

A FIELD INVESTIGATION OF SNOWPACK VENTILATION

by

C

Hardy B. Granberg

A Thesis Submitted to the Faculty of Graduate  
Studies and Research in Partial Fulfilment of  
the Requirements for the Degree of Doctor of  
Philosophy

Department of Geography

McGill University

May, 1981

## ABSTRACT

Snowpack ventilation was studied in the field using a new snow thermometer of high resolution, designed for this purpose. The temperature observations indicate two distinct patterns of temperature variations which appear to be caused by ventilation. One pattern is nocturnal and is apparently driven by density gradients. The second pattern occurs in daytime and is apparently driven by spatial variations in the surface pressure field. Particularly large temporal variations in temperature were observed near noon, when the stratification of the air just above the snow surface is generally least stable. This coincides with the daily maximum temperature of the near-surface snow layers.

The heat balance of the snow cover was measured over 10-minute intervals. The measurements show that in a dry snow cover only a small portion of the absorbed solar radiation is partitioned so as to heat the snow cover itself. A major portion of the absorbed radiation is used to heat the air above the snow. Ventilation of the uppermost few centimeters of the snow cover is suggested as an important heat removal mechanism in this process and offers an explanation of why the near-surface layers of the snow cover do not melt despite the large amount of solar radiation absorbed.

The snow thermometer allows accurate measurements even when

parts of the snow cover are melting. Thermal events associated with a brief period of surface and near-surface melt were recorded, and show meltwater percolating to the base of the snow cover through channels (presumably isothermal at 0 degrees C) in a snow cover that was well below the freezing point.

The rapid temporal variations in the temperature of the near-surface layers suggest two new factors that need to be considered in order to explain the metamorphism of the seasonal snow cover. One is the movement of interstitial air which affects both heat and mass transfers. The second factor is the spatial variation in surface vapor pressure of the ice matrix that is caused by rapid temporal variations in temperature combined with a large spatial variation in thermal inertia of the ice matrix. These two mechanisms may offer an explanation of the rapid "destructive metamorphism" of new snow that is observed in nature but that is not predictable from surface curvatures using Kelvin's equation.

## RÉSUMÉ

La ventilation d'un couvert de neige a été étudiée en utilisant un thermomètre de haute précision, spécialement construit. Les variations temporelles de température présentent la forme d'un signal à deux composantes: la première composante est nocturnale et apparaît d'être causée par des variations spatiales dans la densité de l'air interstitial. La deuxième composante est causée par des variations spatiales de pression atmosphériques près à la surface de la neige. Des variations temporelles particulièrement grandes de température étaient observées près à midi, quand la stratification de l'atmosphère est moins stable près à la surface de la neige et quand on trouve aussi le température maximum de la région surficial de la neige. Par cette coïncidence la ventilation de la neige peut actuellement aider dans le réchauffement de la neige.

Le bilan thermique du couvert de neige a pu être déterminé à toutes les 10 minutes. On a pu en conclure que bien peu de la radiation solaire absorbée par un couvert sec ne sert à le réchauffer lui-même, mais qu'en grande partie cette énergie contribue ultimement à réchauffer l'air au dessus de ce dernier. Il est suggéré que la ventilation des quelques centimètres supérieurs du lit servirait de complément, sinon d'alternative, au mécanisme d'absorption en surface suggéré par Ohmura, (1980) pour expliquer que les couches supérieures ne fondent pas malgré

les grandes quantités de radiation solaire absorbées.

Le thermomètre nival a permis des observations précises alors même qu'une partie du lit était en train de fondre. C'est ainsi qu'ont pu être détectés et enregistrés des incidents thermiques associés à des courtes périodes de fonte à la surface du couvert ou immédiatement sous celle-ci. Ces derniers indiquent que des eaux de fonte ont pu percoler jusqu'à la base du couvert à travers des canaux probablement isothermes traversant la masse de neige elle-même bien en dessous du point de fusion.

Les variations rapides et à l'occasion grandes de la température des couches supérieures suggèrent deux nouveaux processus qui devront être considérés par qui désire comprendre le métamorphisme de la neige. Il y a en premier lieu le mouvement lui-même de l'air qui se repercute à la fois sur les transports de chaleur et de masse. Un second facteur est celui des variations spatiales dans la tension de vapeur en surface de la matrice de glace, résultant de variations temporelles de la température et de variations spatiales de l'inertie thermique à travers la matrice. Ce second facteur pourrait expliquer le métamorphisme destructif rapide la neige fraîche que l'on peut observer dans la nature mais qui n'arrive pas à être expliqué par l'équation de Kelvin appliqué aux courbures de surface.

## ACKNOWLEDGEMENTS

Many persons and institutions have in a direct or indirect way contributed towards this thesis. It is not possible here to mention but a few of those towards who the author is grateful.

I would like to thank Frank H. Nicholson, who supervised the early stages of the thesis, and John E. Lewis, who supervised the later stages of the thesis, for their valuable discussion and support. Bill Howland, Gerry Irwin and Michel Payant have also contributed through many thought-provoking discussions.

Aid in the conversion of a seemingly endless wind chart to computer compatible numbers was given by Riva Flexer, Alan Michalovic and Debbie Newman. Michel Lapointe translated the abstract.

Susan McCallum saved me from many long hours at the keyboards of the typewriter, the keypunch and the computer terminal. So did my wife, Charlotte, who also supported me in many other ways throughout the study.

Financial support was given by PCAC, NSERC and DRES at different stages of the project.

## TABLE OF CONTENTS

ABSTRACT	Page	i
ACKNOWLEDGEMENTS		v
TABLE OF CONTENTS		vi
LIST OF FIGURES		x
CHAPTER I: INTRODUCTION		1
1. The Problem		1
2. Background to the Investigation		2
3. Outline of Thesis		6
4. Site of Study		7
CHAPTER II: THEORETICAL SETTING		8
1. Pressure Variations at a Surface		8
2. Induced Air Flow in the Snow Cover		12
(a) Previous work on air flow in mulches		12
(b) The induced flow		13
3. Detection of Air Movements in Snow		18
(a) Conductive and non-conductive heat fluxes		18
(b) The estimation of air movements from temperature effects		19
(c) A simple indicator of air movements		21

<b>CHAPTER III: INSTRUMENTATION</b>	<b>23</b>
<b>1. Temperature Measurements in Snow</b>	<b>23</b>
(a) Thermal inertia	23
(b) Radiant absorption	24
(c) Heat production by sensor	25
(d) Conduction of heat along the leads of the sensor	26
(e) Some additional problems in snow thermometry	27
<b>2. Some Previously Used Techniques in Snow Thermometry</b>	<b>28</b>
<b>3. Design of the Snow Thermometric Device</b>	<b>31</b>
(a) Some design considerations	31
-Recorders	31
-Scan	31
-Cable characteristics and electromagnetic interference	32
(b) Some initial designs and field tests	32
(c) The new snow thermometer	35
<b>4. Other Instrumentation</b>	<b>39</b>
(a) Snow surface temperature	40
(b) Air temperature measurements	41
(c) In-snow solar radiation	44
(d) Radiation measurements above the snow surface	51
(e) Continuous wind measurement	51
(f) Wind profile measurements	52

## CHAPTER IV: FIELD MEASUREMENTS, CALIBRATIONS

## AND DATA REDUCTION

	55
1. Measurement Schedule	55
2. Snow Property Monitoring	55
3. Meteorological Events Recorded by the Schefferville (A) Weather Station	57
4. Recorder Accuracy and Reading Accuracy	59
5. Reference Thermistor Readings	61
6. Calibrations	61
7. Wind Chart Analysis	62
(a) Method of analysis	63

## CHAPTER V: ANALYSIS OF THE SNOW TEMPERATURE

## MEASUREMENTS

	65
1. Snow Temperature Gradients	65
2. Integrated Snow Temperature Gradients	76
(a) Ventilation patterns	93
3. Snow Surface Temperatures	95
4. In-snow Temperature	98
5. A Meltwater Percolation Event	102
6. Discussion of the Vapor Pressure Regime in a Snow Cover	104
(a) Effects of surface curvature	106
(b) Effects of air movement on void vapor pressure	108

(c) The vapor pressure regime	109
<b>CHAPTER VI: ANALYSIS FOR VENTILATION EFFECTS</b>	<b>111</b>
1. Method	112
2. Run 1	114
3. Runs 2, 3, 4 and 5	122
<hr/>	
<b>CHAPTER VII: CONCLUSIONS AND RECOMMENDATIONS</b>	<b>152</b>
1. Conclusions	152
2. Suggested Modification of the Snow Thermometer	155
3. Suggestions for a Future Experiment	155
4. Some Suggestions for Future Research	157
<b>REFERENCES</b>	<b>160</b>

## LIST OF FIGURES

1. The snow thermometer	Page 36
2. Air temperature mast	42
3. In-snow radiation probe	46
4. Calibration curve for in-snow radiation probe	48
5. In-snow radiation profiles, Schefferville, Quebec	49
6. In-snow radiation profiles, Churchill, Manitoba	50
7. A few wind profiles at the instrumented site	54
8. Millivolt ranges used for recorders A and B	56
9. Weather events as recorded by the Schefferville (A) meteorological station during the measurement period	58
10. Temperature differences over different depth intervals and their first and second time derivatives	66
11. Temperature differences between reference level and different levels in the snow cover and their first and second time derivatives (one-minute intervals)	72
12. Background data for 10-minute intervals	77
13. Background data for one-minute intervals	84
14. Temperature differences between reference level and different levels in the snow cover and their first and second time derivatives	88
15. Snow surface temperature compared to Dew-point, Wet-bulb and Air temperature	97
16. Measured net radiation, heat penetration through	

different levels of the snow cover and computed (residual) turbulent fluxes	99
17. Vapor pressures and vapor pressure gradients	105
18. Run 1. Conductive and total heat fluxes	115
19. Run 2. Conductive and total heat fluxes	123
20. Run 3. Conductive and total heat fluxes	129
21. Run 4. Conductive and total heat fluxes	135
22. Run 5. Conductive and total heat fluxes	143

## CHAPTER I

### INTRODUCTION

#### 1. The Problem

There is one important question regarding the seasonal snow cover that has so far remained largely unanswered. This question concerns air movements inside the snow cover and may be formulated:

- (a) Does the wind above the snow surface induce air flow within the snow cover?
- (b) If so, what are the spatial and temporal characteristics of the induced flow patterns? How do they relate to the wind above the surface and to stability conditions in the near-surface layers of the atmosphere?

Theoretical work and laboratory experiments have shown that, at least near the snow surface, forced, or wind-induced, convection is possible. Forced convection has also been shown to exist in soils and various mulches. However, to the best knowledge of the present author, there has been no successful attempt to evaluate, through field measurements, the spatial and temporal patterns of such forced convection in a natural snow cover.

The reason for this lack of success is, at least partially, found in the properties of snow. Snow is a structurally unstable material that makes disturbance-free insertion of any instrument

nearly impossible. Snow is also, at normal environmental temperatures, quite close to its triple point. Therefore, any thermal disturbance is followed by a structural disturbance because of vapor migration in response to thermal gradients. Thermal disturbances are normally caused by instruments inserted into a snowcover because snow is translucent and allows radiant absorption by the instruments. Even without any radiant absorption, an instrument produces a thermal disturbance since its thermal conductivity usually differs substantially from that of the surrounding snow.

The purpose of this study is to investigate, by field measurement, temporal patterns of snow cover ventilation.

## 2. Background to the Investigation

During a snow survey in a sheltered bay of Knob Lake, near Schefferville, Quebec, the author observed that small pieces (5 - 10 cm in diameter) of the surface layer were missing as though plucked from a few spots on the otherwise smooth snow surface. Fine-grained wind-blown snow had accumulated in a layer approximately 5 mm thick, overlying more porous, recently fallen snow. The author has subsequently observed many such rather inconspicuous features particularly in open woodland but also in a variety of other situations including snow surfaces on rooftops in Montreal.

The reason for the missing surface pieces was not

immediately apparent. It was not until later that the author had the opportunity to observe how the surface feature was formed. The feature was formed by small but relatively strong vortices that lifted pieces of the snow surface layer along their path. Pieces of the thin surface layer of wind blown snow were lifted some 20-50 cm into the air, and, probably on account of acquired rotation and wind shear, disintegrated into a puff of snow grains while airborne.

It is evident that the surface layer could not be lifted without some displacement of air within the snow cover. A survey of the literature, however, revealed very little information on wind induced air movements in snow. An experiment in a wind tunnel by Cura *et al.* (1967) showed a relationship between the air velocity in the tunnel and the air flow at 5 mm below the snow surface in a layer of snow placed in the wind tunnel. Recently, Reimer (1980) concluded, from an analysis of snow and soil temperature variations, that ventilation is important in heat transfers through snow.

The literature on the aeration of soils, a closely related topic, is somewhat more plentiful and shows that wind is an important factor inducing ventilation of soil layers near the surface (Fukuda, 1955, Kimball, 1970; Kimball and Lemon, 1971). The theory of such motion (Fukuda, 1955; Farrel *et al.*, 1966; Scotter and Raats, 1969) is incomplete and has not undergone adequate field testing in either soil or snow. The available

field measurements of vapor transport by air motion in soils (e.g. Kimball and Lemon, 1970; 1971) do not provide detailed information about spatial or temporal patterns.

The process of wind induced ventilation of snow and soils clearly merits attention for it influences life processes in the near-surface layers of the soil and beneath the seasonal snow cover. A better understanding of snow ventilation would also provide a better understanding of processes influencing temporal changes of the seasonal snow cover. At present wind induced ventilation is not even considered a factor in snow metamorphism. Ventilation could, perhaps, help explain the high rates of constructive metamorphism observed in the field but not replicated in laboratory experiments (deQuervain, 1972). The existence of vertical air flows through the snow surface would aid in explaining phenomena such as wind compaction and temporal variations in snow drift transport during snow storms. Such flows would also greatly influence the energy partitioning in the near-surface layers of the snow cover and would aid in the explanation of surface crust formations and many other yet unexplained snow cover features. Of more recent concern is the possible atmospheric filtering action by the snow cover (Gjessing, 1975). If the movement of air through the snow cover results in the deposition of atmospheric contaminants, then the snowpack, as a receptor of atmospheric fallout, must be considered far more complex than is presently believed. If such

filtering occurs, an analysis of the patterns of deposition of suitable contaminants could yield valuable insight into spatial variations in snowpack ventilation.

A suitable anemo-metric device for in-snow operation did not exist at the outset of this study. The purpose of the study thus became twofold. Before the first purpose of the study could be achieved an anemo-metric device suited for this particular application had to be designed. Close to two years of the study were spent on the development and field testing of different such devices before a successful design was accomplished. The work on developing suitable instrumentation thus forms a substantial part of the overall study.

Initially a variety of hot-wire anemometers was developed and field tested. Some success was achieved in that air movements were detected. However, a meaningful interpretation of the observations was not possible mainly because the changing geometry of the cavity surrounding the various devices was unknown.

The method of detection that was eventually adopted employs the observed temperature changes in the snow cover itself to infer the ventilation patterns. One problem with this method is that it requires snow temperature measurements of very high accuracy and a thermometric device that does not significantly disturb internal air flow patterns or internal temperatures of the snow cover. A thermometric device fulfilling these

requirements was designed as part of the study.

### 3. Outline of Thesis

The organization of the thesis reflects the order in which the individual sub-problems were attacked throughout the study. Thus, the theoretical framework is given in Chapter II. This chapter examines the surface pressure variations induced by wind and how such pressure variations may induce air flow in a porous medium. The theory used for the interpretation of air movements from temperature data is also given in Chapter II. Chapter III deals with the experimental procedure. It explores the theoretical and practical aspects of snow temperature measurements and describes the snow thermometric device and other instruments used in the field study. The fourth chapter gives the details of calibrations and data reduction. The fifth chapter is a descriptive presentation of variations in measured and inferred quantities such as snow and air temperatures, in-snow vapor pressures and wind during the measurement period. It presents a unique set of measurements that add significantly to our knowledge about in-snow events just prior to melt. An account of some of these events has been published elsewhere (Granberg, 1978).

The fifth and sixth chapters analyse the patterns of wind induced ventilation, Chapter VII summarizes the conclusions drawn from the study and gives a few suggestions based on the

experience gained during the course of the study.

#### 4. Site of Study

The present study could have been undertaken in any area with a sufficient snow supply. The McGill Sub-Arctic Research Station at Schefferville, Quebec was chosen because of recording equipment, tools and other facilities available at the station. The area also has an ample and reliable supply of snow.

The instrumented site was located some 100 m east of the station, within 100 m of the screen of the Schefferville (A) meteorological station, which afforded valuable backup information for the study.

The measurements reported in this thesis were made in a snow cover that accumulated during one storm. A seasonal snow cover has had a longer time to develop and may therefore be different, particularly in regard to the air permeability of its lower strata, which could be two orders of magnitude greater than the permeability of the snow in which the present measurements were made. The conclusions made in this study are therefore conservative. A natural snow cover with a well developed layer of highly permeable depth hoar might well have indicated much greater air movements than the present snow cover did.

CHAPTER II  
THEORETICAL SETTING

1. Pressure Variations at a Surface

When turbulent air flows past an impermeable surface, different parts of the air flow have different velocities and directions relative to the stationary surface. The surface limits motion to two dimensions and therefore the velocity component perpendicular to the surface is reduced to zero at the surface. In this process momentum is converted into a pressure potential that varies spatially in a fashion determined by the flow. The associated pressure gradient is responsible for the deceleration of air approaching the surface and the acceleration of air away from the surface. Similarly, horizontal gradient components due to spatial variations in the pressure potential accelerate and decelerate the flow horizontally.

If the surface is not perfectly smooth, surface pressure variations are induced through deflections of the flow by the surface. In general, the surface pressure is increased in concave parts of the surface where the surface forces the flow to curve away from its previous direction of motion. Low pressures are generated in convex parts where the surface curves away from the direction of the flow, causing the flow to adjust by expansion.

If there is rotational motion, vorticity, in the flow, a low pressure may be generated at the center of rotation. Such rotation is part of the mechanical turbulence induced by surface roughness. Particularly strong centers of low pressure can be generated at the surface when, during the rise of lower density air, the flow near the surface, possessing vorticity, is forced to converge.

The surface pressure field could, conceptually, be subdivided into two component fields, one of which is quasi-stationary and is related to air deflections by surface roughness elements. The second component field is mobile, is caused by the more or less random turbulence of the air and moves with the flow. These fields respond differently to variations in atmospheric conditions. While the quasi-stationary pressure field, for a given wind direction, depends mainly on variations in the near-surface wind speed, the mobile field, in addition, depends strongly on the density stratification in the near-surface layer. Under stable conditions vertical motions are attenuated resulting in a fairly even surface pressure distribution. In unstable conditions vertical motions are enhanced. Therefore spatial variations in surface pressure can be expected to increase with increasing instability of the air just above the surface.

There is not much direct information available in the literature regarding the possible magnitude of the horizontal

pressure gradients. Farrel et al. (1966) measured fluctuations in pressure difference between two points at spacings of 5 cm, 15 cm and 60 cm on the surface of a grassed area. For a horizontal wind speed of 500 to 700 cm/s, measured with a cup anemometer at a height of 200 cm, they found gradients of 0.0025, 0.0013 and 0.00075 cm of water pressure per cm of horizontal distance respectively for the different spacings (as computed from their figure 1 by the present author). The measurements were made using an induction-type diaphragm pressure transducer. No information was given about the stability conditions during the experiment.

When the mobile pressure field moves past a point on the surface, it is perceived to be an infinite train of pressure waves of varying wavelength and amplitude. Some measurements of pressure spectra are available in the literature. Measurements by Kimball (1970) indicate that the spectral density (microbars<sup>2</sup>/cycle/sec) decreases in a roughly linear manner with a slope of about  $-6/3$  when its logarithm is plotted against the logarithm of frequency over a frequency range from 0.0001 to 100 cycles/sec for all conditions. The spectral density, however, also changes markedly with wind speed. In the frequency range from 0.001 to 0.1 cycles/sec a 500-fold increase was observed between one run when the wind velocity was 68 cm/sec and another when the wind velocity was 552 cm/sec. Similar results are reported by McDonald and Herrin (1975) who report a much greater power

increase in the high-frequency than in the low-frequency part of the spectrum in response to an increase in wind speed. This indicates that the horizontal pressure gradients increase with increasing wind velocity.

There is not enough information in the literature to indicate the effect of stability on horizontal pressure variations. Nor is there much information regarding the maximum and the minimum pressure in the field under different conditions. Theoretically, the maximum pressures are the stagnation pressures for air "parcels" moving towards the surfaces. The minimum pressures could, occasionally, be very low as in the case of the eddies generating the surface erosion feature described in the previous chapter.

The spatial aspects of surface pressure variations are virtually unknown. Spatial information cannot be derived from the spectral information mentioned since it constitutes time averages of the individual pressure variations. It seems reasonable to assume that under stable conditions the areas with a pressure above and below average would be approximately equal in size. The spatial variations in surface pressure would be slight during stable conditions. With increasing instability the area of pressures less than average would decrease and the flow would increasingly be characterized by rising low-density air with near-surface convergence of air possessing vorticity and associated spatially concentrated, fairly intense low-pressures.

The low pressure areas would be interspersed with larger areas of slow subsidence.

## 2. Induced Air Flow in the Snow Cover

### (a) Previous work on air flow in mulches

Until fairly recently it was believed that wind did not have much influence on air flow in soil (or snow). This may, in part, have been due to Romell (1922) who concluded, from inductive reasoning, that diffusion is the most important mechanism in the gaseous exchange between soil and atmosphere. However, experiments by Schmidt and Lehmann (1929) and observations of Diem (1937) led Fukuda (1955) to develop a simple, predictive model for the effect of wind gustiness on air movements in soil.

Farrel et al. (1966) discuss two main limitations of Fukuda's analysis, namely, that it deals only with the case where the soil is of infinite depth and that it ignores horizontal gradients. They developed a model which assumes that the oscillations of air pressure can be described as a train of sinusoidal pressure waves. The model shows that wind has quite an important influence on gas exchange in soil. That wind influences gas exchange in soils has also been shown experimentally by Hanks and Woodruff (1958) who demonstrated that wind can influence evaporation rates at more than 35 cm below the surface of gravel and straw mulches. Later laboratory

experiments by Benoit and Kirkham (1963) and Acharya and Prihar (1969) supported these results. A number of field experiments, notably Evans, Kraner and Schroeder (1962) and Kimball and Lemon (1971) have further shown that wind is an important factor in the aeration of soils.

One main objection to the model by Farrel et al. (1965) is that it treats the input surface pressure field as a wave train of sinusoidal pressure fluctuations. While ventilation by a two-dimensional wave train can be mathematically expressed by analogy to a damped wave, the description of ventilation by a natural surface pressure field requires a more elaborate approach. While a pressure sensor senses a two-dimensional wave train, the three-dimensional nature of the pressure field is evident from the previous discussion. The pressure variations sensed by the pressure transducer are those parallel to the flow. However, the pressure gradients perpendicular to the flow, which are not sensed, are equally important in accelerating the interstitial air.

(b) The induced flow

When the surface and the medium below it are permeable, an internal flow field is initiated in response to the surface pressure field. Once a steady-state condition has been reached, the flow occurs in accordance with Darcy's law so that the macroscopic flow velocity, under laminar conditions (less than 5

cm/sec in fine-grained snow, less than 1 cm/sec in coarse-grained snow; Bender, 1957) is a linear product of the air permeability and the pressure gradient. It is important to note that this law applies only for the condition when the frictional resistance equals the acceleration force. The acceleration force is a linear function of the pressure gradient while the frictional resistance is a power function of the flow velocity for any given air permeability. There is therefore a certain lapse of time before a fluid element in a given porous medium reaches equilibrium velocity in response to a given pressure gradient. This implies that for a step change in pressure at the surface there is a lapse of time before the flow field reaches an equilibrium state, or becomes a potential flow field. One important consequence of this time lag is that the total ventilation rate associated with a given pressure field, as it moves across a porous surface, might, in fact, decrease with increasing wind velocity. This is a result of, on the one hand, the lower internal flow velocity attained as a result of the shorter acceleration time and, on the other hand, the shorter period of influence and therefore distance of actual movement in response to a given pressure gradient. A second consequence of this time lag is that the movement of air in response to the pressure field becomes more surficial as the horizontal velocity of the field increases.

There is not much information available regarding changes in

the horizontal pressure gradients with increasing wind speed. It is therefore not possible to evaluate the relationship between wind speed and ventilation rate. It appears probable however that the increase in ventilation rate with wind speed is most rapid in the low velocity range and that the rate of increase in ventilation rate decreases rapidly with increasing wind velocity. There may possibly even be a net decline in ventilation rates as wind speeds increase beyond a, perhaps fairly small, critical value.

The permeability stratification of a snow cover is also important to the ventilation mechanism. A simple computation using data by Bender (1957) shows that the air permeability of the coarse-grained depth hoar at the base of a seasonal snow cover can be 50 or more times greater than the permeability of new fine-grained snow of the same density ( $0.27 \text{ g/cm}^3$ ) at the surface. This indicates that a given air flow in the near surface layers of a natural snow cover requires a much steeper gradient than the same volume of flow near the base of the seasonal snow cover. This would suggest that near the surface the flow is predominantly vertical, controlled by small scale surface pressure variations, while in the depth hoar layer, near the base of the snow cover, it is mainly horizontal and controlled by larger scale surface pressure variations. It is also likely that spatial variations in surface pressure related to surface drift forms or local topographic variations induce a

slow, more or less horizontal, flow of air in the bottom layers of the snow cover.

Redeposition of matter by vapor transfer can probably also affect the snowpack ventilation mechanism. One important effect of vapor transfer by air moving in pore spaces is that when the air becomes supersaturated relative to the matrix, deposition by sublimation occurs. As a result, when ventilation occurs under a steep temperature gradient, matter is transported from the warm part towards the cold. Deposition occurs within the pores and reduces the air permeability. Thus it appears that the snow cover can provide a negative dynamic response to induced ventilation under conditions when the surface is considerably colder than the internal parts of the snow cover.

It has been observed that the spatial variations in vapor pressure caused by the surface curvatures within the ice matrix are far too small to explain the rapid initial "destructive metamorphism" of newly deposited snow (Colbeck, in press). The process of snowpack ventilation could, however, provide an alternate mechanism that could produce spatial variations in vapor pressure of the necessary magnitude.

Because of variations in mass distribution across individual snow crystals or within the ice matrix of the snow cover, different parts of the snow crystal or ice matrix will respond at different rates to a change in the ambient air temperature. If a stellar crystal is exposed to a change in the temperature of the

surrounding air, the thin spicules of the crystal will adapt more rapidly to the temperature change than will the thicker parts of the crystal. If we let the temperature oscillate between two extreme values, the non-linear relation between vapor pressure and temperature will cause the thin parts of the crystal to experience an average surface vapor pressure that is greater than the average surface vapor pressure of the thicker parts. Consequently, there will be a net transfer of water vapor from the thin to the thick parts of the crystal.

Snowpack ventilation could produce rapidly oscillating temperatures of the interstitial air, particularly in the near-surface layers of the snow cover, where the temperature gradients are often steep and where the induced flow is predominantly vertical and, thus, parallel to the direction of the steepest temperature gradient. Ventilation of the snow cover could therefore help explain the rapid initial "destructive metamorphism" observed in nature.

In summary, a number of interesting features appear to be associated with wind induced ventilation of a seasonal snow cover. First, the stability of the air above the surface appears to influence the ventilation such that maximum vertical flow through the snow surface occurs in unstable conditions. In general this coincides with inversion conditions inside the snow cover. Secondly, there appear to be rapidly diminishing returns in terms of ventilation induced by the moving pressure field in

response to increasing wind velocity. Thirdly, the flow in the highly permeable bottom layer of the snow cover is probably mainly horizontal in response both to the mobile and the stationary surface pressure fields. Fourthly, redeposition of moisture within the snow cover can probably provide a negative feedback to ventilation when steep temperature gradients occur in the snow. Ventilation may also be important in snow metamorphism in that it can induce steep microscale gradients in temperature and vapor pressure within the snow cover.

### 3. Detection of Air Movements in Snow

Air movements influence the rate of propagation of heat, sound and gaseous matter through the snow. Consequently inferences may be made regarding the air movements using observations of the movements of heat, sound or gaseous matter. In this study the heat transfers were monitored in order to derive information about air movements in the snow. Information about air movements can be derived in two ways, one by flux separation and the other by simply monitoring rates of temperature change.

#### (a) Conductive and non-conductive heat fluxes

The heat transfers in snow have been treated in considerable detail by several authors, notably Bergen (1963), Schlatter (1972), Goodrich (1976), Palm and Tveitereid (1979) and Ohmura

(1980). It is convenient for the present study to separate the heat fluxes into conductive and non-conductive fluxes. The conductive fluxes in this context include the transfer of heat by conduction through the ice matrix and the void air spaces and the transfer of heat by vapor diffusion through the air spaces. Both of these fluxes are predictable from knowledge of the temperature gradient, the thermal conductivity of the snow and the coefficient of vapor diffusivity for the given temperature. The effects of still air vapor diffusion are normally included in field determined estimates of the thermal conductivity of snow and may, for the present study, be ignored without much error.

The non-conductive fluxes include solar radiation, thermal radiation and fluxes arising from air movements in the snow. The radiation fluxes can be measured so that their temporal variation is known at all times. This makes it possible to separate the radiant heat fluxes from the total non-conductive heat fluxes which then leaves as a residual the fluxes of heat arising from air movements within the snow cover.

(b) The estimation of air movements from temperature effects

The thermal conductivity of snow can be determined with reasonable accuracy from field measurements of temperature gradients and measurements of temperature change in the snowpack over time. If the snow density is known, the change in snow pack

heat content can be determined with an accuracy that depends largely on the accuracy of the estimate of the snow temperature change. If multi-level temperature measurements are available, the heat flow through different levels of the snow cover can be determined. If the temperature gradient  $dT/dz$  and the heat flow,  $Q$ , are known, the thermal conductivity,  $k_e$  is calculated by:

$$k_e = Q / (dT/dz). \quad 2.1$$

This is the effective thermal conductivity, averaged over the period between the successive temperature measurements, used in order to determine the magnitude of  $Q$ .

The effective thermal conductivity was found by Yen (1962) to be a function of the mass flow rate,  $G$ , such that

$$k_e = 0.0014 + 0.58 G \text{ (cal/cm/sec/degree C)} \quad 2.2$$

for snow of an average density of  $0.426 \text{ g/cm}^3$ . This result was from a laboratory investigation using steady, unidirectional flow. The relationship was tested over a range in  $G$  from 0.001 to about  $0.004 \text{ g/cm}^2/\text{sec}$ . No information outside this range is available in the literature. Nor is there any information regarding the effects of reversal in flow direction. In nature, the flow of air in the snow cover is omnidirectional. This affects the relationship to an unknown degree. It would be necessary to assume the relationship to be valid also for omnidirectional flow. Such an assumption may be justified by the very narrow air voids of the snow cover which would tend to keep the void air in close equilibrium with the surrounding ice matrix

at all times. This latter assumption has some weaknesses, particularly in that the microscale variations in temperature and vapor pressure are ignored.

A more serious problem in using the flux separation method to assess ventilation rates is posed by the internal distillation effects within the snow column. This effect has been discussed in the context of soil freezing by Outcalt (1977). In snow it causes unknown latent heat transfers within the snow column. While the magnitude of this effect is predictable in ideal conditions, there are at least two factors that make it unpredictable in a seasonal snow cover. One is the unknown motion of the interstitial air. The second factor is the Riecke effect and the unknown stress distribution within the ice matrix.

It is therefore not possible to evaluate, with acceptable accuracy, the magnitude of the air movements in the snow cover using the flux separation method. The quantitative estimate of air flow thus derived can, at best, be used as a general indication of air movement magnitude.

(c) A simple indicator of air movements

Only ventilation, meltwater percolation and temporal variations in the absorption of solar radiation can cause sudden temperature changes in a snow cover. All other heat exchanges can only cause relatively gradual changes in temperature. The first and second time derivatives of temperature should therefore

be good indicators of temporal patterns of snowpack ventilation. The thermal effect of a given volume of air moving through the snow depends on the direction of motion and on the steepness of the temperature gradient. A precise, quantitative evaluation of air movements is therefore not possible using temperature measurements. The thermal effects of the air motion can, however, be directly monitored and can be used to indicate temporal patterns of snowpack ventilation.

CHAPTER III  
INSTRUMENTATION

1. Temperature Measurements in Snow

Temperature measurement is usually accomplished by measuring physical changes in a known substance which is inserted into the substance of unknown temperature. The measured quantity may be pressure, volume, electrical resistance or perhaps color change and the temperature of the thermometer substance is inferred from the measured quantity. Furthermore, the assumption is made that the temperature of the thermometer equals the unknown temperature. The failure of this assumption is the most common cause of temperature measurement error. There are a number of reasons why the temperature of the sensor may differ from that of the medium. In the case of snow, the most significant are:

- (a) Thermal inertia effects
- (b) Radiant absorption by the sensor
- (c) Heat production by the sensor
- (d) Conduction of heat along the leads of the sensor

(a) Thermal inertia

If the specific heat of the sensor is greater than the specific heat of the surrounding material, then a lag is introduced such that the sensor will react more slowly to

temperature changes than the surrounding medium. Temperature maxima and minima will therefore not be reached. The sensor thus smooths the time-temperature relationship. This lag effect is usually described as a time constant as described by, for example Doebelin (1976). The value of the time constant increases with increasing heat capacity of the sensor, and with decreasing thermal conductivity and specific heat of the surrounding medium. In snow, therefore, this error can be substantial, since snow, partly because of its porosity, has both low specific heat and low thermal conductivity.

If the sensor has a specific heat that is less than that of the surrounding medium and if it is of similar or greater thermal conductivity it will follow the thermal changes of the surrounding medium without introducing much error.

#### (b) Radiant absorption

When the temperature sensor is exposed to solar radiation the sensor absorbs radiation at a rate that depends on the intensity of the radiation and the albedo of the sensor. The temperature of the sensor increases until an equilibrium is reached where the rate of heat transfer away from the sensor equals the rate of radiant absorption.

If the sensor is assumed to be an infinitely long cylinder in a homogeneous medium, then simple geometry gives that the heat flow per unit area at any distance from the sensor,  $Q_L$ , is

$$Q_r = Q_0/r \quad 3.1$$

where  $Q_0$  is the heat flow per unit area at the surface of the sensor and  $r$  is the distance from the center of the sensor expressed as multiples of the sensor radius.

To accommodate this heat flow the temperature gradient,  $dT/dr$ , declines with distance away from the sensor. Since

$$Q_r = -k(dT/dr) \quad 3.2$$

where  $k$  is the thermal conductivity of the medium, the temperature rise,  $T_r$ , at the sensor required to produce the necessary gradients to conduct away the absorbed heat can be found numerically by integrating the temperature changes over distance from the sensor. Thus,

$$T_r = \int_{r=1}^{\infty} dT/dr. \quad 3.3$$

The radiation error increases with the size of the sensor, with decreasing albedo of the sensor and with decreasing thermal conductivity of the surrounding medium.

### (c) Heat production by sensor

Some sensors may generate heat when the temperature is measured. Such is the case for thermistors or other resistance thermometers. The heating,  $q$  (W/hr) is expressed by the relation

$$q = i^2 r t = e^2/r \quad 3.4$$

where  $r$  is the resistance of the path of the current

$i$  is the current in Amperes (for a/c it is the rms value)

$e$  is the applied voltage

$t$  is the time, in hours, of the flow of the current.

As in the case of radiant absorption, this heating raises the temperature of the sensor until an equilibrium is reached where the amount of heat conducted away from the sensor by the induced temperature gradient equals the amount of heat produced. When thermistors are used in media that have a great ability to conduct or convect heat away from the sensor, the error induced is small. However, when the thermal conductivity of the medium is low such as in snow, the heat generated by a thermistor can seriously affect the accuracy of the measurement, unless special precautions are taken to minimize the current and the duration of measurement.

The size and shape of the thermistor is of some importance since it determines the contact area between the thermistor and the surrounding medium and it also determines the geometry of the heat flow away from the thermistor.

(d) Conduction of heat along the leads of the sensor

If the leads of the sensor pass through zones of different temperature, the conduction of heat by the sensor leads may be sufficiently large to significantly affect the measurement. The heat input, or loss  $Q_1$ , may be estimated by:

$$Q_1 = -ka \frac{dT}{dx} \quad 3.5$$

where  $k$  is the thermal conductivity of the lead

$a$  is the area of the lead and

$dt/dx$  is the temperature gradient along the lead just before the sensor.

Once this quantity has been determined, the necessary temperature change to accomplish steady state condition can be estimated using a technique similar to that outlined in the previous section.

Obviously, the cross-sectional area of the lead is a prime parameter controlling this error, in addition to the parameters mentioned in the previous section. Thus, to minimize this error, the leads should be either as thin as possible or they should be located so as to minimize temperature gradients along them.

(e) Some additional problems in snow thermometry

When snow temperatures are measured, consideration must be given to the peculiarities of the snow cover that arise from the structural and thermodynamic instability of snow. For example, it is almost impossible to insert any kind of sensor into a snow cover without seriously disturbing the surrounding snow structure.

If the sensor induces and maintains temperature gradients around it, the properties of the surrounding snow will change rapidly in response to the gradients. In severe cases a cavity may develop around the sensor, in a fashion similar to the "greenhouse cavity" that develops around twigs in snow.

The snow cover is not structurally stable and settles

gradually over time in response to internal metamorphism. Therefore, between two arbitrary points in the snow there is, usually, a slow relative motion. Any permanent sensor inserted in the snow will therefore experience mechanical stresses. While the mechanical effects of such stresses are easily imagined, the spurious thermal effects that might result in connection with use of different sensors are unknown.

## 2. Some Previously Used Techniques in Snow Thermometry

A wide variety of thermometric devices have been used to measure snow temperatures. The devices have varied depending on the purpose of the measurements. Bader et al. (1939) used mercury thermometers to measure temperature profiles in snow pits in their time-profile study of the snow cover. They observed that radiation heating was a problem. In recognition of this problem, fine thermocouple wires have been used by several subsequent researchers. The "Canadian Snow Kit" includes bi-metal stem thermometers which are inserted into the wall of the snow pit. Provided the thermometers are inserted immediately after the pit has been excavated, the measurements should be accurate to within about 1-2 degrees C, depending on the ambient air temperature, the heat capacity of the thermometers and the thermal properties of the snow.

The settling of the snow cover poses problems in continuous monitoring of snow temperatures. Experiments at Schefferville

have shown that the settling of the snow cover can completely distort a thermistor array suspended on horizontal steel rods 2.5 mm in diameter and about 25 cm long. The rods were firmly anchored in a wooden post at one end (F.H. Nicholson, pers. comm.). Atwater and La Chapelle (1961) and later Bergen (1963) used thermistors attached to the edge of light styrofoam discs which were centered on a guide wire by a mercury contact. The guide wire served as one arm of a bridge circuit which allowed the height of the disc to be accurately measured. The measurements by Bergen (1963) however show a lack of detail in the daytime temperature readings that may be attributable to radiation error, although this is not mentioned by the author.

Attempts at Schefferville to use a Lambrecht soil temperature recorder to obtain multi-level measurements of snow temperatures failed because of the very large thermal inertia of the sensor bulbs. The Lambrecht recorder has mercury filled sensor bulbs of approximately 500 g weight.

In research in the Antarctic, long term records of multi-level snow temperatures have been obtained by several researchers. Liljequist (1956) used thermocouples and multiple recorders to obtain continuous records of snow temperatures. Soviet expeditions have generally also used thermocouples to measure snow temperatures. However, no information is available regarding how control of the depth of the sensor within the snow was achieved.

One recording of snow temperatures extending into the melt season is reported by Kotlyakov (1961). The method of measurement is described as thermocouples at 10 cm intervals throughout the uppermost meter of the near surface layers and the data were plotted every four hours. The measurements give a pattern of very sudden increase in temperature throughout the measured layer, which can be explained by the downward percolation of meltwater. Subsequent sudden drops in temperature below the surface while temperatures both higher up and lower down in the profile are at the melting point (*ibid*, p. 114) cannot be explained by one-dimensional heat flow. The observed temperature changes were probably the result of meltwater percolation along the sensor arrangement with subsequent refreezing by heat loss to surrounding cold snow.

Nowhere in the literature were snow temperature recordings found that gave accurate daytime readings of snow temperatures in near-melt conditions or in conditions that included melting events. It became evident that for the present study a new approach to snow temperature measurements was needed.

### 3. Design of the Snow Thermometric Device

#### (a) Some design considerations

To be useful for the present study the thermometric device should have an absolute accuracy of better than plus or minus 1 degree C. The relative accuracy should be sufficiently good to resolve temperature changes smaller than 0.01 degrees C in the lower part of the profile and smaller than 0.1 degrees C in the upper part of the profile. To achieve this accuracy it became important to consider the following factors in addition to those previously mentioned:

1. Recorders available
2. Matching signal strength with other instruments on scan
3. Cable characteristics

#### Recorders

The recorders available were Esterline Angus potentiometric chart recorders. These recorders accept voltage analog inputs.

#### Scan

A double, 24-point rotary switch (Fairchild mfg.) was used in a continuous 1 rpm rotating mode to scan the various sensors at the instrumented site. The signals were directed to two recorders operating simultaneously either on the 2 and 10 mV

ranges respectively or on the 5 and 20 mV ranges depending on signal conditions. The operating ranges were determined by the solar and net radiometers that were available for the study. To optimize system accuracy, the aim in the design of the thermometric device was a maximum output similar to that of the radiometers.

#### Cable characteristics and electromagnetic interference

A 48-conductor shielded telephone cable was used to link the instrumented site to the recorders in the laboratory. The length of the cable was 100 meters. The resistance of individual conductors was 3 Ohms. By pairing of conductors and by use of common grounds a total resistance of slightly less than 2 Ohms per channel was accomplished. Because of the low cable resistance and the low current in the circuit, errors due to thermally induced variations in the cable resistance are negligible. The cable (Northern Electric No. 2486) has a random-twisted conductor arrangement to minimize signal interference between different channels. The aluminum shielding of the cable minimizes outside electromagnetic interference.

#### (b) Some initial designs and field tests

To obtain some basic information on temperature conditions in the snow, a thermistor cable with five cylindrical, 2.5 mm diameter glass bead thermistors was used. Initially the

thermistors were encapsulated in thin, transparent plastic tubing. This practice was abandoned after temperatures of eight degrees above the melting point were recorded at 5 cm below the surface of a non-melting snow cover on a clear, sunny day. The reading was reduced to +0.8 degrees C when the plastic tubing was removed and the beads painted white. The size of the bead was apparently too large to give a measurement free from radiation error. A specially designed resistance meter was used (Jessop, 1968) which minimizes the current through the thermistor and thus minimizes the self-heating effect. The thermistors were calibrated to an accuracy better than  $\pm 0.01$  degrees C, using calibration facilities at the Earth Physics Branch of the Dominion Observatory in Ottawa. It is therefore believed that most of the error was caused by the absorption of solar radiation by the sensor. The heat thus generated could only slowly be dissipated by the surrounding snow because of its low thermal conductivity, raising the temperature of the sensor.

One of the initial designs of snow temperature sensors that was used concurrently with the thermistor string was a string of bunched 10-junction thermopiles with sensor levels at 0, 2.5, 7.5, 37.5 and 77.5 cm below the surface. The device was comprised of insulated 36 AWG copper-constantan wire. The string was moulded into acrylic plastic and painted white. To measure surface temperatures, the individual upper junctions of the uppermost thermopile were spread over an area of approximately 10

cm radius. Spring action by the nylon-insulated wires held the junctions against the snow surface. This design also suffered from considerable radiation error near the surface. On warm days with air temperatures just below freezing, this led to melting near the surface and meltwater percolation downwards along the string. There were also apparent problems with conduction of heat along the sensor string. The absence of short-term slight variations in temperature at 2.5 cm below the surface indicated that the thermal inertia of the sensor was too high.

To reduce the error caused by radiation and by conduction along the sensor string, a thermopile string was designed where the junctions protruded about 10 cm horizontally from the main cable. To install this cable it was necessary to dig a pit and to insert the sensors horizontally into the pit walls. Although the radiation error and the thermal inertia effects were reduced by spreading the junctions individually at each level, the method generated far too great a disturbance of the snow pack to be practical.

To minimize radiation error and conduction, a translucent probe of 8 mm diameter with 13-junction thermopiles was designed. The sensing levels were at 0, 2.5, 5, 10, 15, 25 and 35 cm below the surface. The leads from the thermopiles were packed in plastic foam inside the hollow stem of the probe. At the base of the probe, at the level of the lowest set of junctions, a calibrated thermistor was embedded in the foam. Although this

probe was reasonably free from thermal inertia error, there was some radiation error in evidence just below the snow surface with a tendency for meltwater conduction along the probe on warm days. It was also apparent from multiple insertions and excavations that the probe could not be inserted with a tight fit along its entire length. Usually the snow would collapse and air pockets develop along part of the probe. It was felt at this stage that the conventional methods of thermometer design had been exhausted and that a radically new approach was needed.

(c) The new snow thermometer

The snow thermometer is shown in Figure 1. The design incorporates a number of features which make it suitable for accurate monitoring of snow temperatures. It consists of a series of 20-junction copper-constantan thermopiles suspended on nylon wires within a metal frame. Each thermopile spans a vertical distance of 5 cm. At each end about 25 cm of nylon wire accommodate vertical motion due to settling of the snow cover. The thermocouple wire used is AWG 32 and the junctions were twisted and soldered. This gives them a diameter of approximately 0.4 mm including a thin layer of white, dielectric lacquer. The radiation error is somewhat difficult to compute due to the change in effective diameter at the junction and the presence of the nylon wire but according to estimates using cylindrical geometry, an effective diameter of 0.5 mm and a

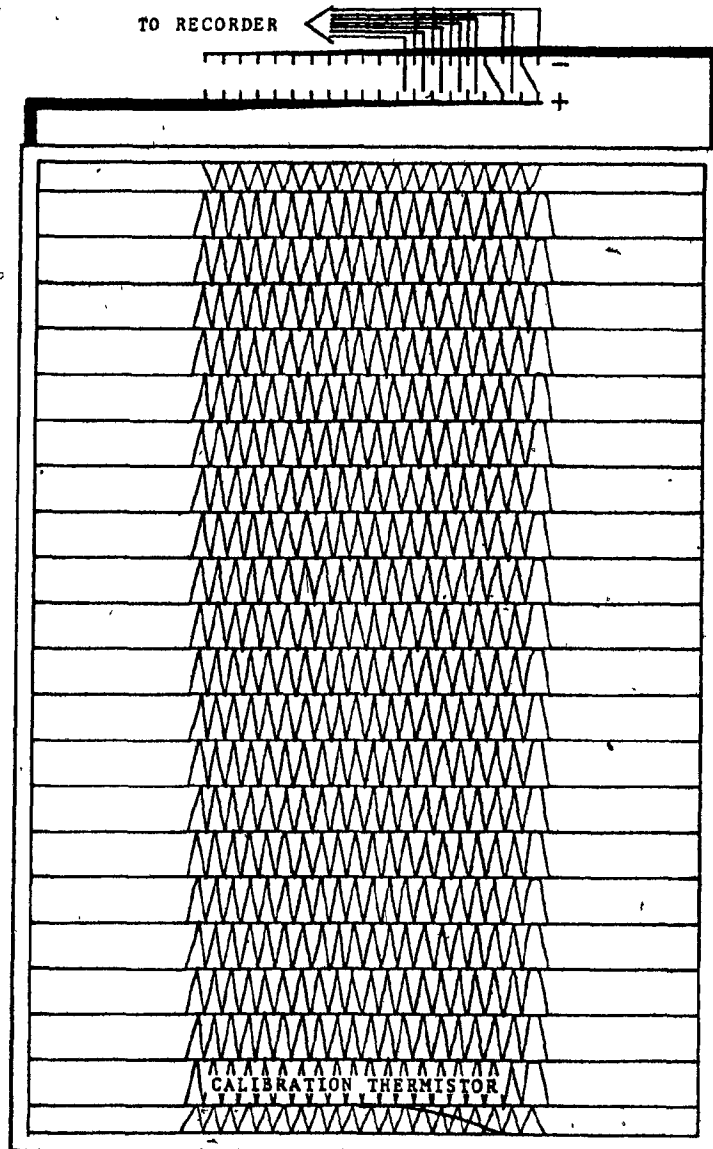


Figure 1. The snow thermometer.

sensor albedo of 0.9 a radiation error greater than 0.1 degrees Celsius can occur only in the uppermost centimeter of the snow cover. Below this level, radiation loads, according to field measurements, do not exceed 0.4 ly/min for the snow conditions that prevailed at Schefferville during the experiment. The snow thermal conductivity was computed using Abels' formula, assuming a snow density of 0.2 g/cm<sup>3</sup>.

Because of the geometry of the snow thermometer it does not conduct meltwater downwards. The conduction of heat along wires is minimal because of the small gauge wire used and is further reduced by the diagonal arrangement of the wires.

The thermometer is installed by allowing it to be buried by snowfall or drifting snow. Since it is not easy to predict what depth of snow will accumulate it was necessary to furnish a programming unit so that the depth intervals over which measurements are taken may be altered depending on snow depth. Because thermopiles were used the depth intervals can be extended to different multiples of 5 cm simply by connecting the thermopiles in series. The error introduced by the increased circuit resistance is negligible.

The reference temperature is determined by using a calibrated thermistor at the lowest sensor level. The temperature differences between different sensor levels are then added. Since the thermistor was located within 5 cm of the ground/snow interface it was assumed that temperature changes

would be gradual, and that therefore interpolations between intermittent readings of the thermistor would be sufficient to provide an accurate reference temperature. This assumption will be further discussed in Chapter V.

In the design 20 junctions of the upper and 20 junctions of the lower thermopile alternate at each level. This gives a reasonable certainty that both thermopiles measure the same average temperature at each level. Within a snow cover there are microthermal variations due to the surface curvatures of the ice matrix (Colbeck, 1973). When the temperature sensor is small, as in the present case, the measured temperature can vary slightly depending on the characteristics of the ice matrix close to the sensor. There may also be slight local variations in temperature due to spatial inhomogeneities in the thermal properties of the snow cover.

The number of junctions per thermopile (2 x 20) also ascertain that calibration differences between individual thermopiles are minimized. Although great care was taken in the manufacture of the thermocouple junctions, it is impossible to make them all identical with regard to electromotive force. When a large number of junctions are used in a thermopile, individual variations are averaged over the total number of junctions. Thus a thermopile can measure a given temperature difference far more accurately than a single pair of thermocouple junctions can without special calibration.

When thermocouples are used it is essential to minimize all other potential sources of electromotive force in the circuit. Whenever cables are joined, either by plugs of material dissimilar to that of the cable or by soldering, it is essential that each plug or joint is kept at a spatially even temperature - otherwise an electromotive force may be induced. By thermally insulating the joints, temperature differences across them can be eliminated. The cable leading to the recorders was shielded to prevent electromagnetic interference. The metal frame of the snow thermometer helped eliminate possible electro-potential gradients through the snow. Such gradients can possibly be generated as a result of snow drifting.

#### 4. Other Instrumentation

In addition to 6-level temperature measurements in the snow on a minute-by-minute basis, the following measurements were made:

- (a) Snow surface temperature (measured once per minute)
- (b) 3-level air temperature (as above)
- (c) Net radiation (as above)
- (d) 3-level in-snow solar radiation (as above)
- (e) Reflected solar radiation (as above)
- (f) Incoming solar radiation (continuous record)
- (g) Wind velocity (continuous record)
- (h) 3-level wind speed (intermittent)

Meteorological observations from the nearby Schefferville (A) meteorological station were also available as backup information.

(a) Snow surface temperature

The snow surface temperature was measured using a 2 x 5-junction thermopile, one end of which was encased in a high thermal inertia device with a calibrated thermistor. The individual junctions at the other end were spread out on the snow surface over an area of about 20 cm diameter. The thermopile was manufactured from 32 AWG copper-constantan wire, twisted and soldered and painted white with electrically insulating paint. The twisted tips, about 5 mm long were inserted into the snow until the T-shaped junction was flush with the surface.

The uncertainties associated with the measurement of surface temperatures of soil, vegetation and water are quite well known from the literature. Marlatt (1967) provides a good summary of the errors inherent in different measurement methods. The snow surface temperatures may be slightly less prone to error because of the high albedo and the porosity of the surface.

The radiation error, computed according to the method outlined earlier in this chapter, is, for a thermocouple of this size at a radiation level of 1 ly/min, approximately 0.5 degrees C for homogeneous snow of a density of  $0.2 \text{ g/cm}^3$ . However, since half of the medium surrounding the thermocouple is snow and half is air, some uncertainty is introduced because of the

variable ability of air to transport heat away from the sensor. It is estimated that in calm conditions the error may be as much as 1 degree C, provided the contact between the snow and the sensor is good. If it is not good, the error may be greater. The maximum error may therefore be approximately +1.5 to +2.0 degrees C in perfectly calm weather. The error decreases with increased ventilation of the sensor. During the period of measurement calm conditions occurred only during the night and early mornings when little or no shortwave radiation was present. The overall accuracy of the surface temperature measurements is therefore regarded as good with the error only rarely exceeding +0.5 degrees C.

(b) Air temperature measurements

Air temperatures were measured at three levels, 0.5 and 1.0 m apart using the thermometric ladder technique (Figure 2). Two 2 x 15-junction thermopiles were used and a third thermopile with 2 x 5 junctions was used to connect the lowest sensing level to the same reference thermistor as was used for the snow surface temperatures. The ends of adjacent thermopiles were housed in glass vials of equal size (6 mm outer diameter), with individual junctions randomly dispersed within the common bundle of junctions from the two thermopiles. This gives three vials with differing numbers of junctions within each. The top vial contained 15 junctions, the middle vial 30 junctions and the

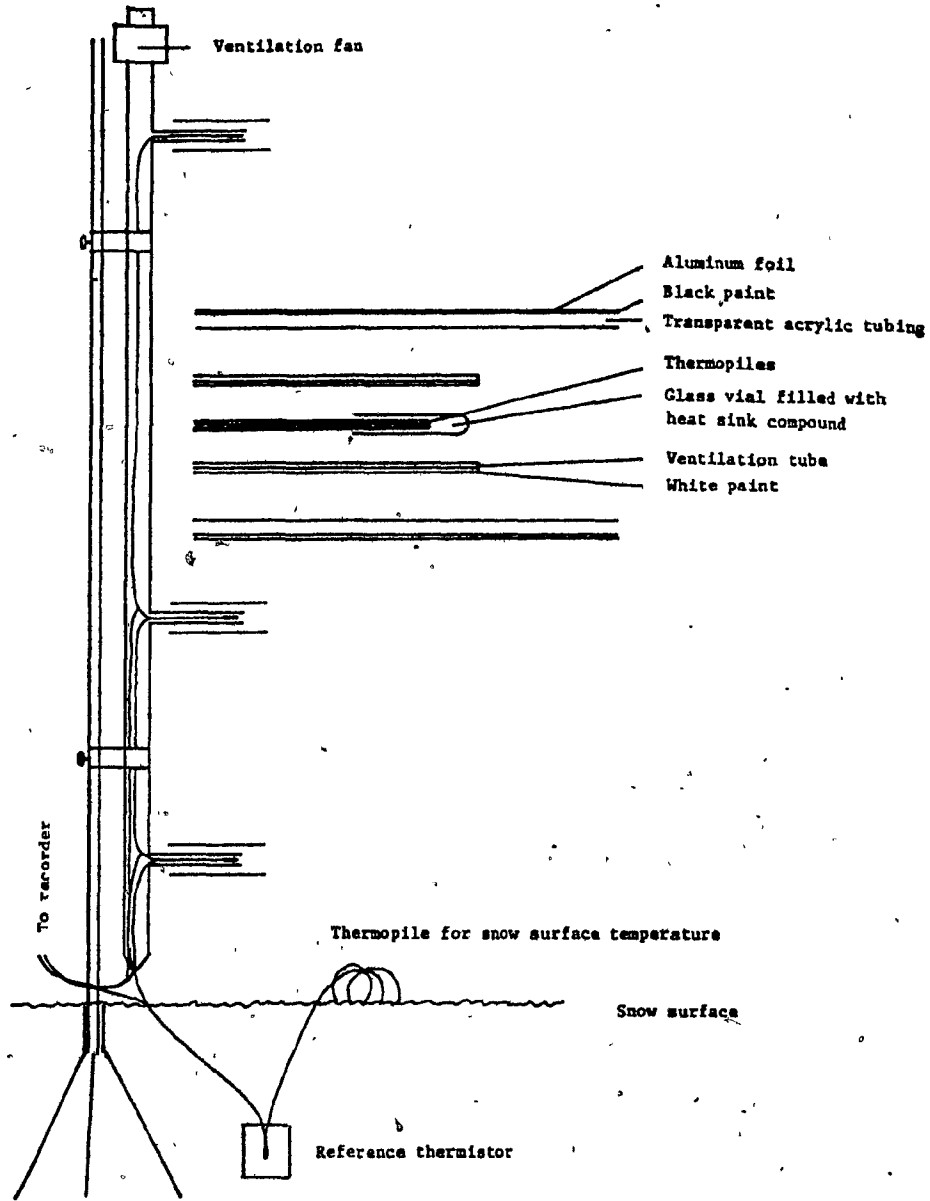


Figure 2. Air temperature mast

bottom vial 20 junctions.

The vials were encased in ventilated housing manufactured from acrylic plastic. A small vacuum fan was used for ventilation. Double radiation shielding was used. The inner shield was painted white while the outer radiation shield was first painted black on the outside and then clad with aluminum foil. The theory of this arrangement is that the solar radiation that enters the shield is absorbed where it can easily be removed by sensible heat transfer to the ambient air.

Initially, a fairly large radiation error resulted, despite the shielding, because the small amount of radiation that entered the vials was quite efficiently trapped inside. The vials simply acted as a greenhouse. To overcome this problem the vials were filled with heat sink compound (Dow Corning No. 18). Heat sink compound is a white paste that has a high thermal conductivity. In the present application it served two purposes, to block incoming radiation and to balance the response of the individual sensors. The time constant of the sensors can be changed by varying the amount of heat sink compound and by varying the ventilation rate. Because of deficiencies in the ventilation system caused by the narrow ductwork used, the time constants of the three sensors were unequal. Some compensation was achieved by altering the amount of heat sink compound but the time constants could not be accurately equalized. Consequently, there may be spurious temperature gradients measured when the air

temperature is rising or falling rapidly. There are also radiation errors due to poor ventilation and fan breakdowns. The daytime air temperature measurements are therefore not very accurate and may occasionally indicate a stable stratification closely above the snow surface when, in fact, the stratification was unstable.

(c) In-snow solar radiation

Solar radiation intensity was measured at three levels of 10, 20, and 30 cm below the snow surface. The radiometers were designed by the author, using silicone photoelectric elements. The reader is referred to IRC-handbook No. 3 (1966) for details regarding spectral response characteristics. The peak sensitivity of the sensor is at 0.83 microns.

To measure solar radiation inside a multiple scattering medium such as snow is a rather difficult task. Any absorbing object inserted into such a medium will alter the radiation intensity locally. In-snow radiation measured by two different radiometer probes may thus differ depending on the amount of radiation disturbance caused by each probe.

Another problem is that, because of the difference in refractive index between ice and void air, the light intensity in the ice may be different from that in the air. The measured intensity may therefore depend on the area of contact between the ice matrix and the sensor. For a probe inserted temporarily into

the snow the area of contact would depend on snow density, grain size and water content. For a permanently installed probe it would depend on time-dependent contact changes.

The radiometer probe is shown in Figure 3. It consists of a silicone photocell mounted inside a 10 mm brushed aluminum tube. The aperture of 6 mm diameter is covered by a diffuser lens of opalescent acrylic plastic. The lens is cemented directly onto the silicone cell and the front of the diffuser is matted, using fine emery cloth, to produce a good cosine response. The circumference of the diffuser was painted opaque black to avoid stray light. It was necessary, for calibration purposes, to allow radiation to enter only through the flat front surface of the diffuser.

A load resistor of 50-150 Ohms (depending on desired sensitivity) was used to match the sensor output range to that of other instruments on the scan. The load resistor also to some extent linearizes the output of the sensor.

Since thermal variations encountered in operation would produce less than about 10 per cent variation in voltage output (under constant resistance) and the ratio of voltage to current is high, the total error due to thermal effects is small. The sensors were therefore used without temperature compensation.

Calibration was accomplished by recording the outputs of the in-snow radiometers parallel with an Eppley solarimeter the calibration of which was known. The in-snow radiometers were

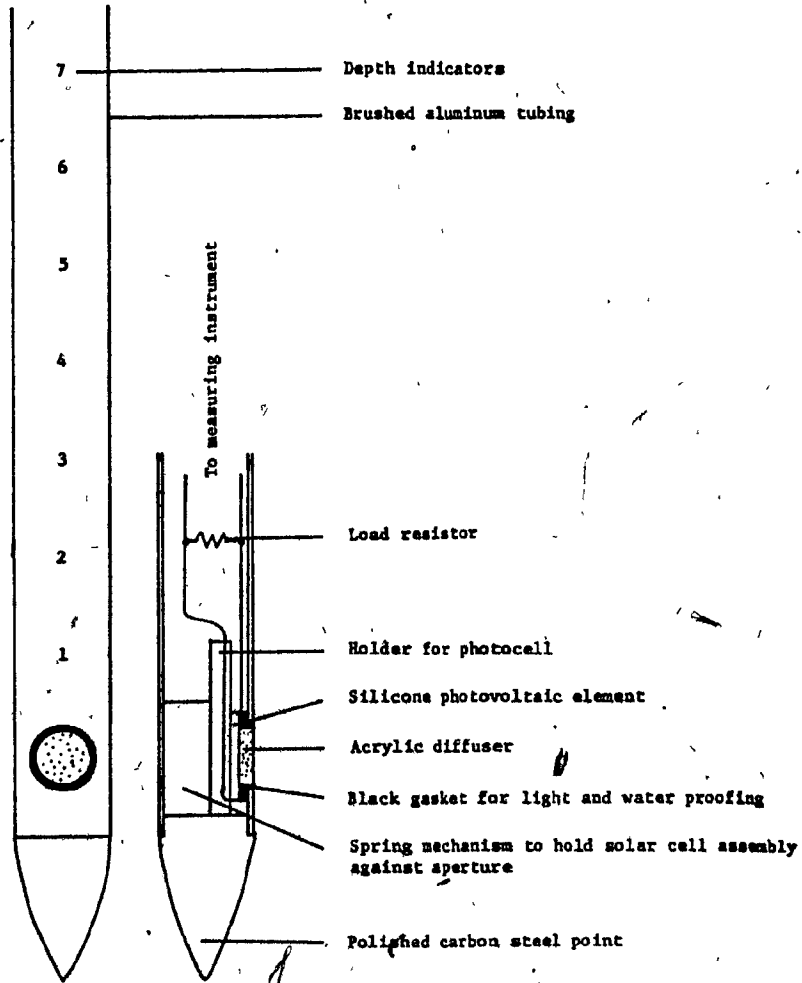


Figure 3. In-snow radiation probe

placed near the solarimeter with the front surface of the diffuser horizontal. A typical calibration curve is shown in Figure 4.

At times, melting occurred around the probes in the region just below the snow surface. The melting was caused by radiant absorption by the probe and caused meltwater to percolate downwards along the probe. On warm days melting caused the probes to lean over and they had to be repositioned quite frequently. Use of the probes in a stationary mode in near-melting conditions is thus not feasible. The continuous measurements were therefore not suited for further analysis.

The probes appear useful, however, if they are applied in a portable mode. Figure 5 shows some radiation measurements that were taken in Schefferville on a clear day at about 1300-1400 hrs. The measurements were taken along the eastern shore of Knob Lake and some of the variations in the measured radiation density reflect slight variations in the iron ore dust content of the snow. Another set of measurements (Figure 6) were taken in clean snow at Churchill Manitoba. The profiles were obtained within a few meters from each other on an open willow-buskeg site. These variations in radiation density are related to variations in the amount of vegetative matter within the snow. Profile 3 shows the effect of a willow branch acting as a local radiation sink. Below the branch, the radiation density increases again after reaching near zero adjacent to the branch.

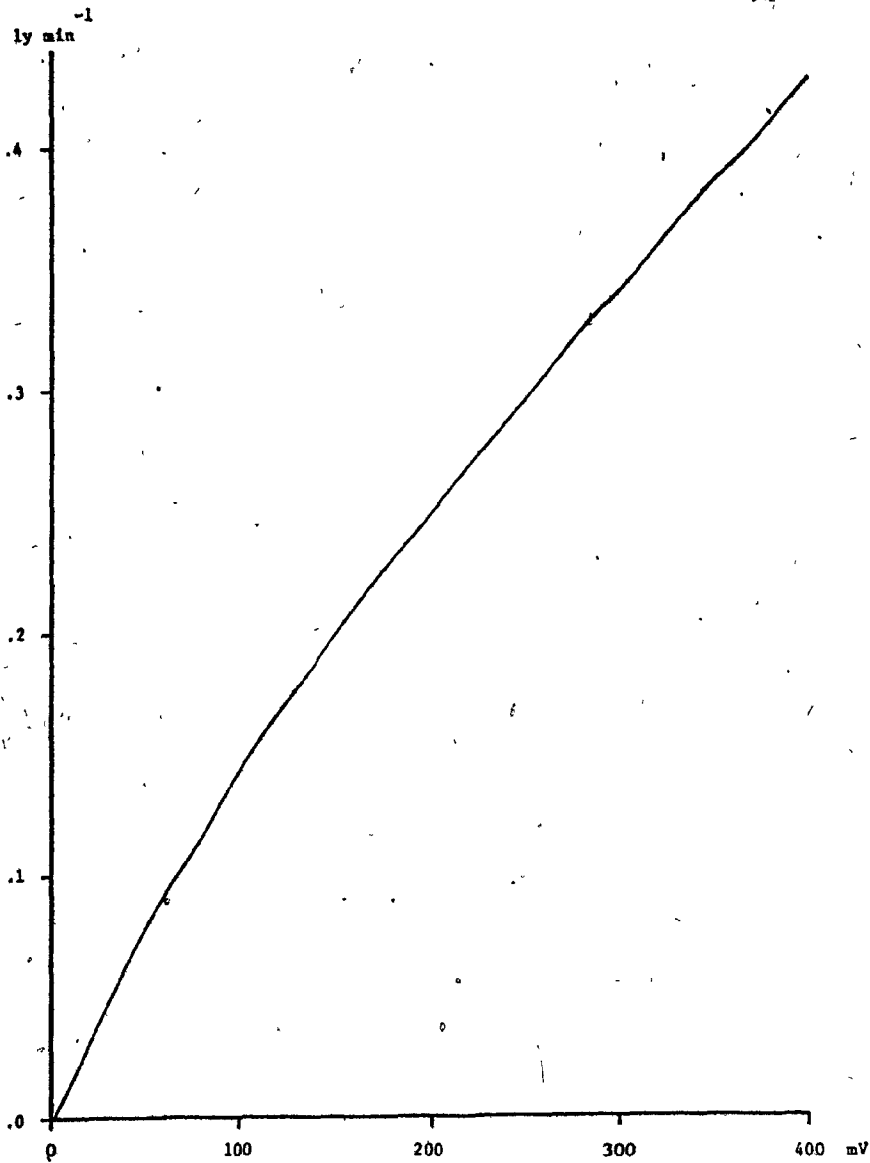


Figure 4. Calibration curve for in-snow radiometer probe.

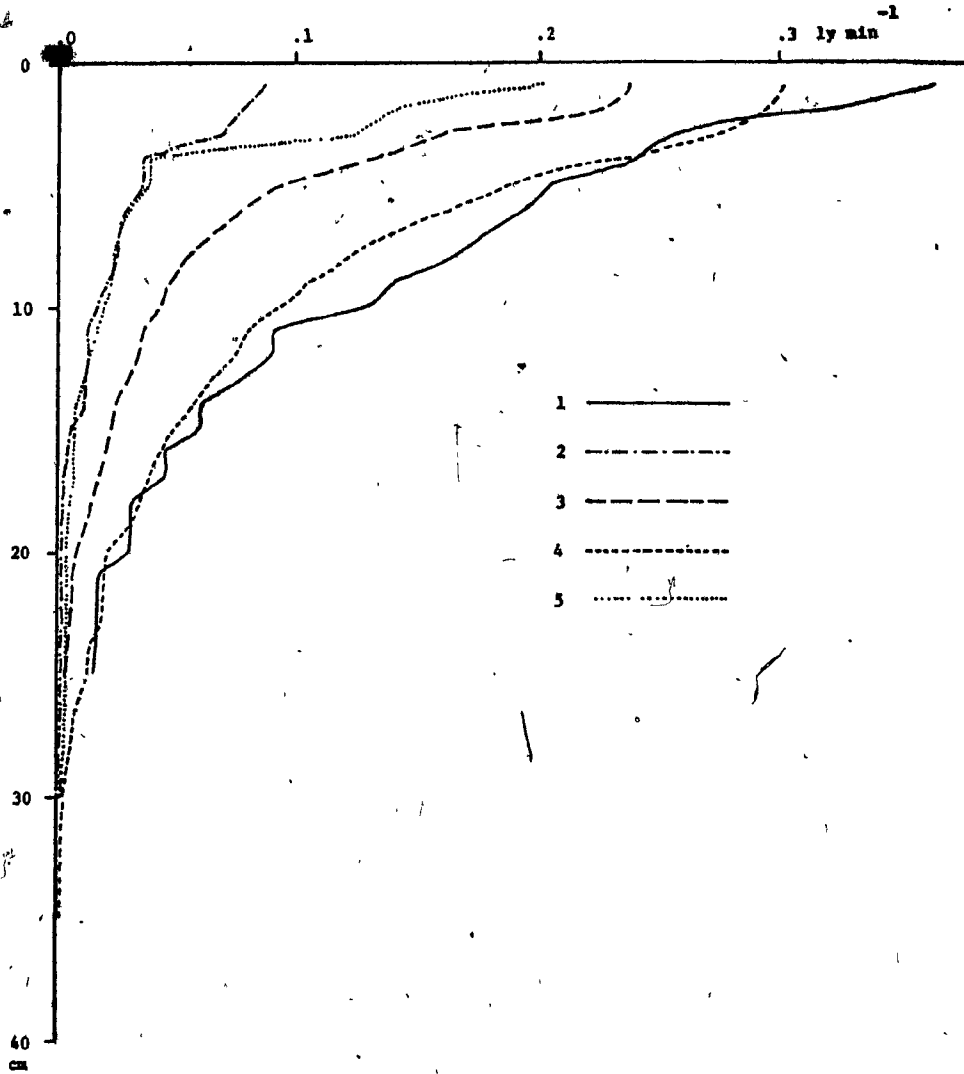


Figure 5. In-snow radiation profiles, Schefferville, Quebec.

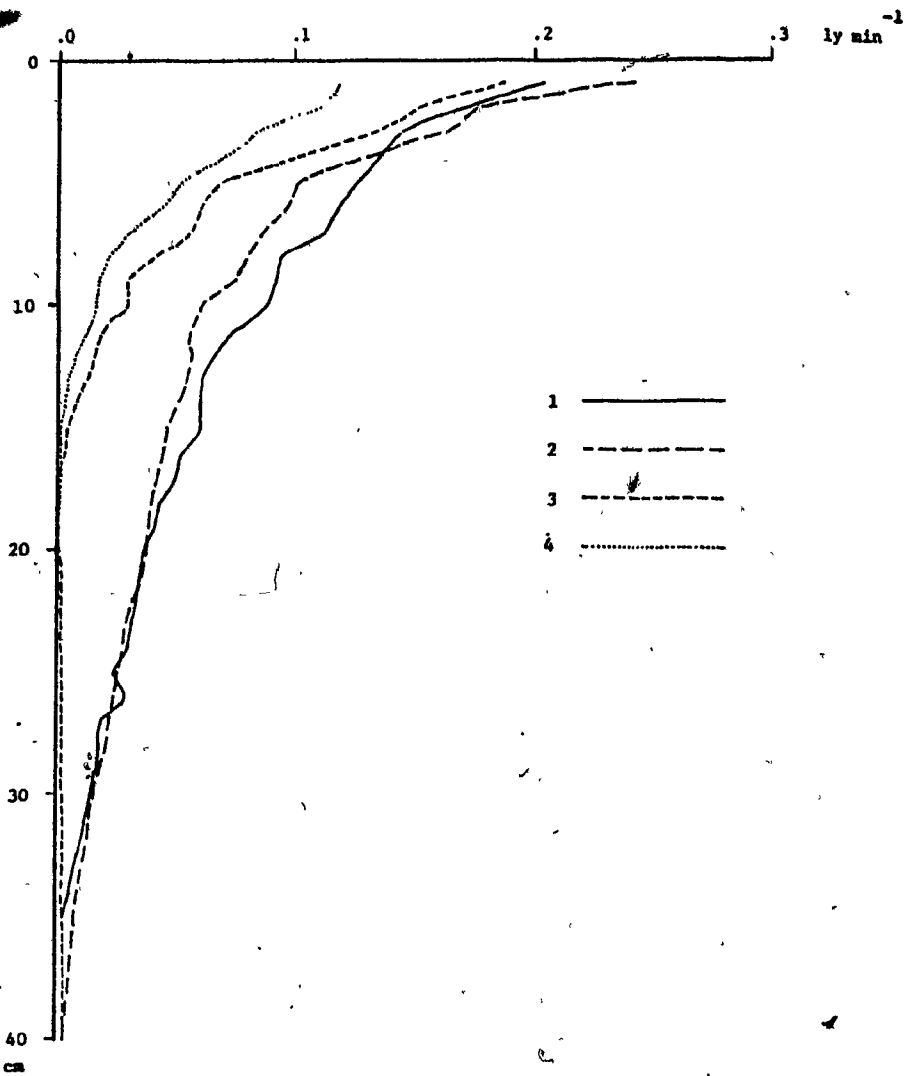


Figure 6. In-snow radiation profiles, Churchill, Manitoba.

(d) Radiation measurements above the snow surface

Net radiation was measured using a Fritschen net radiometer. The radiometer was suspended at a height of approximately 1.25 m above the snow surface, at a distance of 1 m from the snow thermometer.

Reflected solar radiation was measured using an inverted Eppley pyranometer suspended at a height of 1.0 m above the snow surface about 2 m from the snow thermometer.

Global radiation was measured continuously using an Eppley pyranometer. The recorder used was a Science Associates No. 644 pyranometer recorder. The sensor, a permanent installation at the McGill Sub-Arctic Research Station, is located approximately 80 meters from the instrumented site.

(e) Continuous wind measurement

A continuous record of wind velocity was obtained using a conical-cup direct-current generator type anemometer (Science Associates No. 406) at a height of 2.0 m at the instrumented site. The recorder was an Esterline Angus Potentiometric Chart Recorder.

The anemometer has a starting speed of approximately 1 m/s. The output voltage is linear and directly proportional to cup-wheel rotation with an output of 5.0 V (open circuit) at a wind speed of 47 m/s.

(f) Wind profile measurements

Intermittent measurements of wind speeds were made at three levels using anemometers that were manufactured by the author. The bearing assembly and switching mechanism is made by modifying a small 3-pole electric motor. The motor's collector is turned into a switching device by removing the permanent magnets and the rotor winding and by shorting two of the three poles on the rotor. This changes the motor into a rotary switch that switches on and off twice per revolution. The cup assembly is manufactured using a hub, machined from plexiglass. Three hemispherical plastic cups, 55 mm in diameter are suspended on arms of 2 mm carbon steel rod. The radius of the cup assembly is 175 mm.

The three anemometers were each series-connected with a totalizer (Hecon GO 856 002-3) which operates on 12 VDC power and is capable of 20 counts per second. The three counters were connected with a common on-off switch for simultaneous operation of the counters. The anemometers at the instrumented site were connected to the laboratory via a separate, shielded cable as a precaution against electromagnetic interference with signals from other instruments.

Calibration was accomplished by running the three sensors at the same height against the calibrated generating anemometer and against each other. A set of nine anemometers was manufactured and in all nine cases the inter-reproducibility was within plus

or minus 5 per cent over 10 minute runs for individual pairs of sensors at the same height.

Figure 7 shows some wind profiles measured during the experiment. The range in roughness length determined by log-linear extrapolation is from about 0.003 to 0.5 m. There is a marked difference between the roughness lengths measured over the various height intervals. A much lower surface roughness is indicated by the upper interval. No attempt will be made here to assess the cause of this difference. It is not caused by instrumental error, for the anemometers were shifted around when the effect was noticed, and the shifting did not change the results. The temporal trend suggests that the cause may be a stability gradient, but it is also possible that slight spatial variations in surface roughness may have produced the effect.

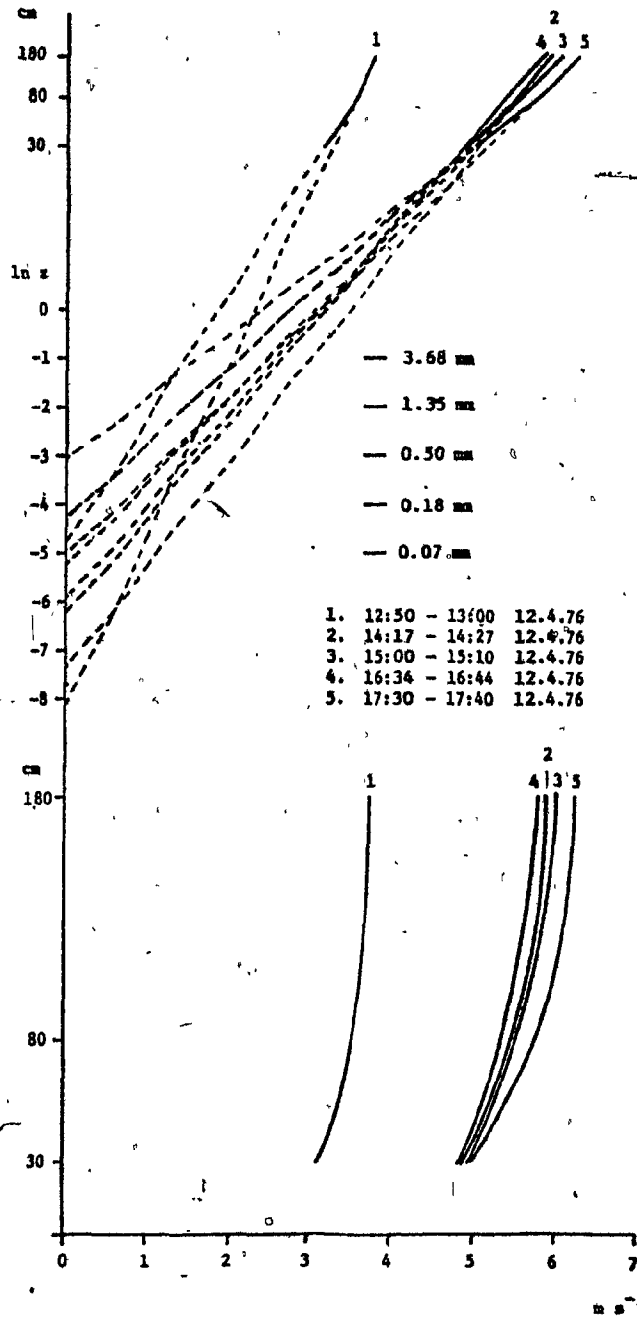


Figure 7. A few wind profiles at the instrumented site

## CHAPTER IV

## FIELD MEASUREMENTS, CALIBRATIONS AND DATA REDUCTION

1. Measurement Schedule

A nine-day continuous set of measurements using the new snow thermometer was obtained from April 12 to April 21, 1976. A heavy snowfall allowed the snow thermometer to be buried by drifting snow backfilling a wide depression in which the snow thermometer was centered. The measurement period ended when one of the junctions in the thermometer yielded to the stress buildup due to snow settling.

The two chart recorders that were used to monitor the snow temperatures were used at different ranges throughout the measurement period. This was necessary because signal strength varied considerably depending on conditions. The measurement error depends somewhat on the range used. Figure 8 shows the times when the recorders were operated at different ranges throughout the survey.

2. Snow Property Monitoring

The requirement of an undisturbed snow cover in the vicinity of the snow thermometer precluded the simultaneous monitoring of snow properties since there was no equipment available for non-destructive monitoring of snow cover changes.

The snow density was measured after the end of the

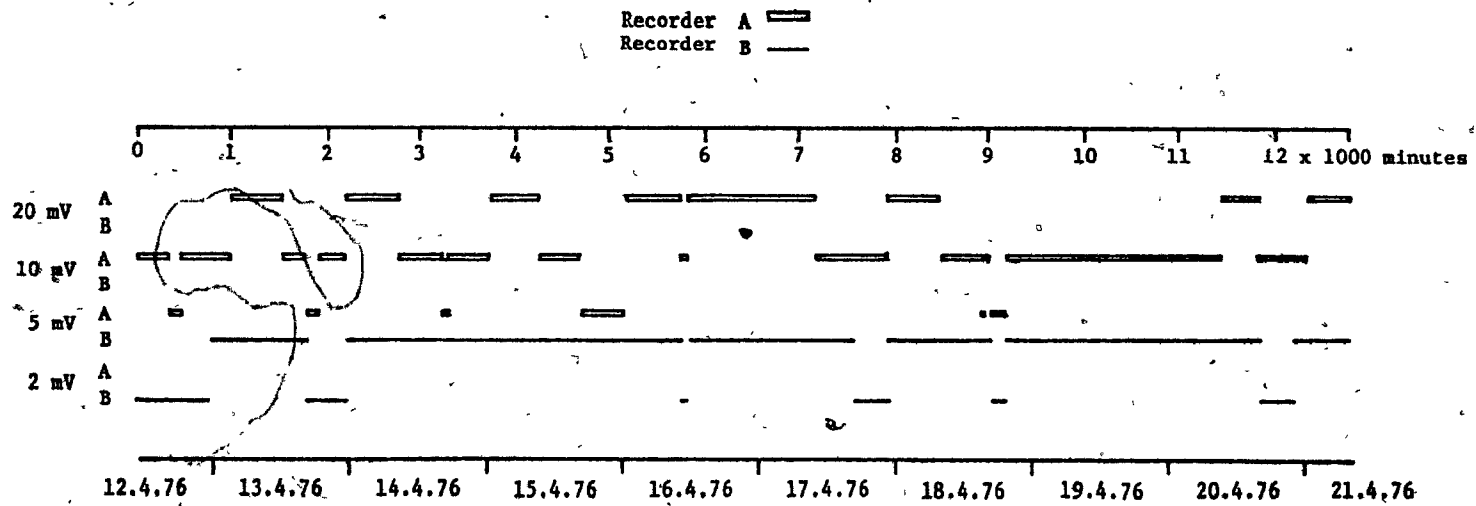


Figure 8. Millivolt ranges used for recorders A and B

measurement period when the thermometer was excavated. Three 250 cc samples were taken at five levels at the snow thermometer site, parallel to the snow thermometer and within 20 cm of it. The density was quite uniform, ranging from 0.21 to 0.25 g/cm<sup>3</sup>. Much of the densification occurred after the end of the measurement period, before the snow thermometer was excavated. The most probable density range during the period of measurement is 0.16 to 0.20 g/cm<sup>3</sup>.

The snow cover at the site may be characterized as a moderately fragmented wind slab. It consisted of fine-grained snow of low air permeability throughout its depth. The snow cover lacked the basal layers of highly permeable depth hoar that are normally found in seasonal snow covers of similar depth.

### 3. Meteorological Events Recorded by the Schefferville (A) Weather Station

The weather events recorded by the Schefferville (A) weather station are shown in Figure 9. Although the period of measurement is relatively short it encompasses a fair variety of weather events. Three frontal systems moved through the area during the period. The first was an occluded system moving south of the field area on April 13. The second, which exhibited a fairly typical warmfront-coldfront situation moved through during April 14 - April 16. The third, of which the low pressure center passed north of Schefferville caused some snow surface melt

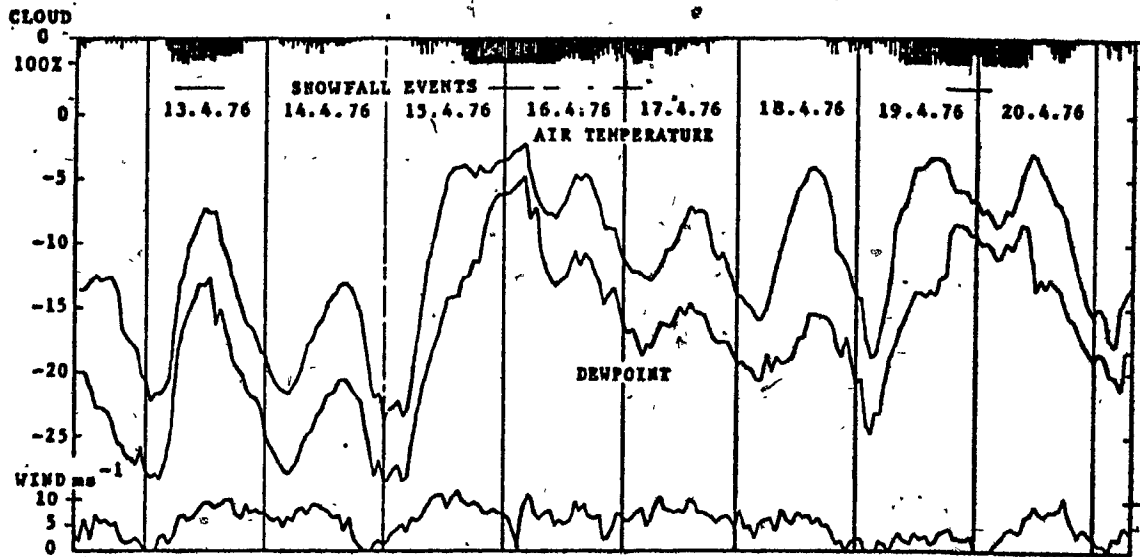


Figure 9. Weather events as recorded by the Schefferville (A) meteorological station during the measurement period.

during the passage of the warm sector on April 20. The screen temperature, however, did not exceed 0 degrees Celsius throughout the period.

The screen instrumentation is standard for A.E.S. Class A stations. The screen temperature is measured using a remotely sensed thermistor. The lithium chloride dewpoint cell is also sensed remotely from the weather station. It is described in the Atmospheric Environment Instrument Manual No. 32. According to A.E.S. personnel at Schefferville the dewpoint system performed normally throughout the survey period. Unfortunately, the continuous wind recorder at the meteorological station had broken down before the measurement period. Therefore the windspeeds indicated in Figure 9 are observer estimates from the windspeed dial instead of the wind chart.

#### 4. Recorder accuracy and reading accuracy

The signals from the different instruments were recorded onto charts and thence transferred to computer cards for the analysis. Errors are added to the signal in both of these steps. The manufacturer quotes a recording accuracy for the recorders used of 0.5 per cent of full span and a dead band of 0.25 per cent. A full scale reading of 150 mm on the 10 mV scale corresponds to a temperature difference of 12.5 degrees C for the snow thermometer. The accuracy with which this temperature difference is recorded is thus plus or minus 0.065 degrees C.

Similarly, the error due to the dead band is 0.031 C on the 10 mV scale. On the 2 mV scale it is 0.006 degrees C with the present snow thermometer. For the snow surface temperature sensor the accuracy on the 10 mV scale is 0.25 degrees C per temperature difference of 12.5 degrees C between the snow surface and the reference thermistor. The error due to the dead band is 0.13 degrees C on the 10 mV scale and 0.06 degrees C on the 2 mV scale. The overall effect of the dead band is to reduce somewhat the sensitivity of the recorder to minor fluctuations in the input signal.

The charts were analysed using a transparent ruler with subdivisions to the nearest half millimeter. The charts were read to the nearest 0.1 mm which is about 0.06 per cent of full scale or about one order of magnitude better than the nominal recorder accuracy. The field accuracy of the thermometric instrumentation is discussed further in Chapter V.

The charts were analysed for 10 minute intervals between observations throughout the period. Except for the radiation measurements, the rates of change in the parameters measured were not sufficiently great to seriously affect the assumption of simultaneity of measurement. Where the rate of change is high, such as in the case of near-surface snow temperature gradients, the scan was arranged so that the level nearest to the surface was measured first and then the subsequent two levels on one recorder while the second recorder simultaneously scanned the

three levels farther down. The on-time for each instrument was six seconds.

#### 5. Reference Thermistor Readings

The resistances of the two reference thermistors were measured at approximately hourly intervals, though from time to time longer intervals were necessitated by the absence of the observer. The thermistors were calibrated at the Earth Physics Branch of the Dominion Observatory in Ottawa to an absolute accuracy better than plus or minus 0.01 degrees C.

It was assumed that the change in temperature at the reference level could be reasonably represented by a least squares semi-linear approximation between temperature measurements. This assumption was valid for the calibration thermistor cavity for the air and snow surface temperatures, which was of high thermal inertia. For the snow thermometer reference, however, it will be shown that this assumption was not valid.

#### 6. Calibrations

Imperfections, and slight variations in alloy composition and differences in the method of manufacturing can cause individual copper-constantan thermocouples to vary their electromotive force by as much as 2 per cent. Due to their designs, the snow thermometer and the air and snow surface

thermometers are somewhat difficult to calibrate. The nominal output per pair of junctions is 0.039 mV per degree C, which for the snow thermometer gives a nominal output of 0.78 mV per degree C. For the snow surface temperature and the lowest air temperature sensor the outputs are 0.2 mV per degree C. Since all of these instruments were manufactured from the same batch of thermocouple wire and the junctions were made in a similar manner for all instruments and were manufactured by the same person, similarity between the different instruments could reasonably be assumed. In addition, the multi-junction design would tend to average out individual variations.

The brief event of surface melt between 9 and 11 hrs on April 20 indicated that the calibration factor supplied by the manufacturer could be used directly. There is a slight non-linearity in the relationship between temperature difference and electromotive force. The error introduced by this non-linearity is about +2 degrees C for a temperature of -25 degrees C when the reference is at +25 degrees C, an insignificant error for the purpose of this study. Since the reference was usually at between -5 and -10 degrees C, and the lowest temperature extreme was about -28 degrees C, no correction was applied.

#### 7. Wind Chart Analysis

In this study it was necessary to have information about the

character of the wind for the interval over which thermal changes were measured. In particular, wind speed and wind speed variation data were regarded as essential; the first because it indicates the wind stress at the surface and the second because it indicates accelerations and decelerations and thus pressure gradients within the flow. It was assumed that the turbulence recorded at 2 m above the site is indicative of the microscale turbulence that is responsible for snow cover ventilation. This assumption may not be valid under the sometimes extreme stability conditions occurring over snow.

(a) Method of analysis

The wind chart was marked at intervals synchronous with the scan intervals. Each 10-minute period was subdivided into 20 intervals of 30 seconds each. The maximum and minimum wind speed in each 30-second interval was recorded and punched onto computer cards for further analysis.

Average wind speed,  $U_{mean}$ , over each 10-minute period was computed by

$$U_{mean} = \left( \sum_{i=1}^N (U_{xi} + U_{ni}) / 2 \right) / N \quad 4.1$$

where  $U_{xi}$  is the maximum wind speed in the 30-second interval,  $i$ .

$U_{ni}$  is the minimum wind speed in the 30-second interval,  $i$ .

and  $N$  is the number of 30-second intervals.

The average wind speed range,  $R_{mean}$ , over each 10-minute period was computed by

$$R_{mean} = \frac{\sum_{i=1}^N (U_{xi} - U_{ni})}{N}.$$

4.2



## CHAPTER V

## ANALYSIS OF THE SNOW TEMPERATURE MEASUREMENTS

1. Snow Temperature Gradients

The temperature differences over the different depth intervals in the snow cover are shown in Figure 10. The time interval between measurements is 10 minutes.

The elevation of the snow surface varied from about 45 to about 40 cm above the reference throughout the period of measurement. The greatest decrease in surface elevation occurred on April 12, the first day of measurement, and was caused by initial settlement of the snow deposit. Subsequent variations in surface elevation were slight. Some snowfall occurred during the measurement period, accompanied by snow drifting, but these events did not change the depth of snow by more than one to two cm. The temperature differences measured at the uppermost level thus occur at a depth of 5 cm or more below the snow surface. Figure 10 also shows the first and second derivatives of the temperature gradients.

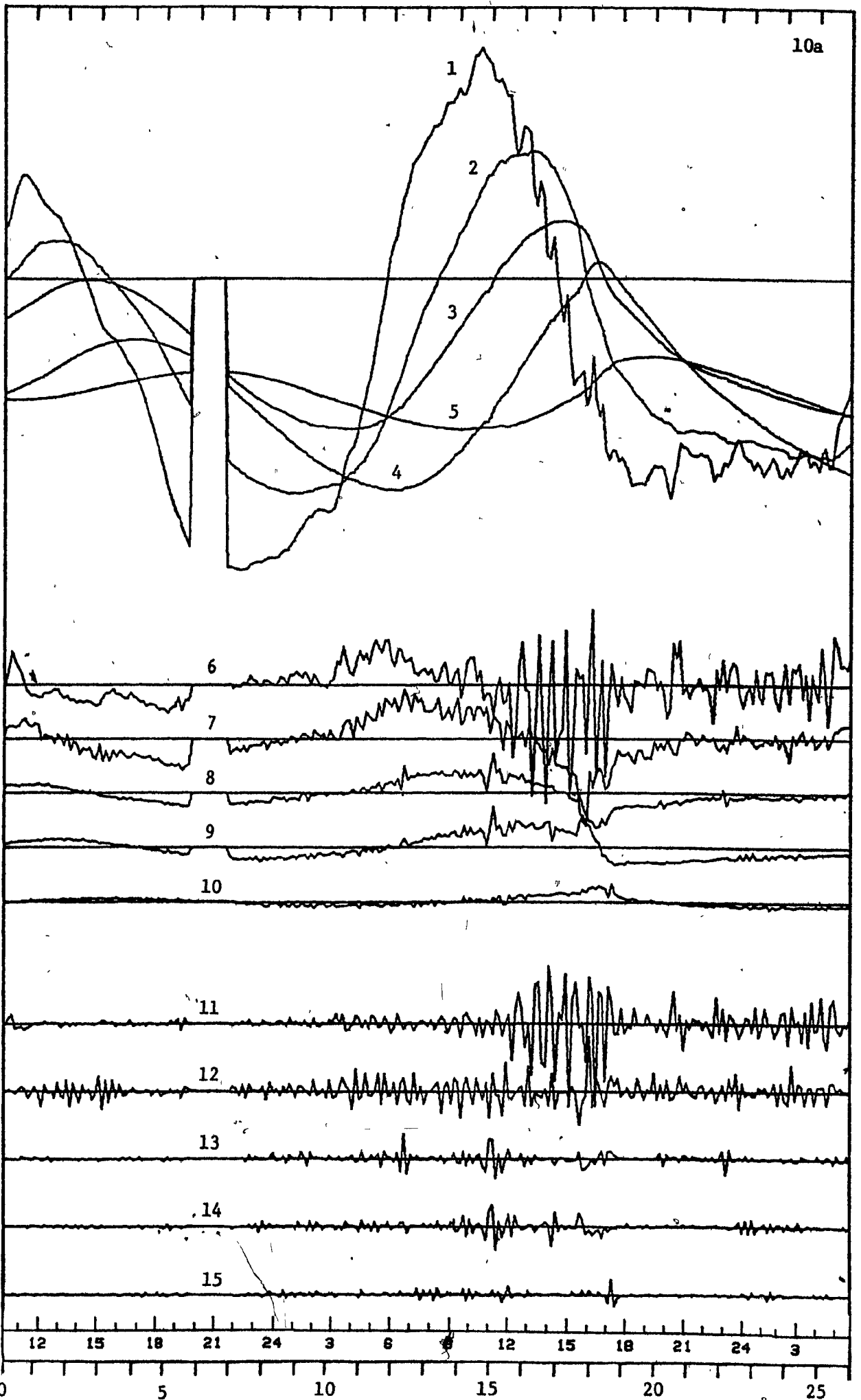
To estimate the noise inherent in the measurements through errors in recording and data reduction, readings were taken at one-minute intervals to obtain the record shown in Figure 11. In comparison to the readings taken at 10-minute intervals (Figure 10), this figure shows an essentially smooth line at the lowest level, where real changes in temperature over one-minute

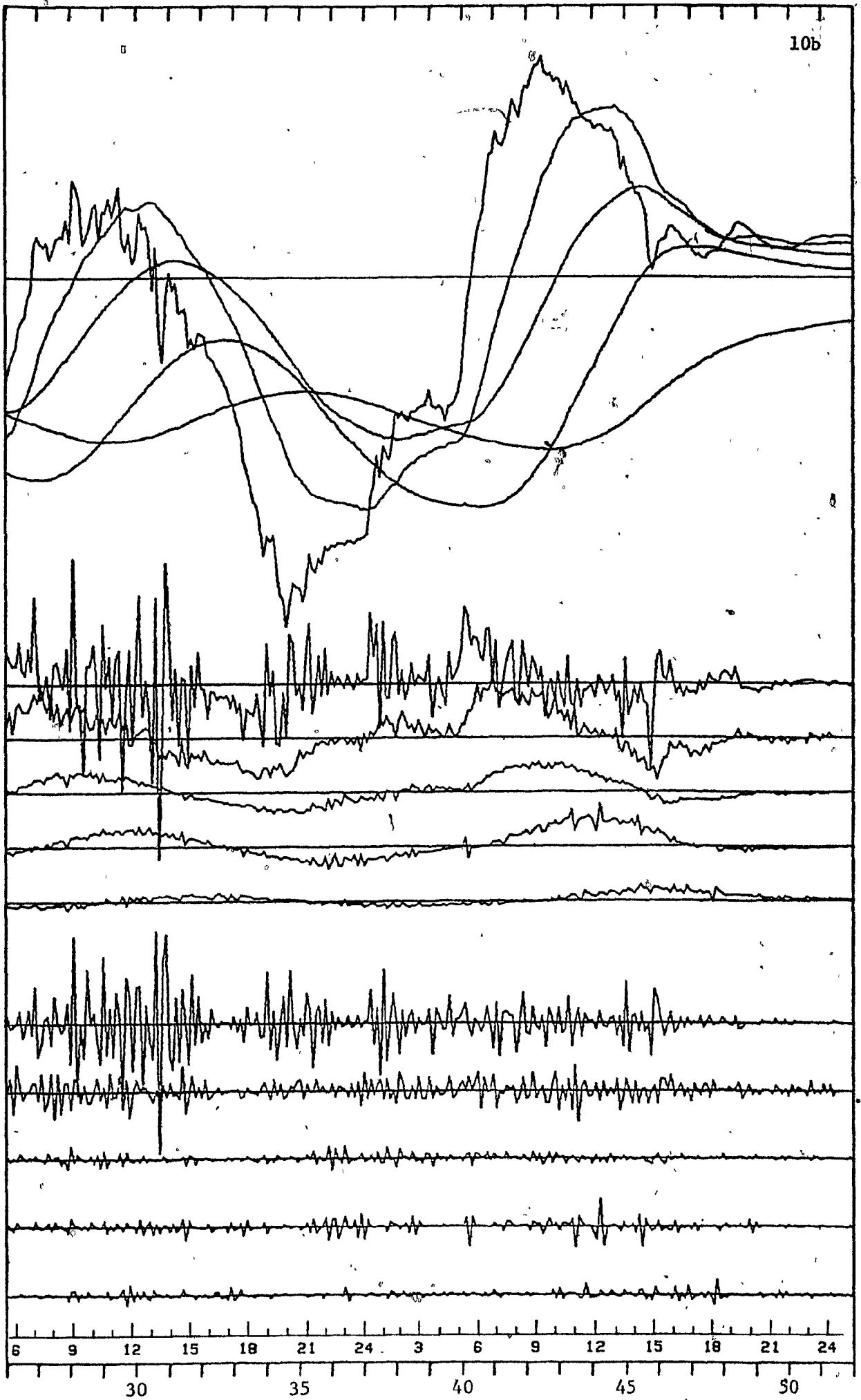
Figure 10. Temperature differences over different depth intervals and their first and second time derivatives.

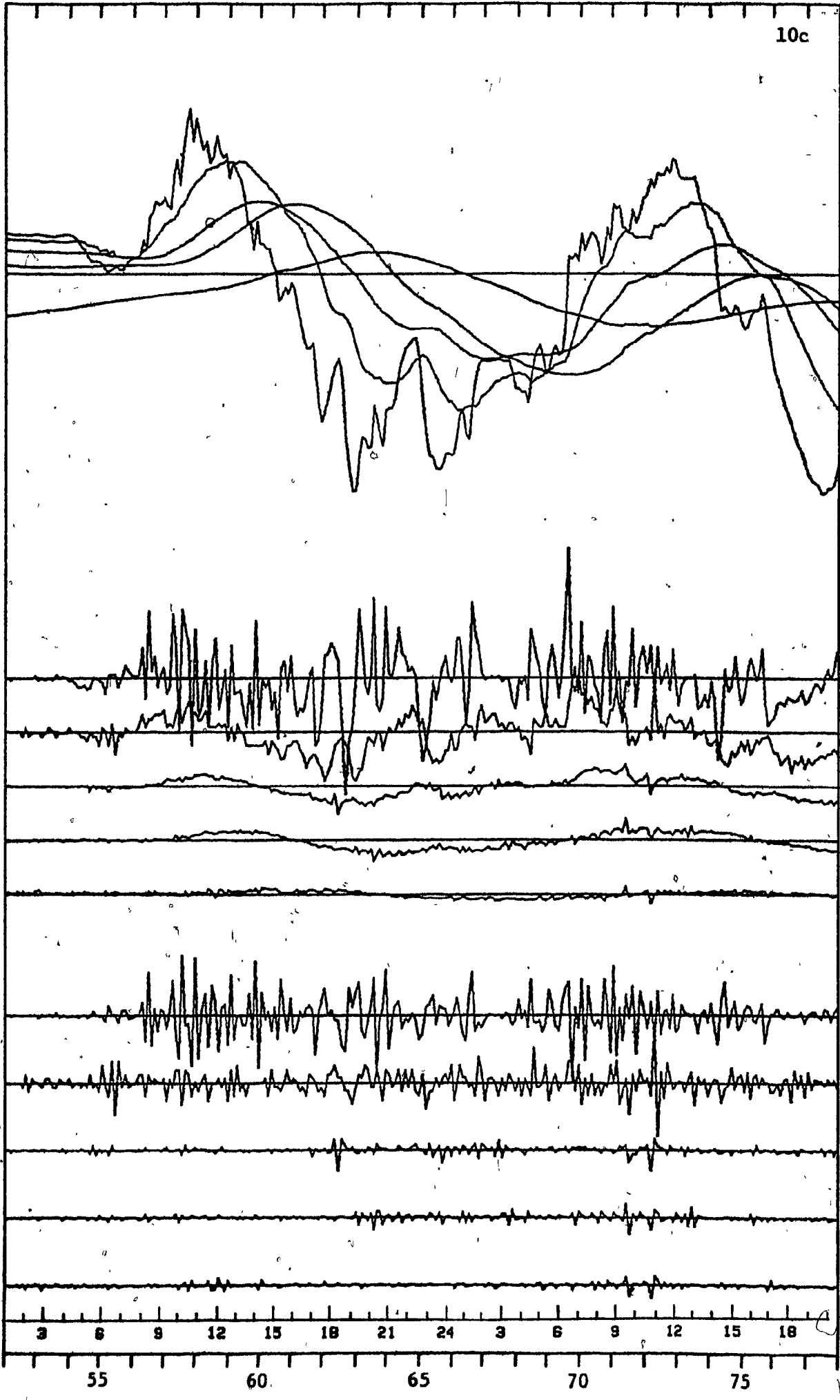
(a.r. - above reference)

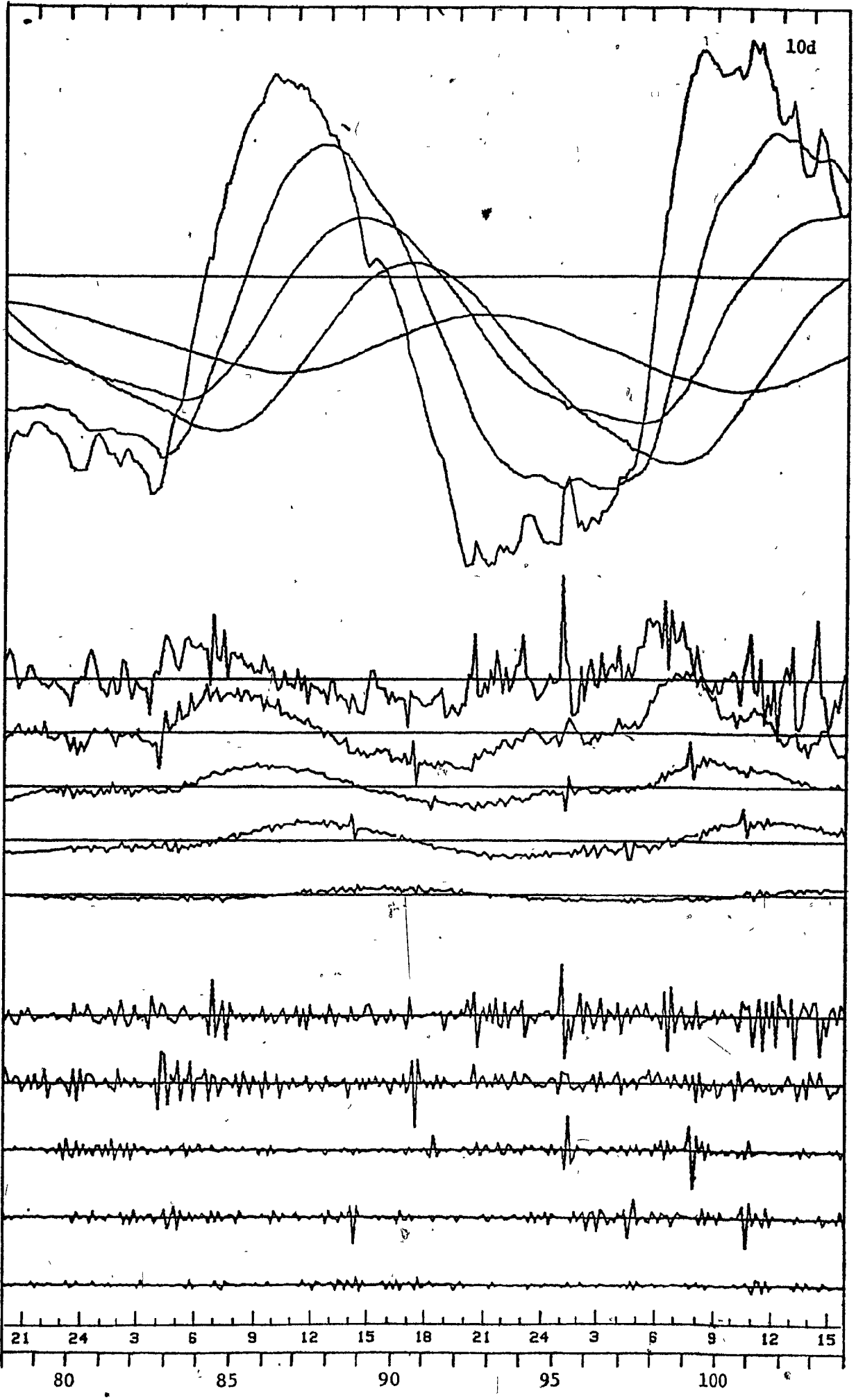
	<u>Scale</u>
1. Temperature difference 35 cm a.r. to 30 cm a.r.	1 inch - 2.0 °C
2. Temperature difference 30 cm a.r. to 25 cm a.r.	1 inch - 2.0 °C
3. Temperature difference 25 cm a.r. to 20 cm a.r.	1 inch - 2.0 °C
4. Temperature difference 20 cm a.r. to 10 cm a.r.	1 inch - 2.0 °C
5. Temperature difference 10 cm a.r. to reference	1 inch - 2.0 °C
6. First derivative of 1.	1 inch - 1.0 °C
7. First derivative of 2.	1 inch - 0.5 °C
8. First derivative of 3.	1 inch - 0.5 °C
9. First derivative of 4.	1 inch - 0.5 °C
10. First derivative of 5.	1 inch - 0.5 °C
11. Second derivative of 1.	1 inch - 2.0 °C
12. Second derivative of 2.	1 inch - 0.5 °C
13. Second derivative of 3.	1 inch - 0.5 °C
14. Second derivative of 4.	1 inch - 0.5 °C
15. Second derivative of 5.	1 inch - 0.5 °C

Time interval between measurements is 10 minutes









10e

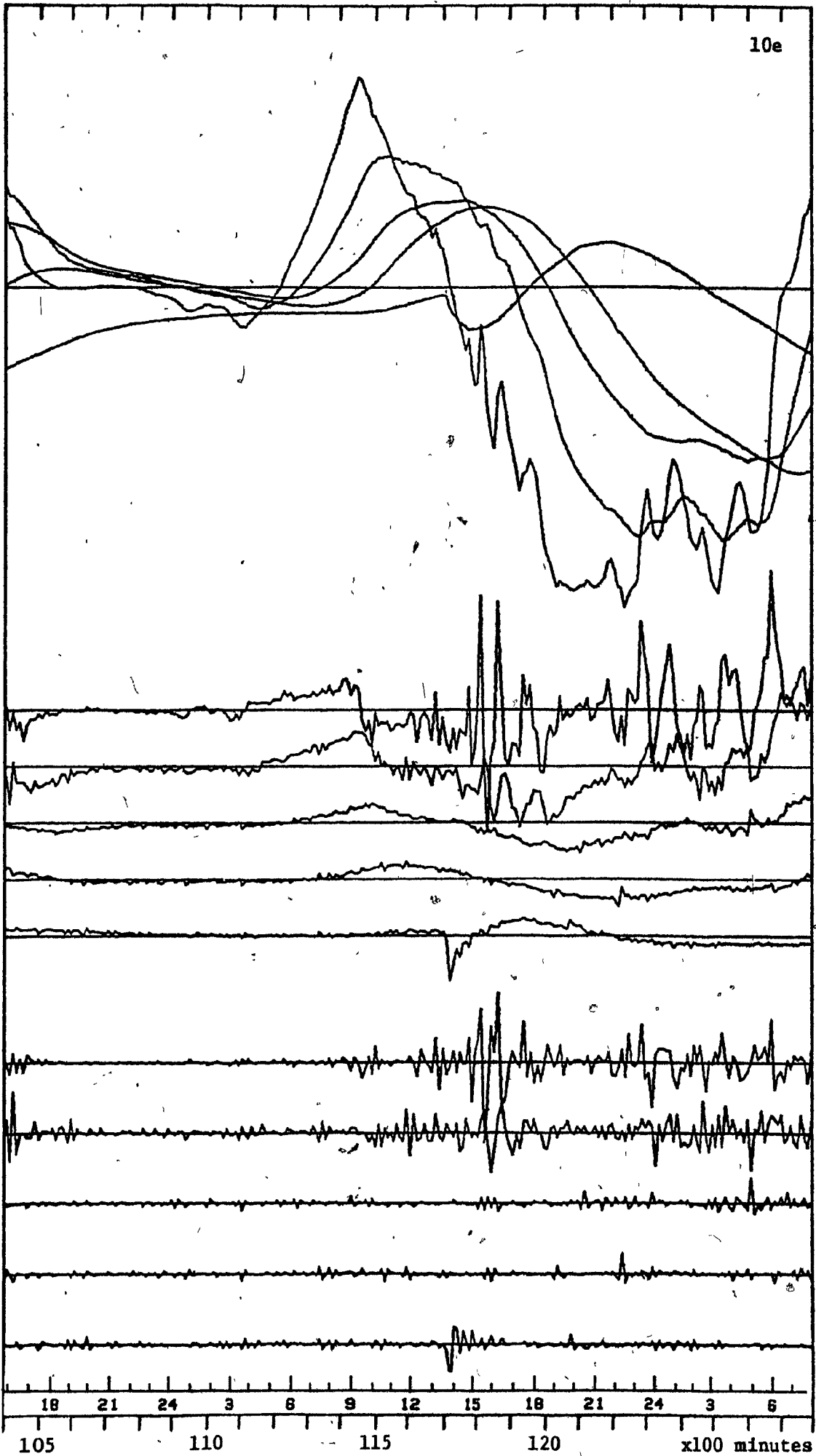


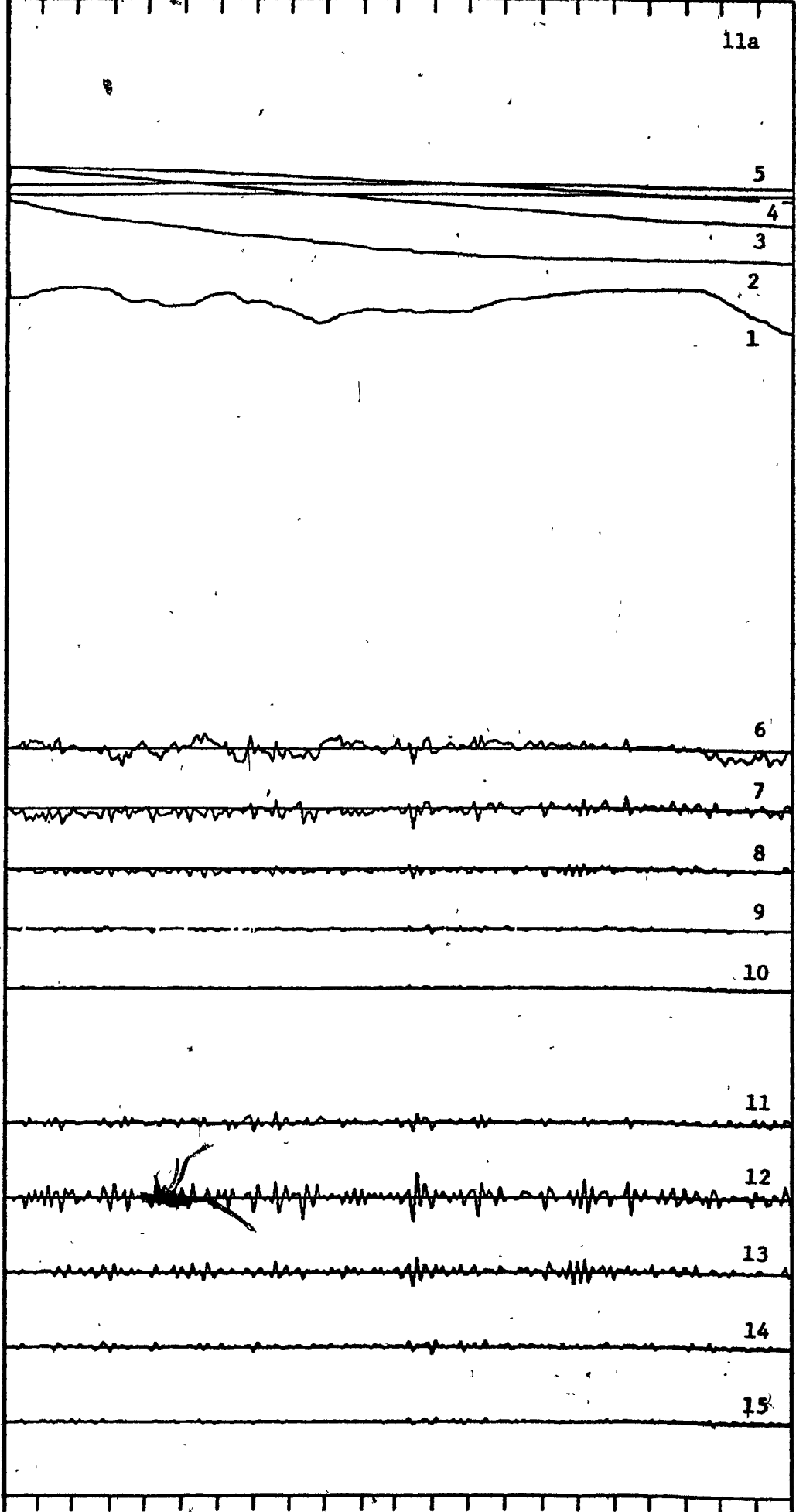
Figure 11. . . Temperature differences between reference level and different levels in the snow cover and their first and second time derivatives (one-minute intervals).

(a.r. - above reference)

	<u>Scale</u>
1. Temperature difference reference to 35 cm a.r.	1 inch - 5.0 °C
2. Temperature difference reference to 30 cm a.r.	1 inch - 5.0 °C
3. Temperature difference reference to 25 cm a.r.	1 inch - 5.0 °C
4. Temperature difference reference to 20 cm a.r.	1 inch - 5.0 °C
5. Temperature difference reference to 10 cm a.r.	1 inch - 5.0 °C
6. First derivative of 1.	1 inch - 1.0 °C
7. First derivative of 2.	1 inch - 0.5 °C
8. First derivative of 3.	1 inch - 0.5 °C
9. First derivative of 4.	1 inch - 0.5 °C
10. First derivative of 5.	1 inch - 0.5 °C
11. Second derivative of 1.	1 inch - 2.0 °C
12. Second derivative of 2.	1 inch - 0.5 °C
13. Second derivative of 3.	1 inch - 0.5 °C
14. Second derivative of 4.	1 inch - 0.5 °C
15. Second derivative of 5.	1 inch - 0.5 °C

Recorders were operating on the 5 mV and 20 mV (lowest accuracy) ranges respectively throughout the measurement period.

11a



5

4

3

2

1

6

7

8

9

10

11

12

13

14

15

630

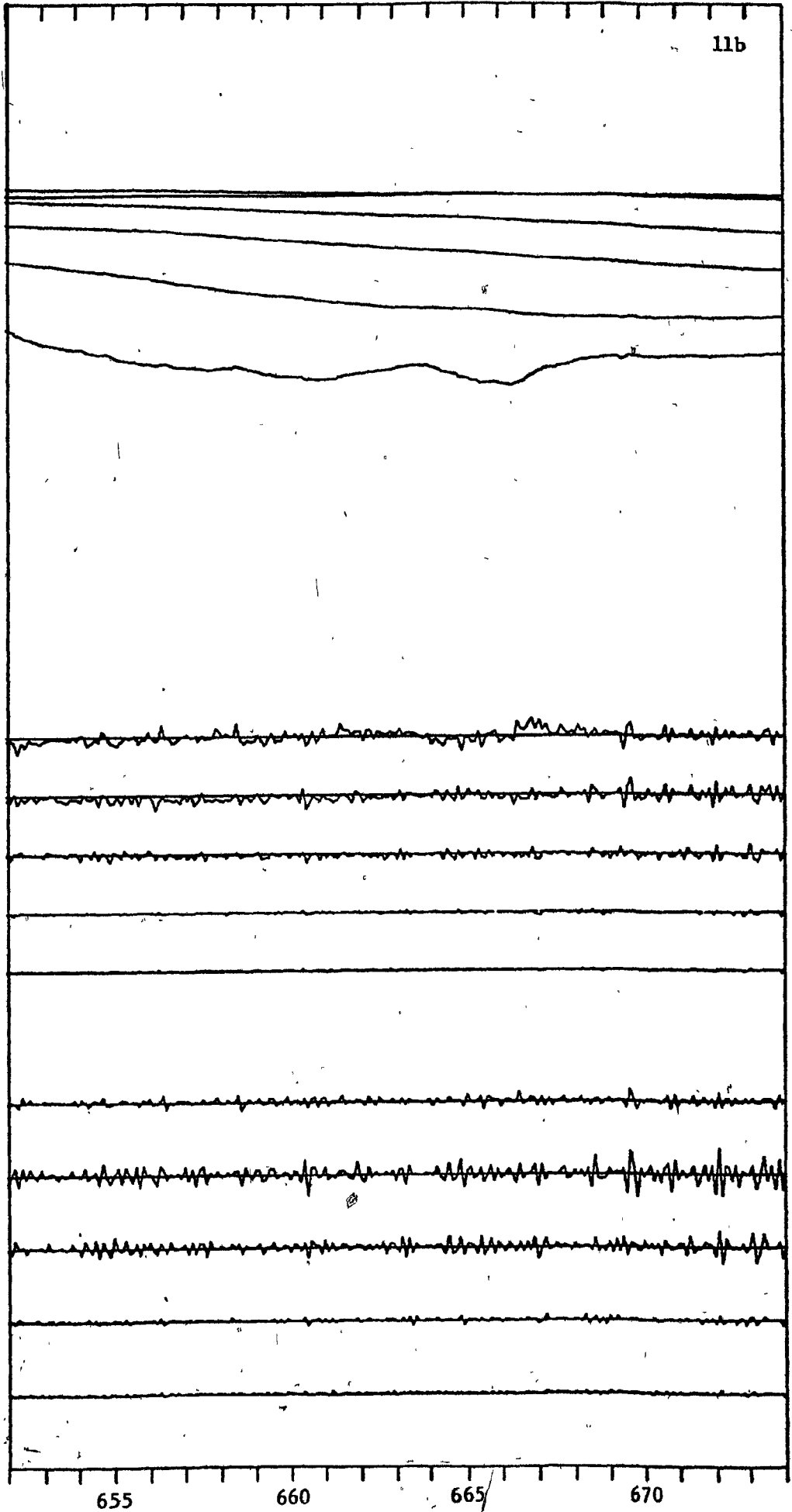
635

640

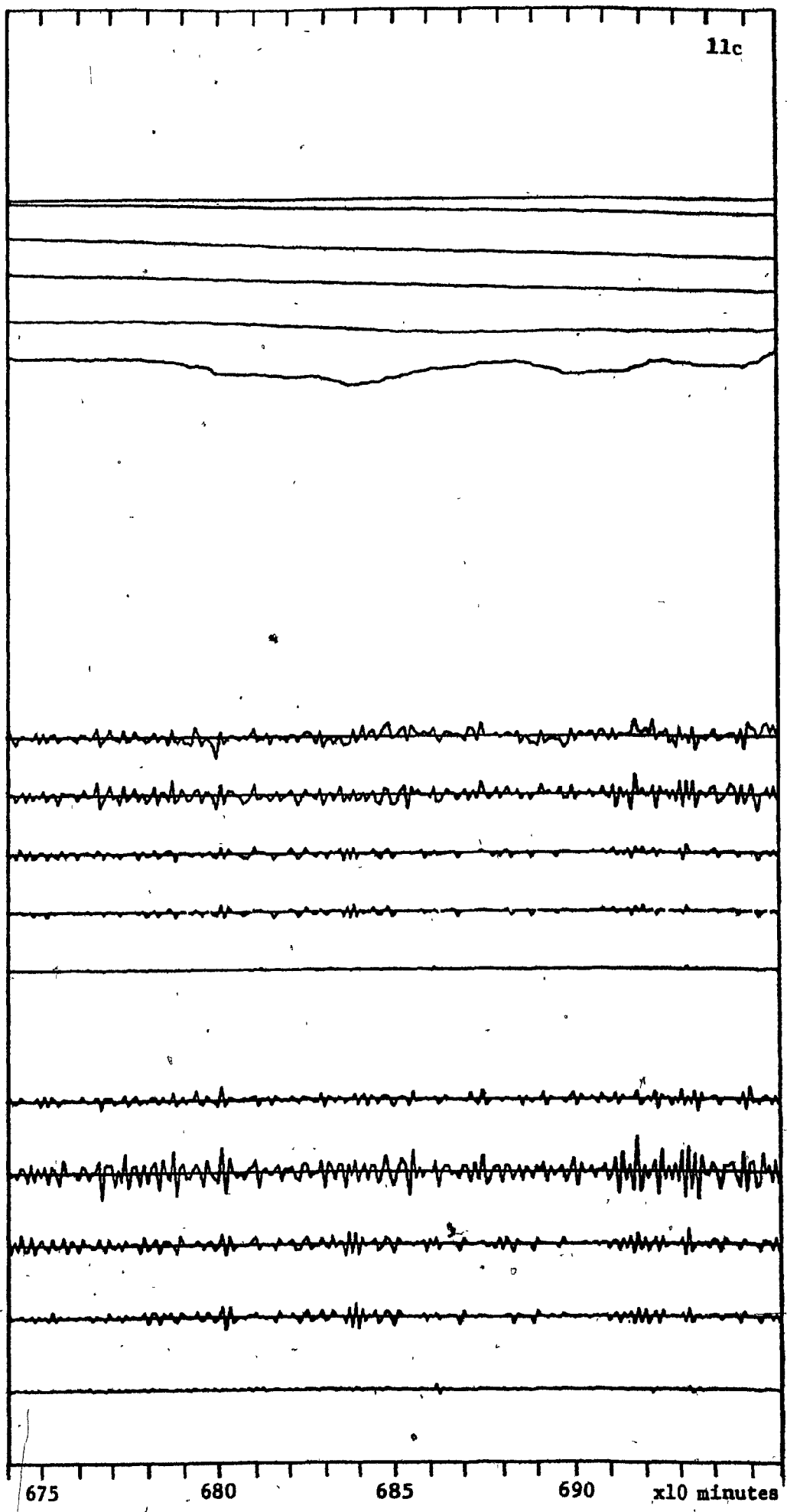
645

650

11b



11c



675 680 685 690 x10 minutes

intervals are slight. Since the same data reduction procedure was used we may conclude that data transfer errors are slight and that the majority of the observable variations represent real thermal events in the snow cover. There is no apparent relation between the variations shown by Figure 10 and the changes in recording ranges shown by Figure 8.

A series of large, rapid temporal variations occurs in the uppermost layer during days when the net radiation also varies strongly (Figure 12). These variations might at first seem to indicate a possible radiation error in the snow thermometer. However, they are about one order of magnitude larger than the computed maximum radiation error. Variations of similar magnitude also occur at night. Therefore it must be the whole snow layer and not just the temperature sensor that heats and cools. The likely causes are variations in radiant absorption and heat transfer by ventilation of the near-surface layers.

## 2. Integrated Snow Temperature Gradients

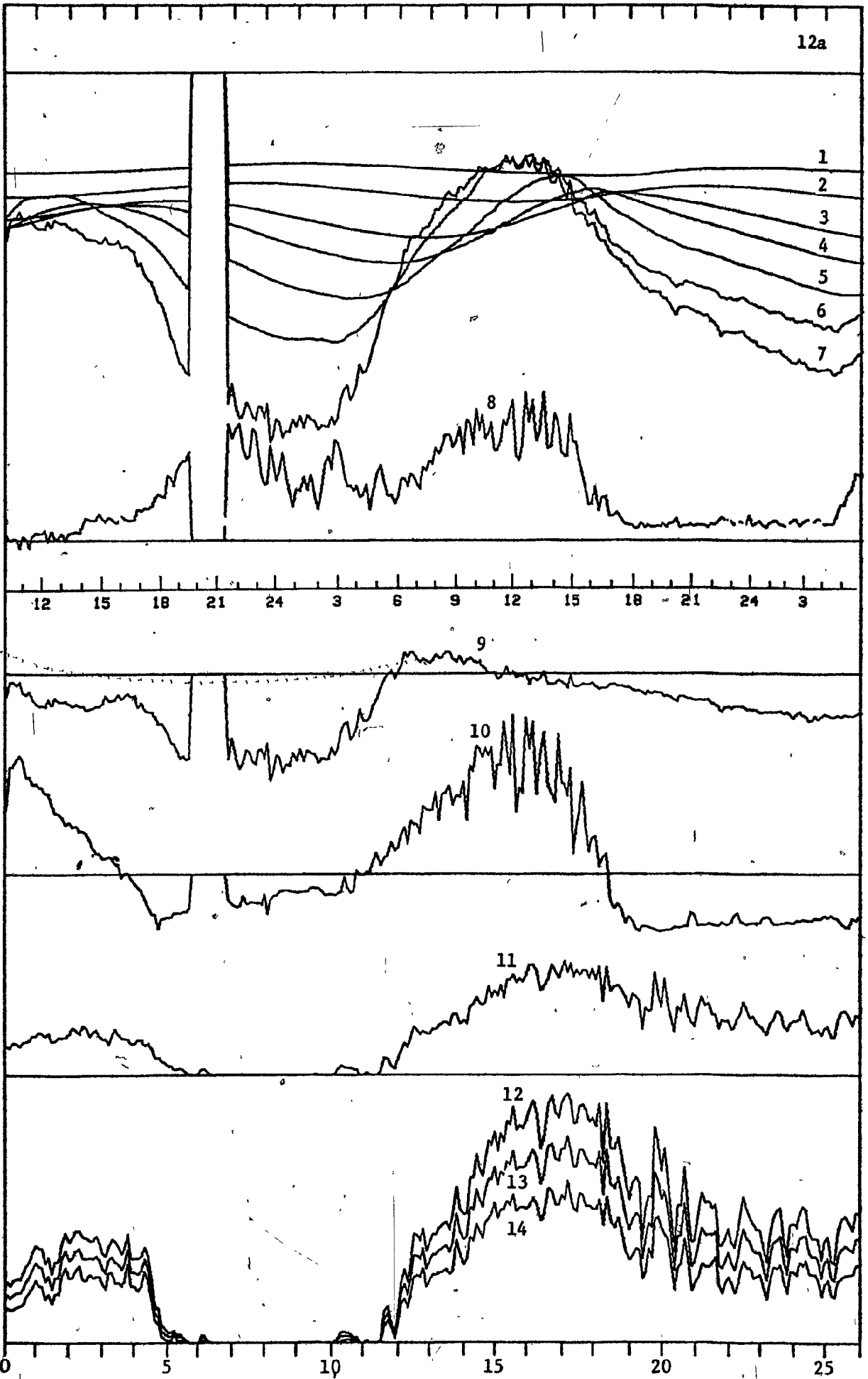
The change in temperature inside a snow cover is not smooth and gradual. This is shown both by Figure 11 and Figure 14. In these figures, the temperature gradients have been integrated over depth to yield snow temperatures with the reference temperature not yet added (snow temperatures with reference temperature included are shown in Figures 12 and 13).

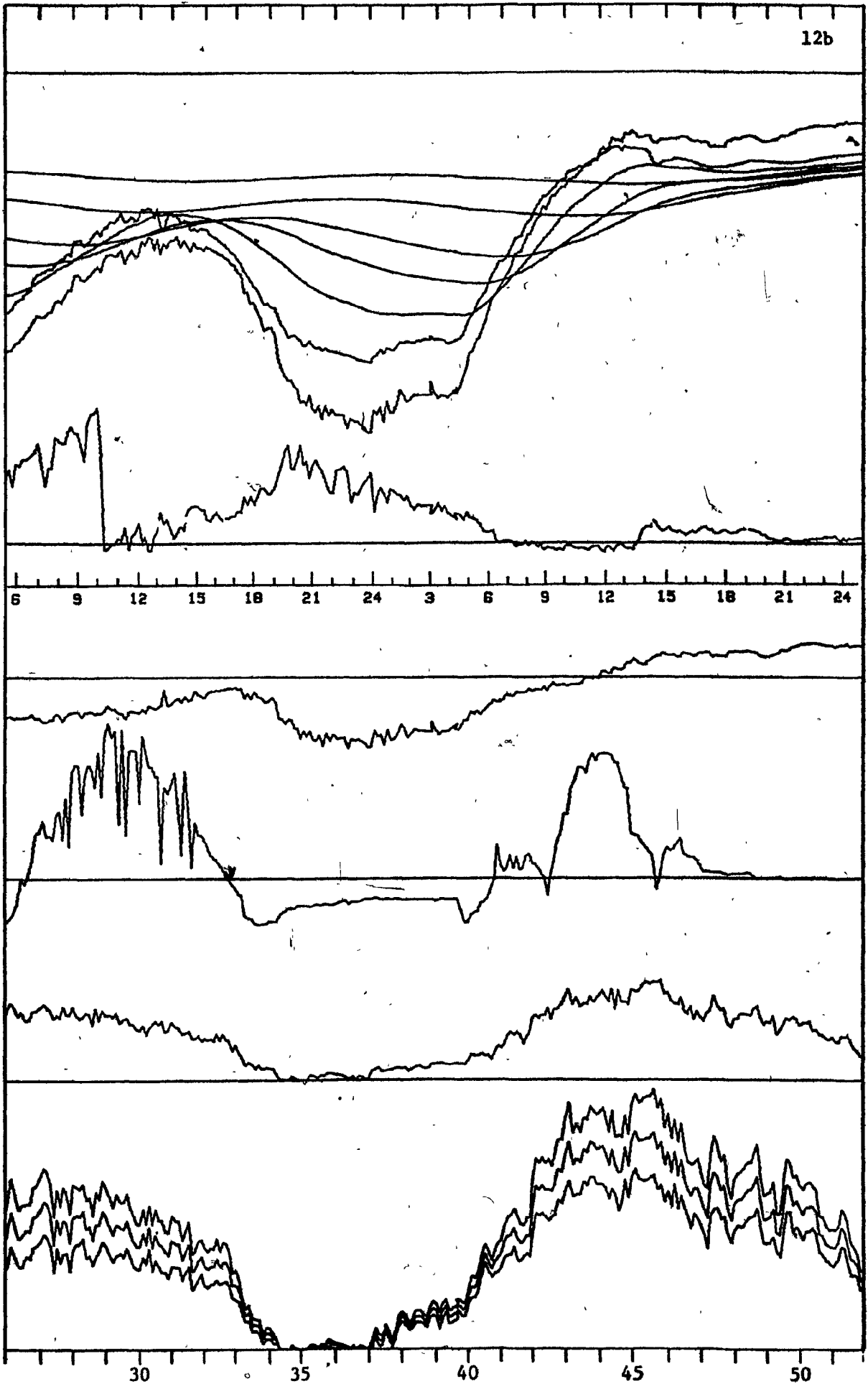
Figure 12. Background data for 10-minute intervals.

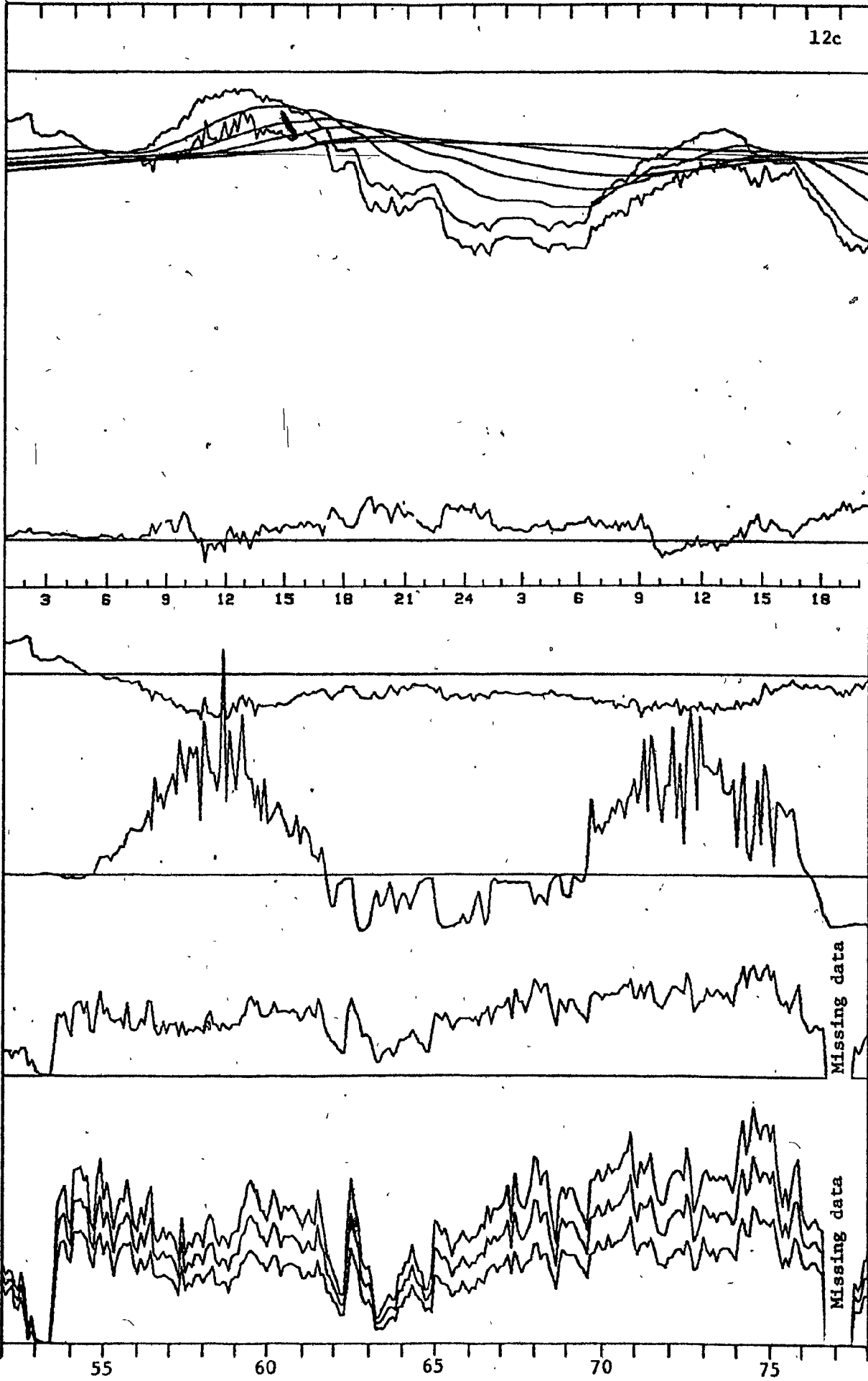
(a.r. - above reference)  
(a.s. - above surface)

	Scale
1. Temperature at reference level	1 inch - 10.0 °C
2. Temperature at 10 cm a.r.	1 inch - 10.0 °C
3. Temperature at 20 cm a.r.	1 inch - 10.0 °C
4. Temperature at 25 cm a.r.	1 inch - 10.0 °C
5. Temperature at 30 cm a.r.	1 inch - 10.0 °C
6. Temperature at 35 cm a.r.	1 inch - 10.0 °C
7. Surface temperature (approximately 40 cm a.r.)	1 inch - 10.0 °C
8. Temperature difference, 30 cm a.s. to surface	1 inch - 5.0 °C
9. Temperature difference, surface to 35 cm a.r.	1 inch - 10.0 °C
10. Net radiation	1 inch - 0.2 ly min <sup>-1</sup>
11. Wind speed range	1 inch - 10.0 m s <sup>-1</sup>
12. Mean maximum wind speed	1 inch - 10.0 m s <sup>-1</sup>
13. Mean wind speed	1 inch - 10.0 m s <sup>-1</sup>
14. Mean minimum wind speed	1 inch - 10.0 m s <sup>-1</sup>

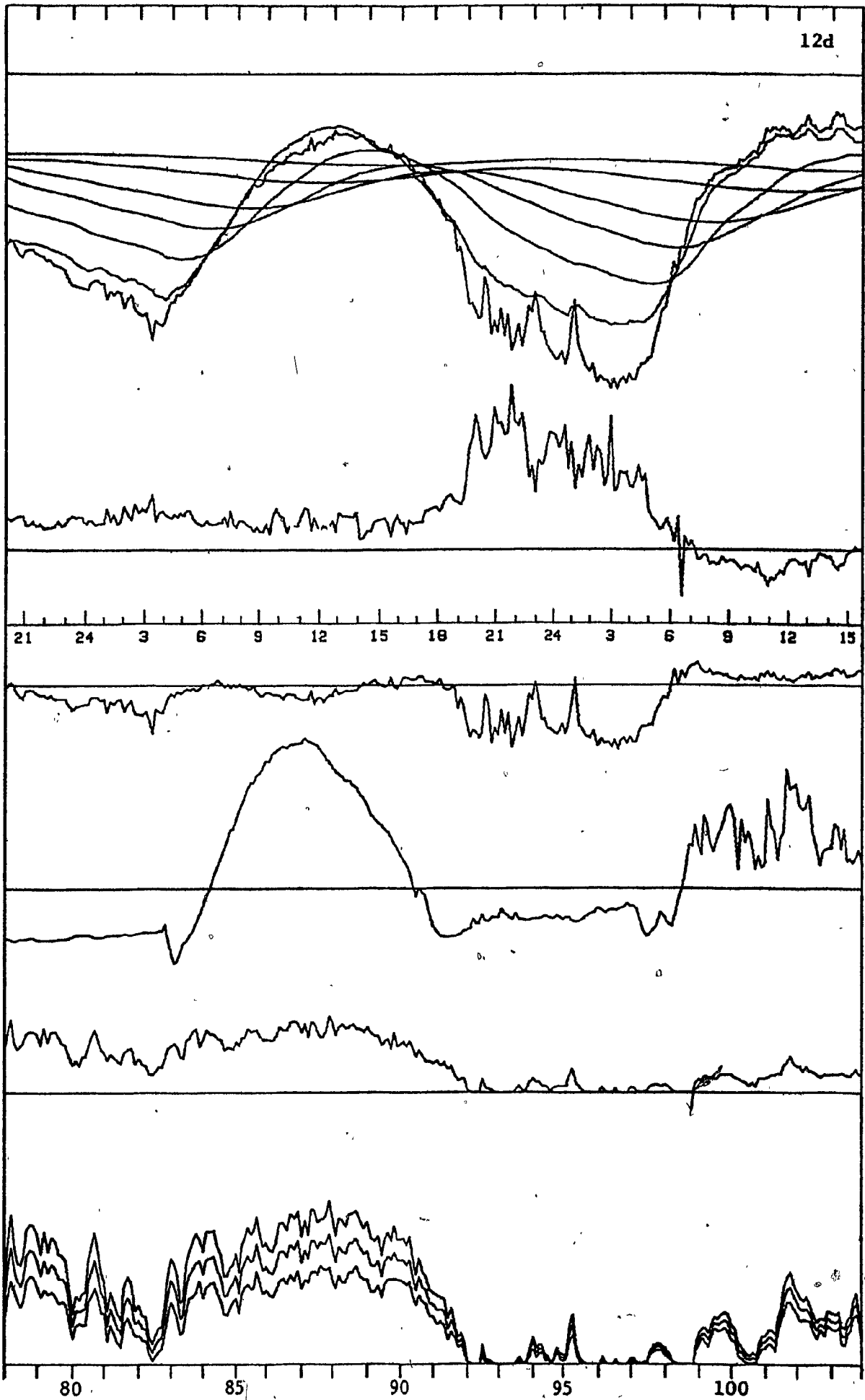
12a







12d



12e

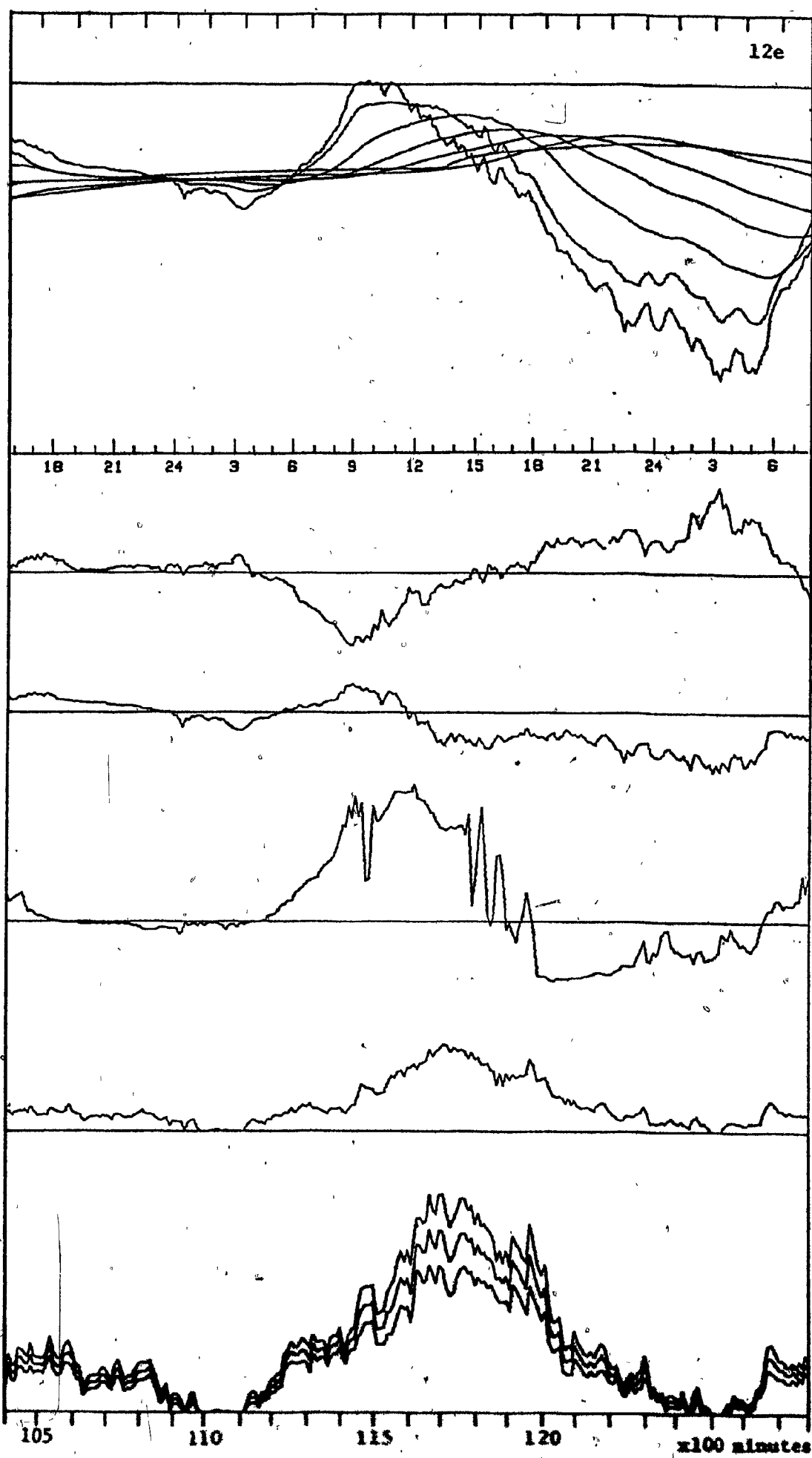
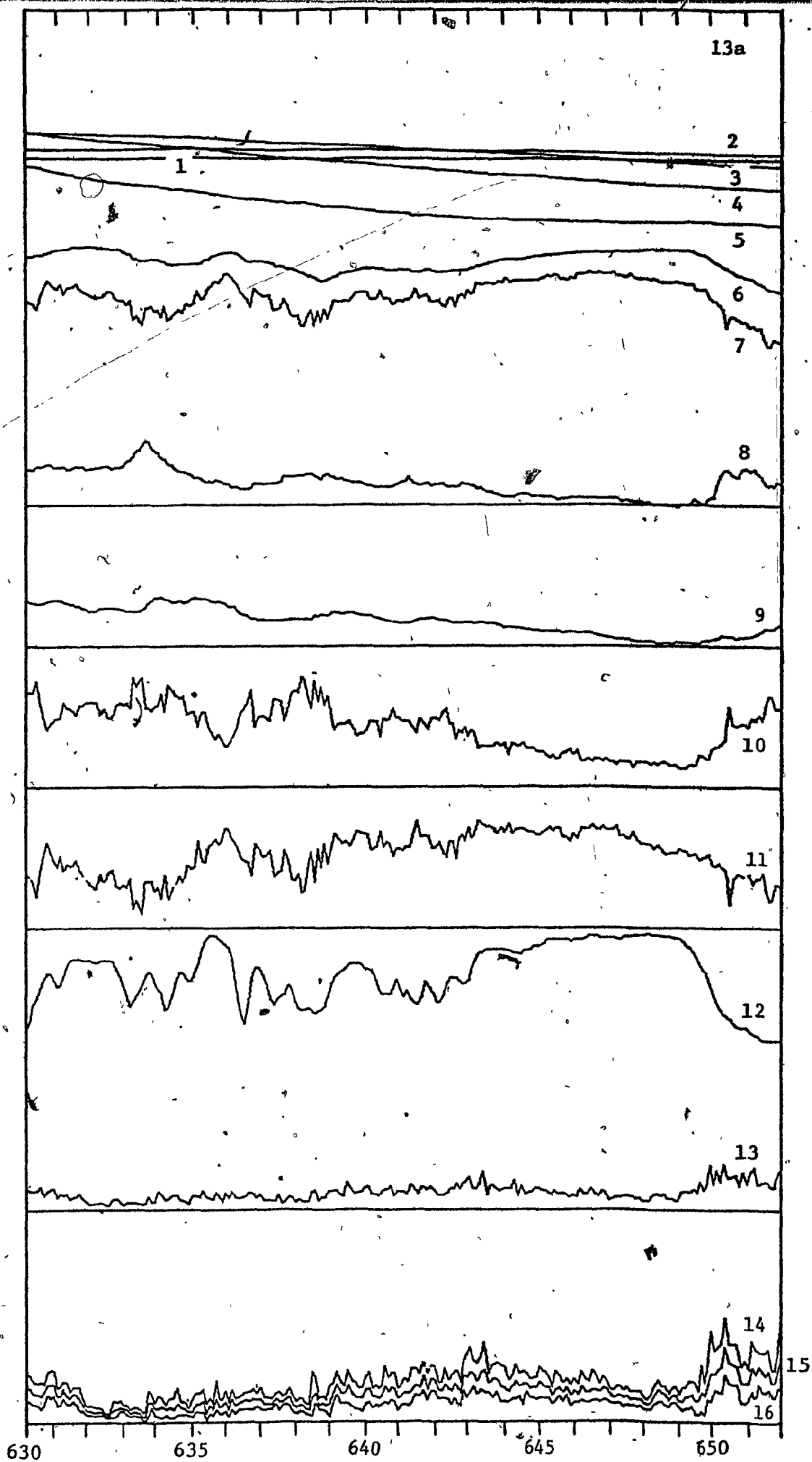
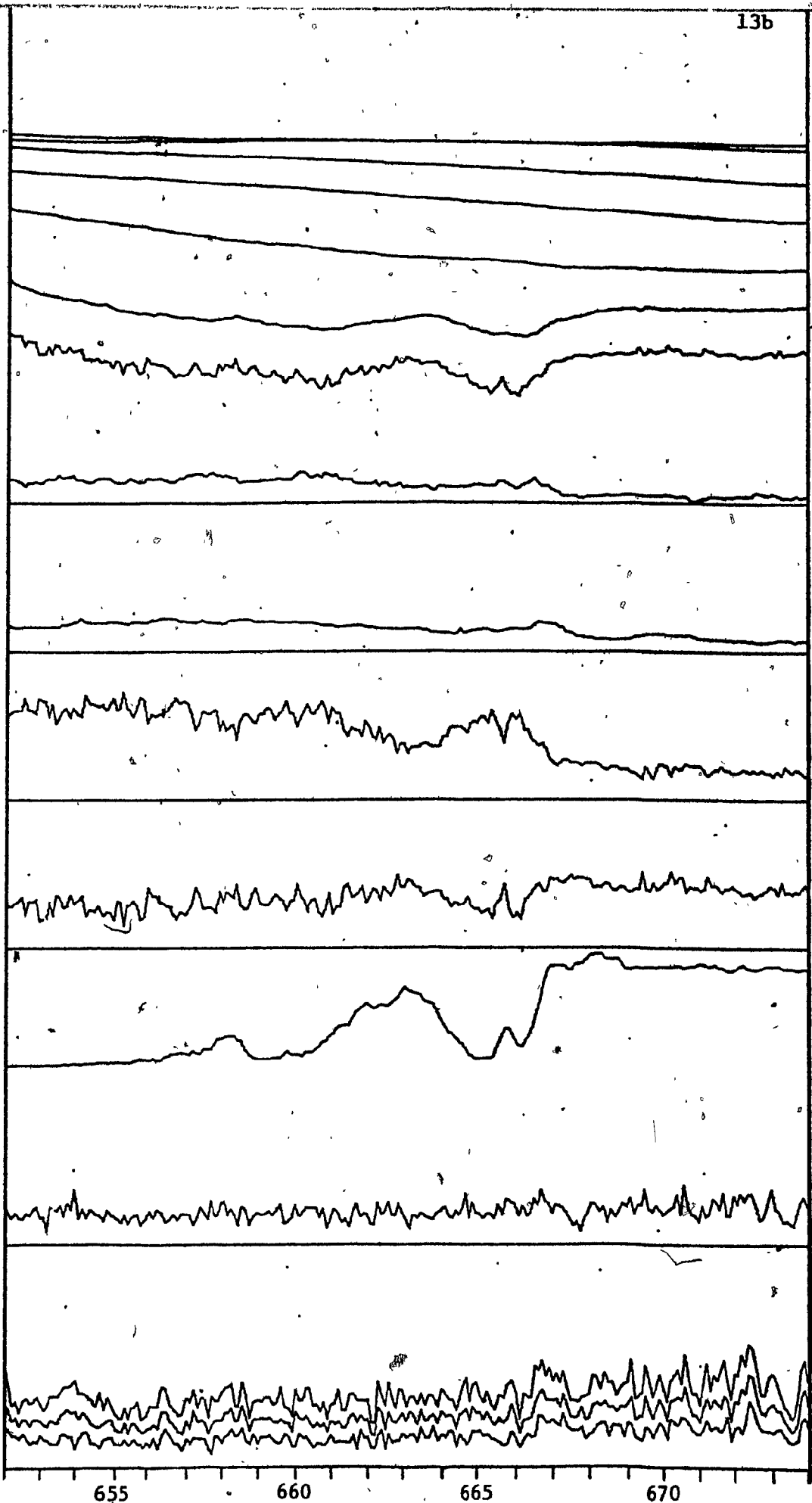


Figure 13. Background data for one-minute intervals.

(a.r. - above reference)  
(a.s. - above surface)

	<u>Scale</u>
1. Temperature at reference level	1 inch - 5.0 °C
2. Temperature at 10 cm a.r.	1 inch - 5.0 °C
3. Temperature at 20 cm a.r.	1 inch - 5.0 °C
4. Temperature at 25 cm a.r.	1 inch - 5.0 °C
5. Temperature at 30 cm a.r.	1 inch - 5.0 °C
6. Temperature at 35 cm a.r.	1 inch - 5.0 °C
7. Surface temperature (approximately 40 cm a.r.)	1 inch - 5.0 °C
8. Temperature difference, 180 cm a.s. to 80 cm a.s.	1 inch - 0.5 °C
9. Temperature difference, 80 cm a.s. to 30 cm a.s.	1 inch - 1.0 °C
10. Temperature difference, 30 cm a.s. to surface	1 inch - 3.0 °C
11. Temperature difference, surface to 35 cm a.r.	1 inch - 3.0 °C
12. Net radiation	1 inch - 0.1 ly min <sup>-1</sup>
13. Wind speed range	1 inch - 10.0 m s <sup>-1</sup>
14. Mean maximum wind speed	1 inch - 10.0 m s <sup>-1</sup>
15. Mean wind speed	1 inch - 10.0 m s <sup>-1</sup>
16. Mean minimum wind speed	1 inch - 10.0 m s <sup>-1</sup>





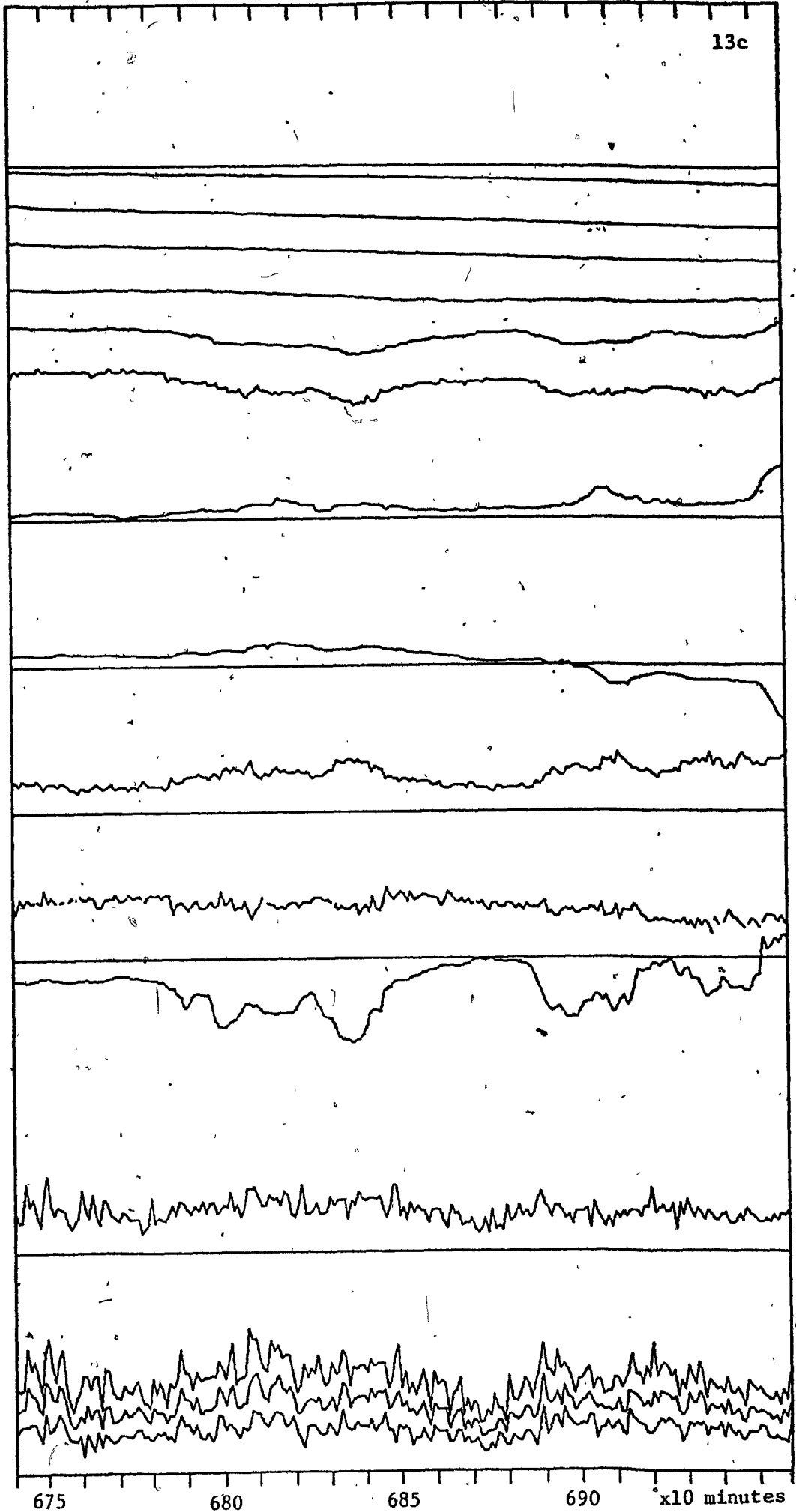
655

660

665

670

13c



675

680

685

690

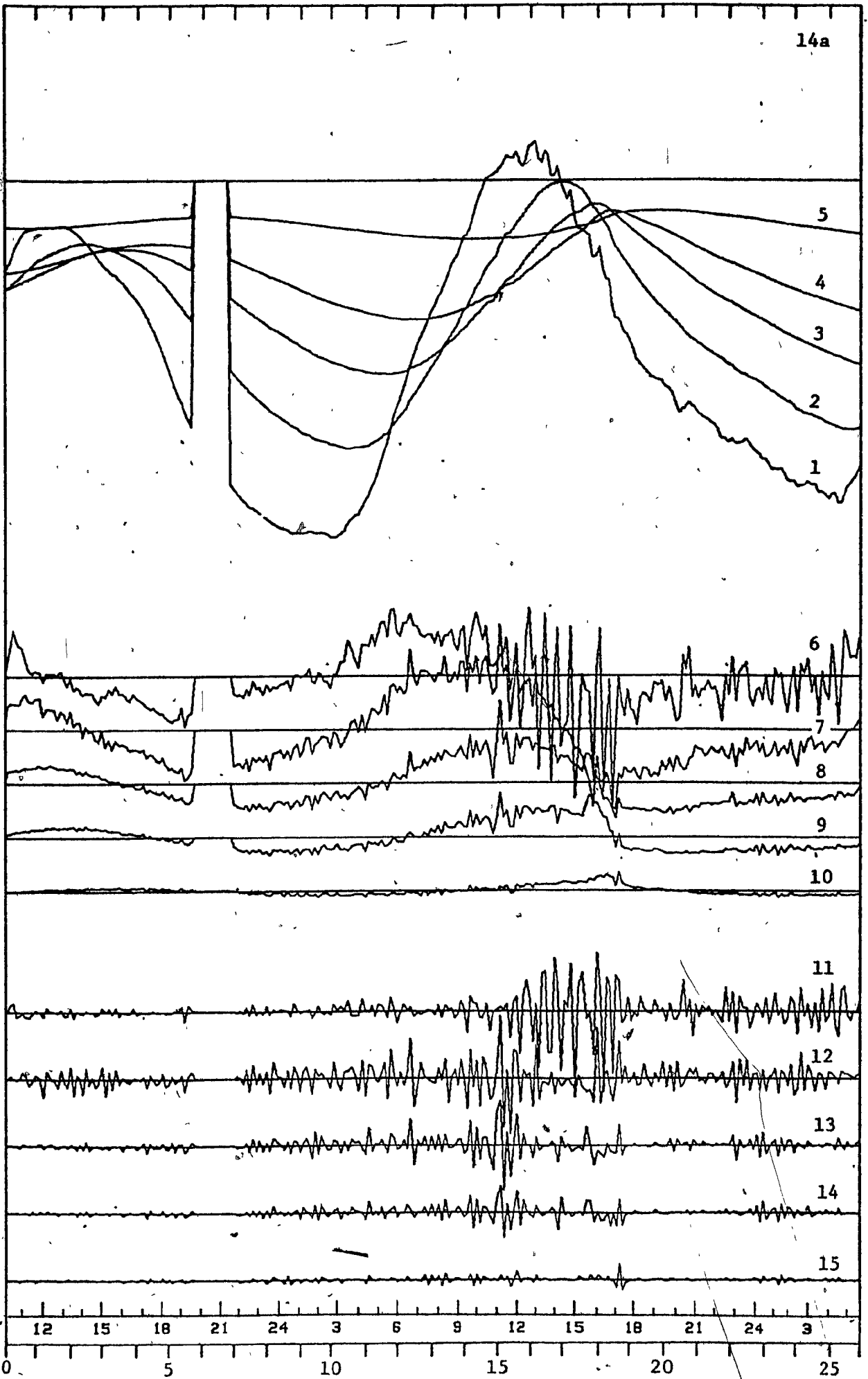
x10 minutes

Figure 14. Temperature differences between reference level and different levels in the snow cover and their first and second time derivatives.

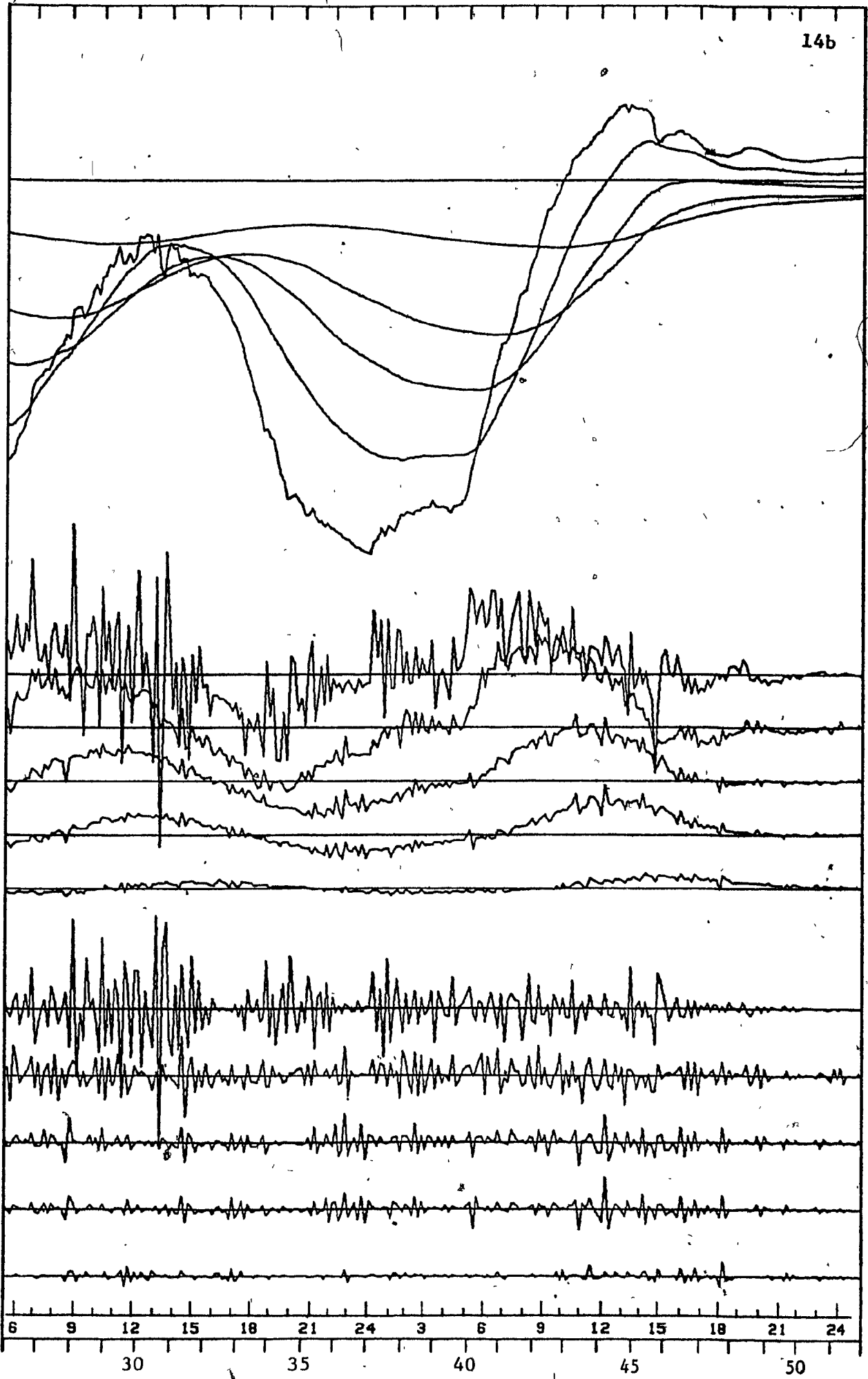
(a.r. - above reference)

	<u>Scale</u>
1. Temperature difference, 35 cm a.r. to reference	1 inch - 5.0 °C
2. Temperature difference, 30 cm a.r. to reference	1 inch - 5.0 °C
3. Temperature difference, 25 cm a.r. to reference	1 inch - 5.0 °C
4. Temperature difference, 20 cm a.r. to reference	1 inch - 5.0 °C
5. Temperature difference, 10 cm a.r. to reference	1 inch - 5.0 °C
6. First derivative of 1.	1 inch - 1.0 °C
7. First derivative of 2.	1 inch - 0.5 °C
8. First derivative of 3.	1 inch - 0.5 °C
9. First derivative of 4.	1 inch - 0.5 °C
10. First derivative of 5.	1 inch - 0.5 °C
11. Second derivative of 1.	1 inch - 2.0 °C
12. Second derivative of 2.	1 inch - 0.5 °C
13. Second derivative of 3.	1 inch - 0.5 °C
14. Second derivative of 4.	1 inch - 0.5 °C
15. Second derivative of 5.	1 inch - 0.5 °C

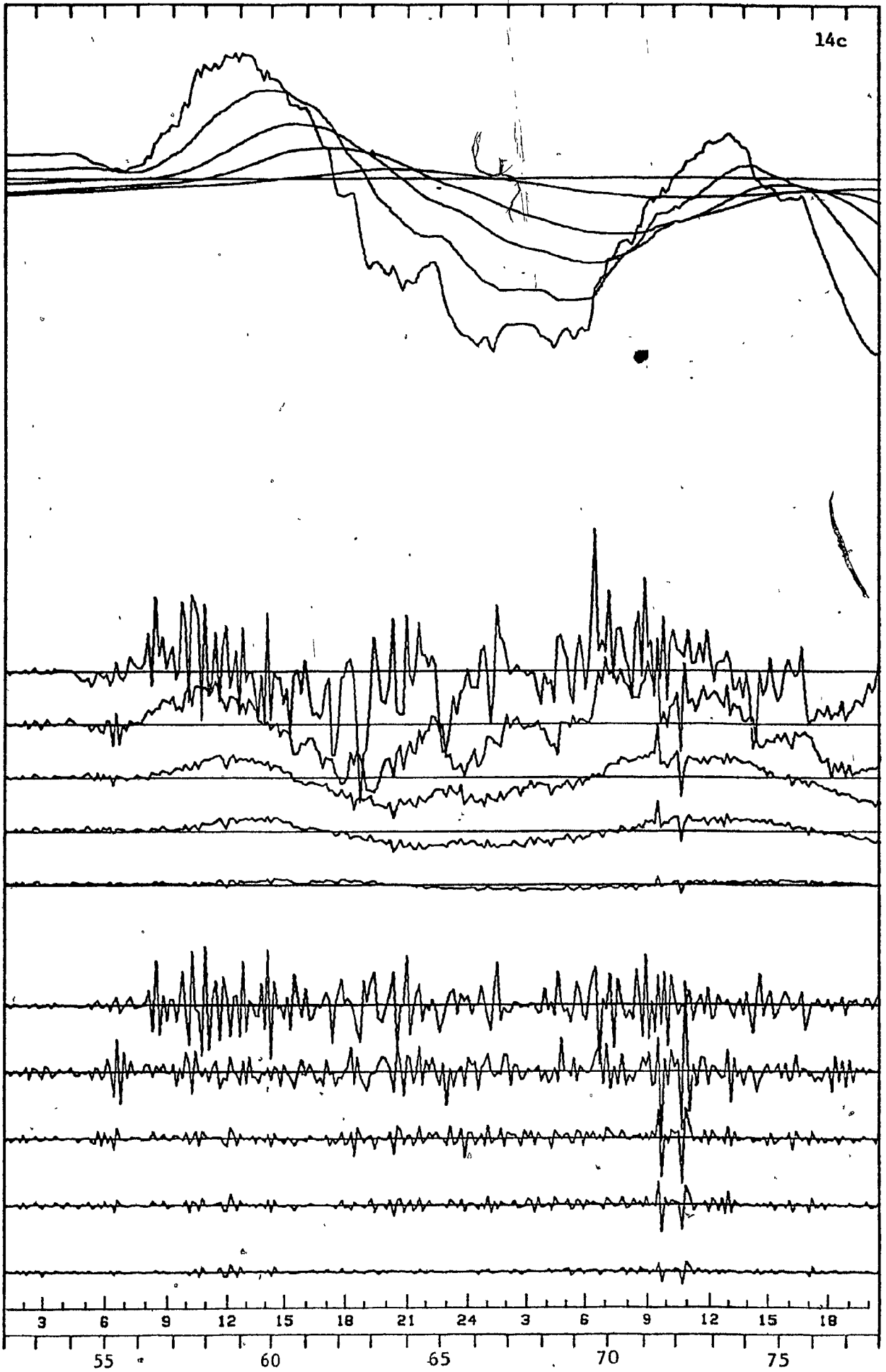
Time interval between measurements is 10 minutes

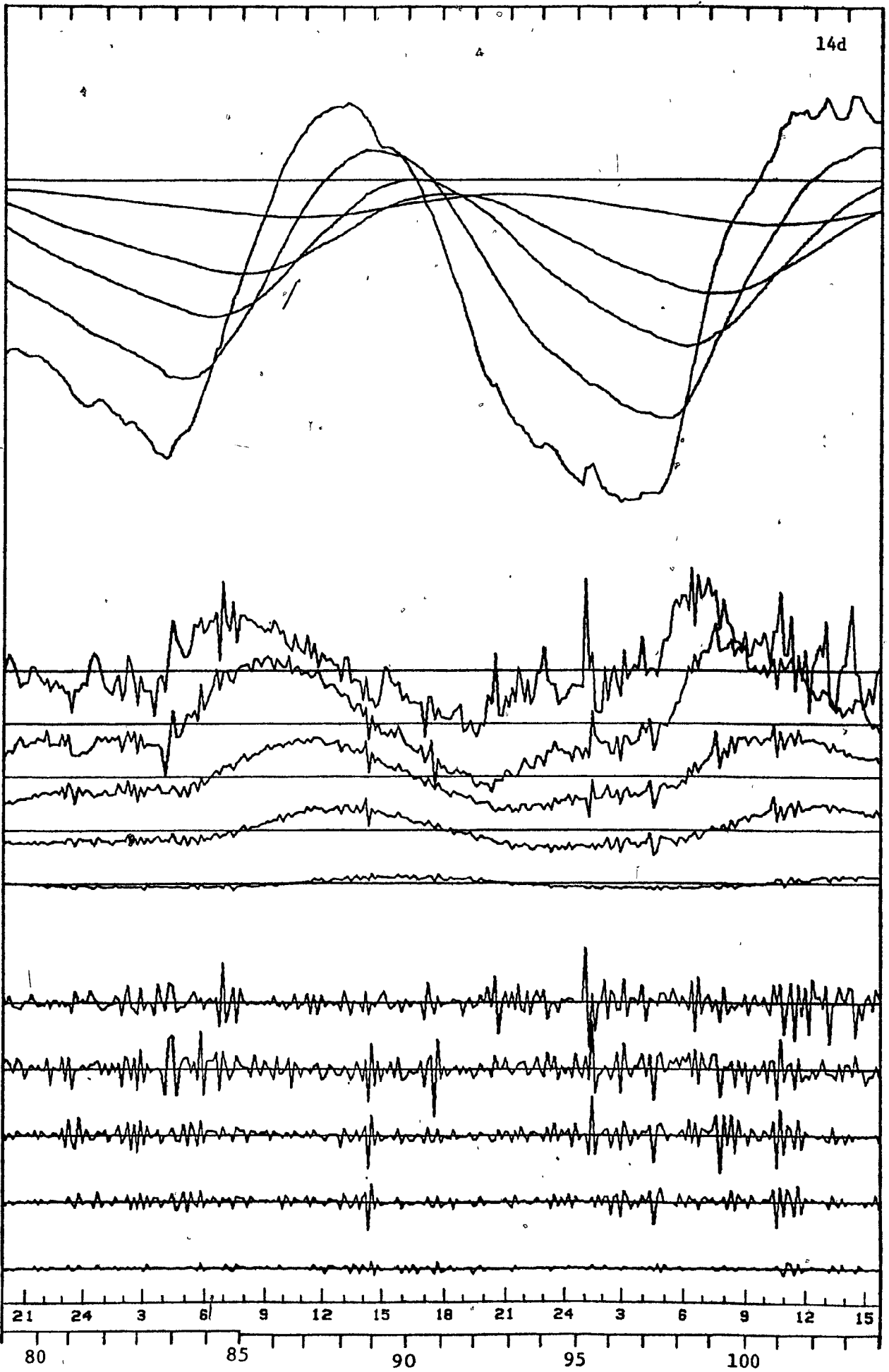


14b

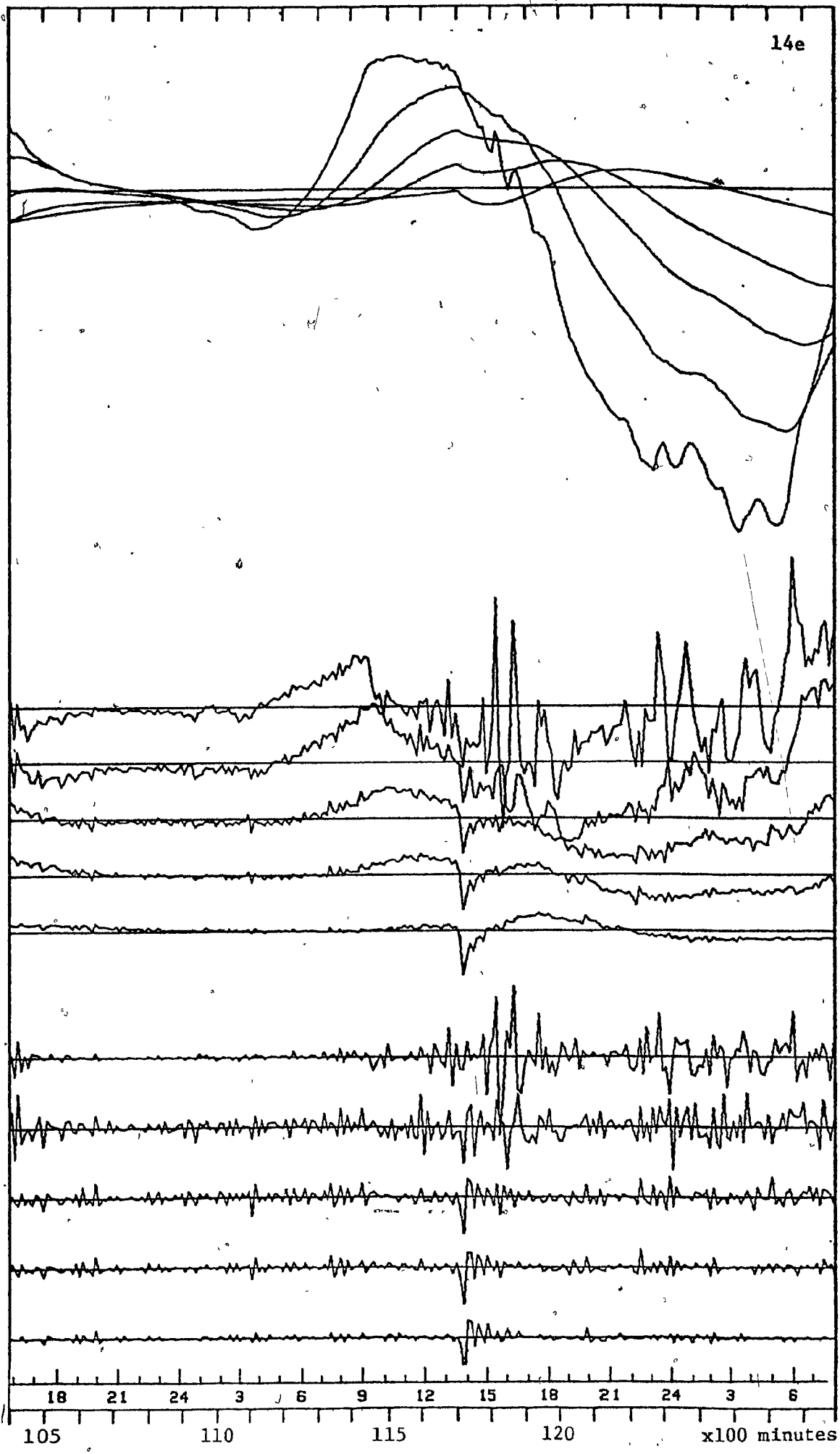


14c





14e



(a) Ventilation patterns

There are two patterns present in the variations indicated by the first and the second derivatives in Figure 14. One occurs at night and is characterized by variations that gradually penetrate deeper into the snowpack. The pattern apparently is related to the overall steepness of the negative temperature gradient in the snow cover. The pattern is absent around 5200 and 11000 minutes when the gradients were slight. This pattern is believed to be a result of free convection inside the snow cover as a response to the unstable stratification (Scheidegger, 1960). The pattern is consistent with results obtained by Bergen (1963) who reports free convection in a Rocky Mountain snowpack.

It is often claimed that the pores of a snowpack are too small to allow free convection. This assumption arises from the treatment of the pore spaces as closed cells in which the driving force becomes equal to the viscous dissipation at fairly large pore sizes. Since, however, a low density snowpack has interconnected pores throughout, a simultaneous return flow within the same pore space is not necessary. The flow in any one pore space is therefore at any instant unidirectional. The resistance to such flow is velocity dependent and approaches zero at zero velocity, without exceeding the driving force. A slow flow of air is therefore possible in the snow cover even at moderate density gradients.

Except for the near-surface layers, the pattern is

apparently unaffected by wind above the surface as indicated by the similarity of the patterns at 900 and 2300 minutes. However, at 9500 minutes, during a night with intermittent wind at low speeds, fairly large variations extend deep into the snowpack. These may be related to individual gusts of wind. The near-surface temperature gradient was steep and variable on that night and this may have influenced the convection at greater depths below the surface.

The second pattern occurs in daytime. The depth penetration of the variations is usually greatest at around noon but it may vary from day to day. Unfortunately the temperature gradients measured above the snow surface are not very reliable. If, however, we use the temperatures at the meteorological screen, we find that the depth penetration is generally better developed when the snow surface temperature is near or greater than the screen temperature. This indicates conditions of relatively steep horizontal surface pressure gradients.

The observed temperature variations cannot easily be explained without assuming the existence of convective heat transfer through the snow cover. The temporal patterns indicate that two driving processes are involved. It is concluded that one pattern is wind-induced and related to the unstable density stratification of the air that occurs just above the surface in daytime. The second pattern is an apparent result of free convection caused by the unstable air density stratification

inside the snow cover at night.

The very rapid changes in temperature of the near-surface snow layers could be sufficiently large to produce the previously discussed spatial variations in vapor pressure of the ice matrix.

### 3. Snow Surface Temperatures

One characteristic feature of snow surface temperatures is their rapid temporal variation (Figures 12 and 13). The fluctuations coincide with fluctuations in temperature recorded at deeper levels in the snow and they also correlate with observed air temperature variations. The rate of temperature change is high, as can be expected for a surface material of low (still air) thermal conductivity and low heat capacity. The greatest temporal variations tend to occur particularly on clear nights with strong radiative cooling. On such nights, in the absence of wind, the surface temperature drops towards the dewpoint, but even minor gusts of wind raise the temperature, presumably towards that of the wetbulb.

These rapid fluctuations show that the surface temperature is very strongly influenced by changes in the magnitude of the turbulent fluxes. Thermal scanning of snow surface temperatures could therefore be a useful tool in studying spatial variations in the turbulent fluxes. The rapid fluctuations also show that spatial variations in the turbulent fluxes may be far more important than the heat flux through the snow in determining the

temperature of the snow surface.

In snow hydrology, for the purpose of estimating heat fluxes, three common assumptions regarding snow surface temperatures are:

- (a) The snow surface temperature equals screen air temperature when this temperature is below 0 degrees C (e.g. Wendler, 1971).
- (b) The snow surface temperature equals the screen dewpoint temperature when the latter is below 0 degrees C.
- (c) The snow surface temperature equals the screen wet-bulb temperature when the air temperature is colder than 0 degrees C (Price et al., 1976; FitzGibbon, 1977).

The data presented in Figure 15 shows that screen temperature is generally the best estimator. At night, in calm, clear conditions the dewpoint temperature may give the best estimate. In windy conditions at night, the best estimate is often given by the wet-bulb temperature.

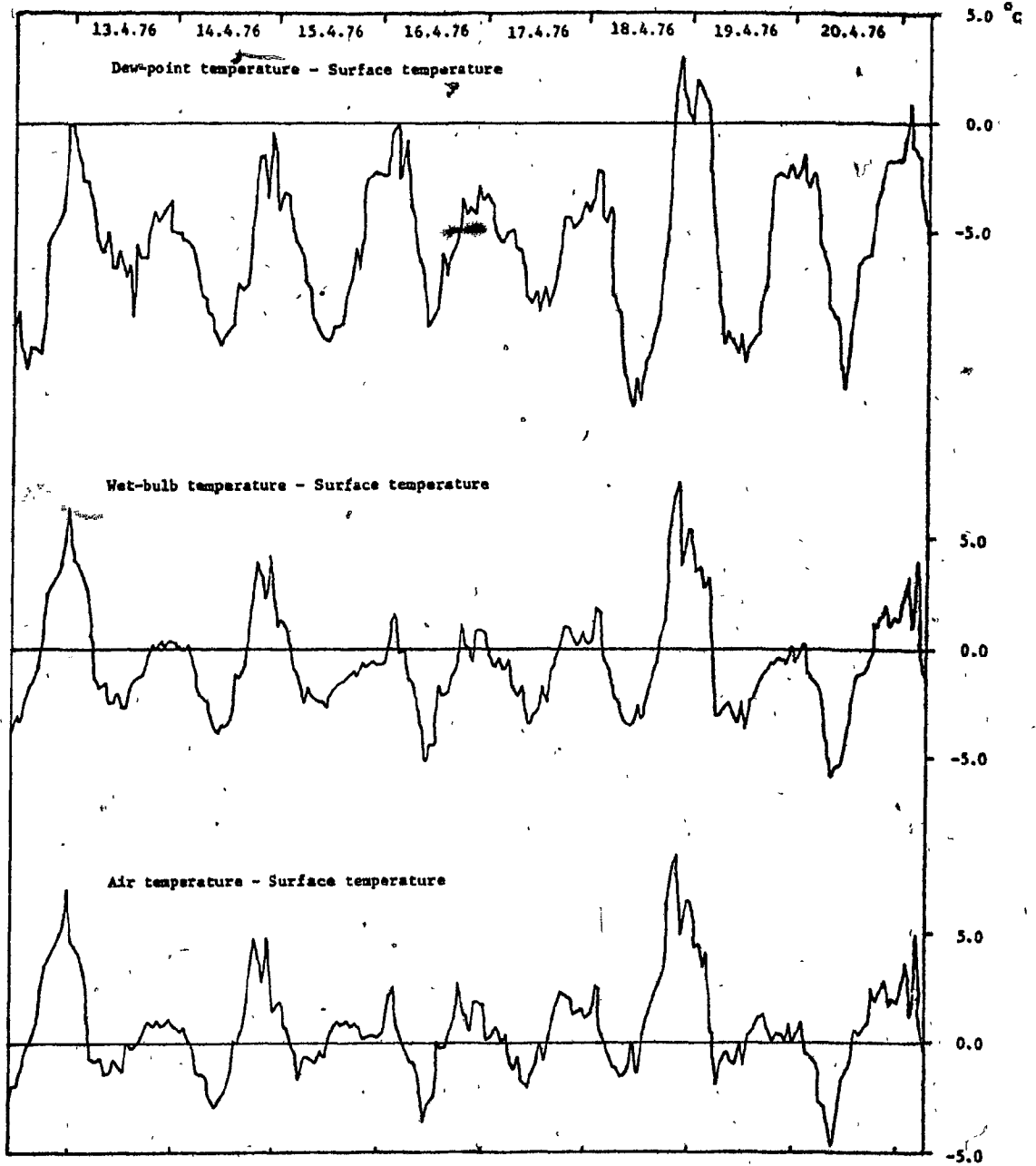


Figure 15. Snow surface temperature compared to Dew-point, Wet-bulb and Air temperature.

#### 4. In-Snow Temperature

An important factor influencing snow temperature variations is the internal absorption of solar radiation. From Figures 5 and 6 it may be seen that the amount of radiation available for absorption is at a maximum within the uppermost centimeter of the snow cover and declines quite rapidly with depth below the surface.

The temperature measurements show that on several days the temperature at 5 cm below the surface was considerably warmer than the surface temperature. This indicates, when we consider the radiation profile, that a major part of the absorbed radiation must be used to heat the air above the snow. Figure 16 shows this to be the case. This figure shows the measured net radiation, the computed heat penetration through different levels of the snow pack, and the computed turbulent fluxes. The turbulent fluxes were computed over 10-minute intervals as a residual from the measured net radiation and the computed change in heat content of the snow cover.

When the snow cover is isothermal, in a melting state, a much greater proportion of the net radiation has been observed to go towards (melting of) the snow (McKay and Thurtell, 1978). This can partially be explained by the fact that when the snow cover is isothermal, there is no gradient to conduct the heat from internal radiant absorption towards the surface. One basic condition for isothermal snow, however, is that the turbulent

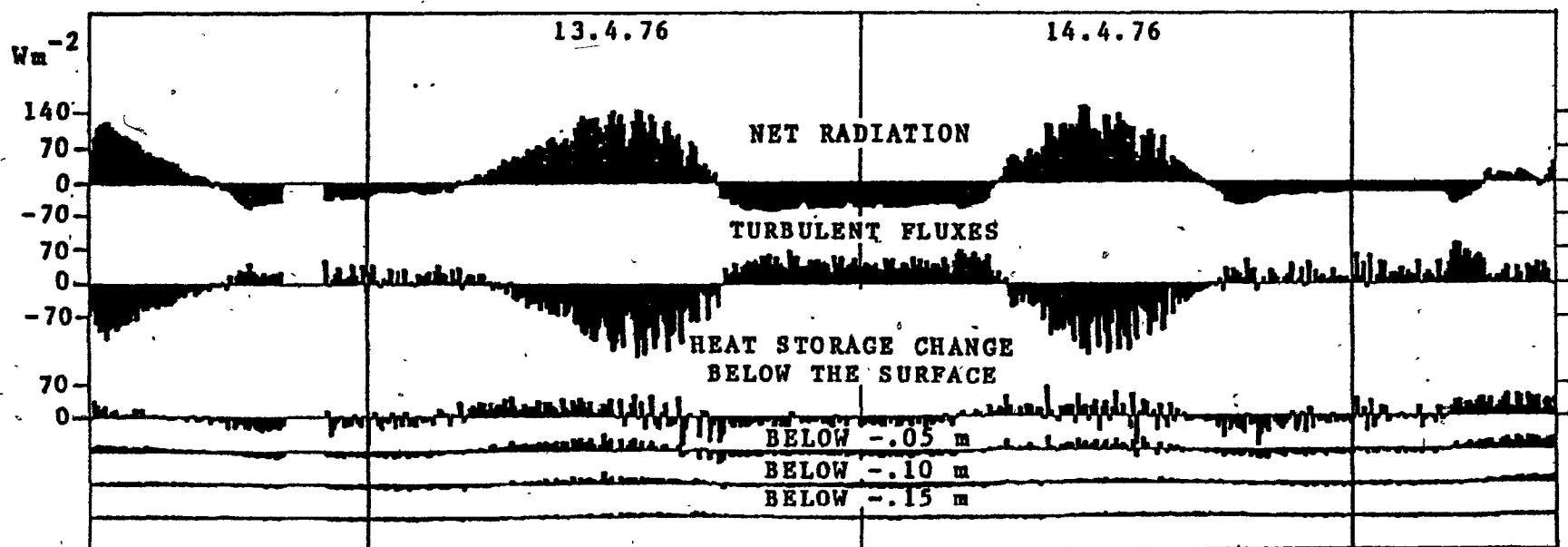
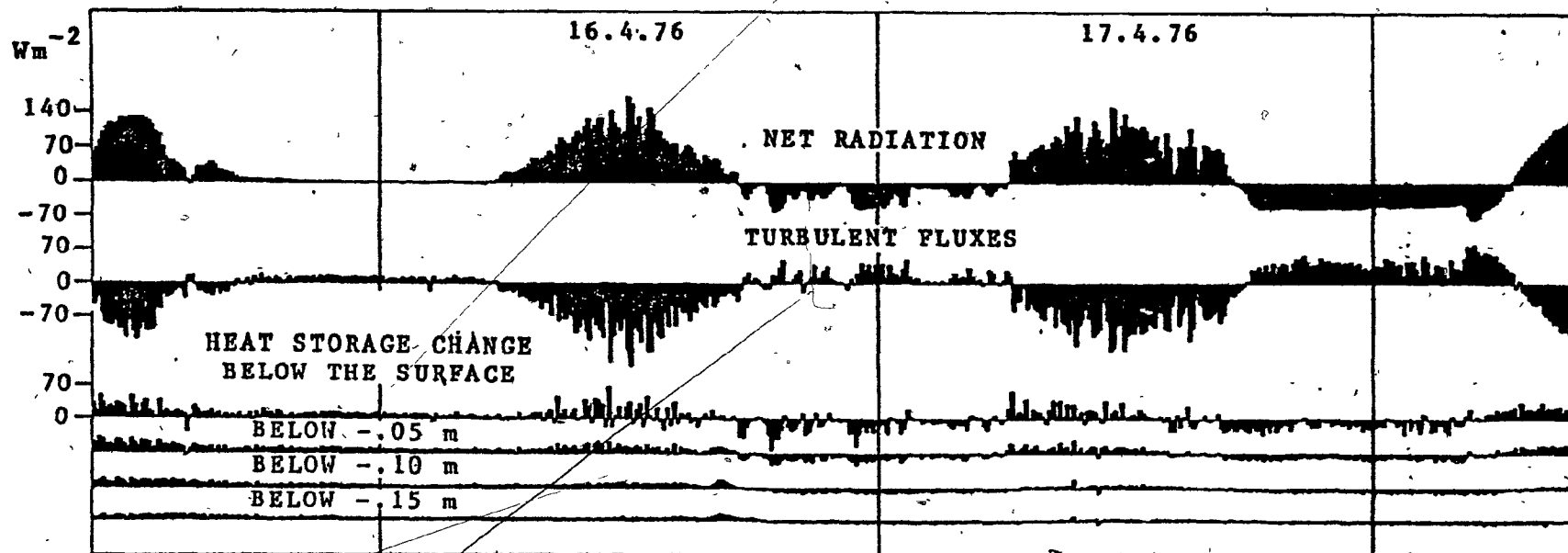


Figure 16a. Measured net radiation, heat penetration through different levels of the snow cover and computed (residual) turbulent fluxes.



100

Figure 16b. Measured net radiation, heat penetration through different levels of the snow cover and computed (residual) turbulent fluxes.

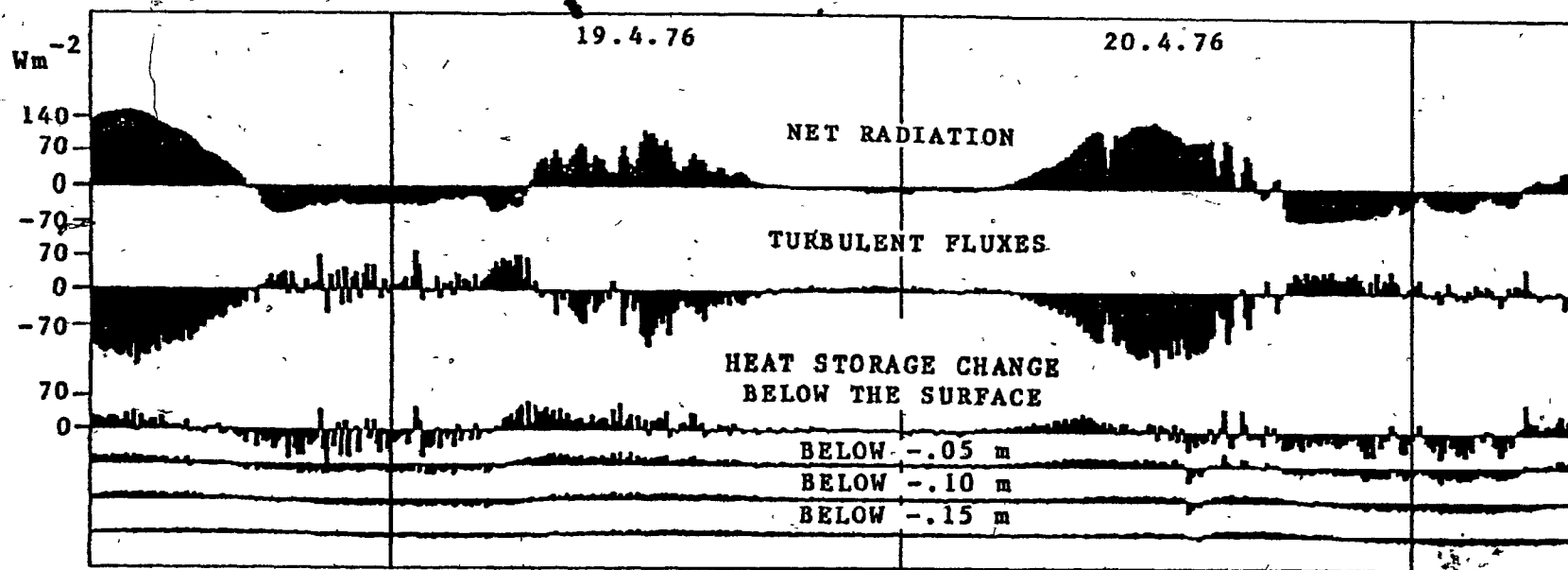


Figure 16c. Measured net radiation, heat penetration through different levels of the snow cover and computed (residual) turbulent fluxes.

fluxes are directed towards the surface or, at least, do not transfer much heat away from the surface.

It is interesting to note that the internal absorption of solar radiation provides a very efficient mechanism for the recovery of nocturnal heat losses. This allows the base of the snowpack to balance at a higher temperature than would be possible without internal absorption. On several days surface temperatures well above the melting point would have been required in order to conductively replace nocturnal heat losses.

##### 5. A Meltwater Percolation Event

The soil heat deficit plays an important role during snow melt and is probably quite significant both hydrologically and ecologically. The data obtained in the present study give some observations relating to this topic.

At the study site, the temperatures at the snow/soil interface were about  $-6$  degrees C. With the ground frozen to a depth of 1 m and a volumetric heat capacity of  $4.2 \text{ MJ/m}^3$ , the winter soil heat deficit is sufficient to refreeze about 4 cm of water or about one day's melt at above average rates (cf Price et al., 1976). In Schefferville, winter soil heat deficits may vary considerably, particularly in tundra locations (cf monthly tauchrones shown by Annersten, 1964, pp 59-62). Not much of the latent part of the winter heat deficit is recovered during melt as is evidenced by the ground often remaining frozen quite

close to the surface after the snow has melted. A large portion of the non-latent winter heat deficit is moved to the bottom layers of the snow cover in the early stages of melt when water from brief melting events percolates to the base of the snow pack and then refreezes. The refreezing is a result of the non-latent heat deficit of the ground. In this process a layer of snow ice is formed at the snow/ground interface. Measurements by Annersten (1964, p. 68) clearly show the effect of such meltwater percolation on soil temperatures at a tundra site near Schefferville.

One brief melting event with percolation of meltwater occurred on April 20 when surface melt was recorded between 900 and 1100 hours. For two hours the surface was at the melting temperature and then the temperature dropped below freezing after a reduction in the humidity occurred at about 1100 hours. Melting must have continued, however, in a layer just below the surface. At 1300 hours meltwater percolated through to the base of the snow cover causing a sudden increase in temperature at reference level. The total increase amounted to about 0.5 degrees C. The temperature at 5 cm below the surface remained well below 0 degrees C and reached a maximum of about -1.4 degrees C exhibiting a characteristic "zero curtain effect" as a result of the surface and near-surface melting.

Many snow melt prediction models and snow hydrology textbooks state that it is necessary for the snow cover to be

isothermal at 0 degrees C for snowmelt runoff to occur. However, the present data set shows that this is not a necessary condition. The recording, which shows meltwater percolation through 40 cm of relatively cold snow, shows that it is not necessary for the snow cover to recover the nocturnal heat deficit before meltwater percolation and, presumably, runoff can start. It shows that in cold snow, funnels (presumably isothermal) develop through which the runoff occurs. These funnels are surrounded by areas of cold snow where temperatures, in deep snow, may remain well below the melting point for days after the meltwater percolation has started. Funnels would tend to develop around stems and twigs in the snow cover where metamorphic processes have already produced routes of least resistance for the meltwater. The character of the vegetation at a site may in this way be important to the character of the runoff from that site.

On excavation of the snow thermometer, a few percolation paths were identified in its vicinity. Snow ice had formed where the funnels reached the ground surface.

#### 6. Discussion of the Vapor Pressure Regime in a Snow Cover

Vapor pressures were computed at 100-minute intervals, assuming equilibrium with a plane ice surface, and are shown by Figure 17. This figure also shows the variations in vapor pressure gradients at different levels in the snow.

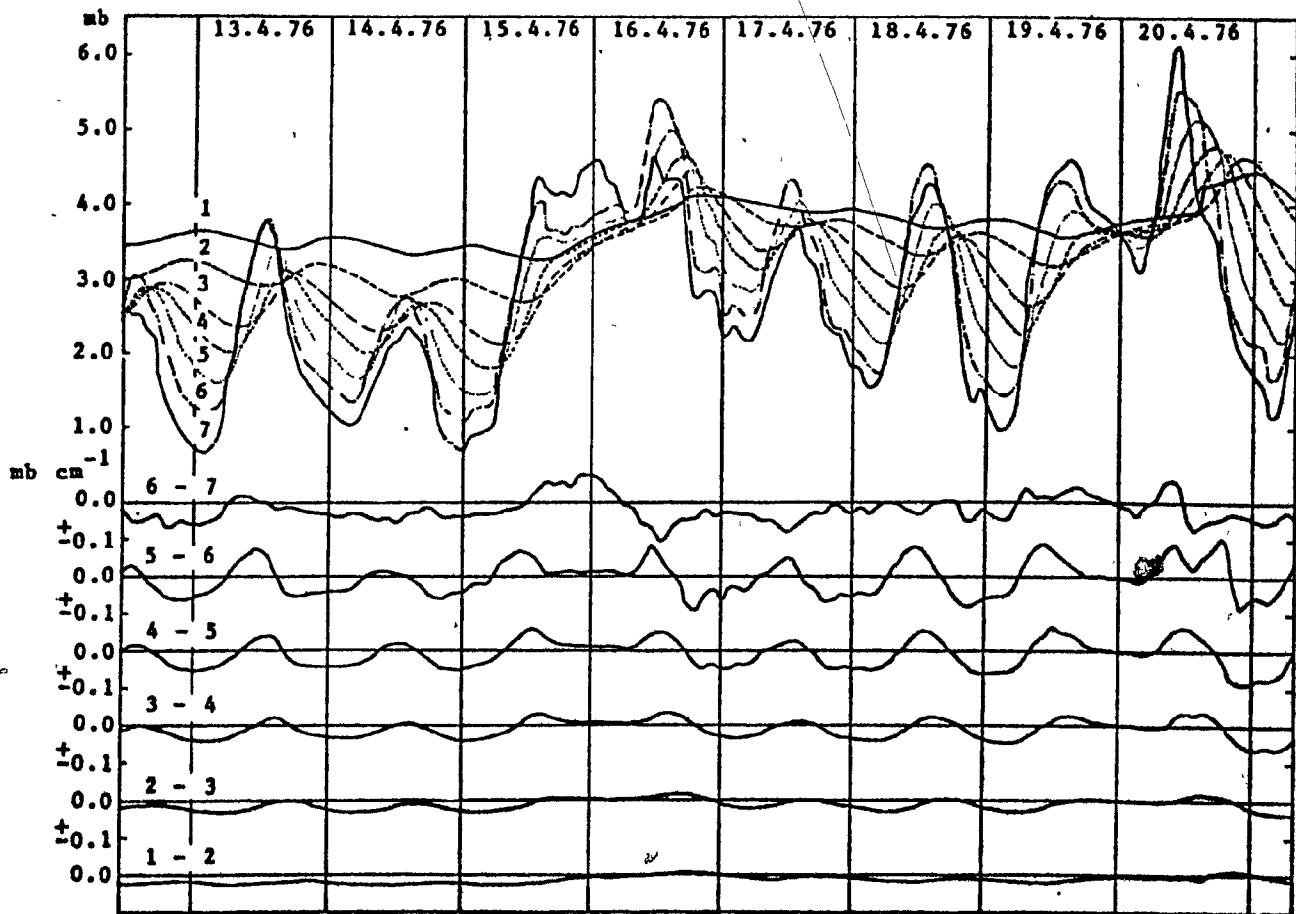


Figure 17. Vapor pressures and vapor pressure gradients.

- 1 - reference level
- 2 - 10 cm a.r.
- 3 - 20 cm a.r.
- 4 - 25 cm a.r.
- 5 - 30 cm a.r.
- 6 - 35 cm a.r.
- 7 - surface (approximately 40 cm a.r.)

The computations of in-snow vapor pressures were made using the formula:

$$\log e = tu/(t+v)+w \quad (\text{Tetens, 1930}) \quad 5.1$$

where  $t$  is the temperature (degrees C)

$e$  = vapor pressure (mb)

$w$  = 0.7858 for vapor pressure in mb

$u$  = 9.5 over ice

$v$  = 265.5 over ice

This formula gives only an approximate estimate of vapor pressure. For the present purpose, however, it is quite adequate, as a greater potential error lies in the assumption of equilibrium with a plane ice surface inside the snow pack.

(a) Effects of surface curvature

A porous snow cover could produce an average in-snow vapor pressure different from that above a plane ice surface. Some field measurements by Van Haveren (1971) using a thermocouple psychrometer (Brown, 1970) indicate that the relative vapor pressure of snowpack void air, or the ratio of the measured to the computed vapor pressure is normally less than unity and can reach values below 0.985. Van Haveren postulates that this undersaturation is caused by ventilation of the snow cover. However, the saturation profiles do not clearly support this idea since, in several of the profiles the greatest saturation deficit is found, not at the surface, but at some depth below it.

The temporal variations in vapor pressure deficit displayed by Van Haveren's profile measurements show that the shape and size of capillaries cannot be the only factor influencing the vapor pressure measurements. Although a laboratory accuracy of 0.0005 units of relative vapor pressure is claimed, Van Haveren does not indicate the field accuracy of his vapor pressure measurements. It is evident, however, (Figure 9b, Van Haveren, 1971, p. 181) that the time allotted for the probe to come to an equilibrium with the snow temperature was insufficient. Considering that the probe length is 60 cm, the temperature change that is indicated is quite unusual when compared to the in-snow temperature changes recorded in this thesis. On p. 180, Van Haveren indicates that ambient temperatures need to be held within 0.001 degrees C during the 30-40 second measurement period. From the temperature graphs in the accompanying figures it is, however, evident that this requirement was not fulfilled.

Given that the aforementioned factors introduce but negligible error, the measurements indicate that the error caused by assuming equilibrium with respect to a plane ice surface is generally less than 0.1 mb vapor pressure in the old snow pack at Van Haveren's test site. In a new snow pack the error could probably be considerably greater. Figure 17 should be viewed with these constraints in mind.

(b) Effects of air movement on void vapor pressure

An interesting effect of surface curvature on vapor pressure is that it probably makes the equilibrium vapor pressure of the voids a function of the velocity of flow, for the most sharply convex parts of the ice matrix protrude into the airstream while the concave parts are more sheltered from the moving air. In still air both convex and concave parts are of similar importance in determining the average void vapor pressure, but with increasing rates of air movement, the vapor pressure at the protrusions would take an increasingly dominant role. Thus, the vapor pressure of the void air should increase as the rate of flow increases. No suitable measurements are available in the literature to evaluate whether or not such a velocity dependence exists. Neither Yosida's (1950, 1955) nor Yen's (1962, 1963, 1965) experiments include measurements suitable to answer the question. Yen's experimental apparatus could, however, be used for this purpose, if the moisture content of the air were also measured just before the wet test meter.

If we re-interpret the relative vapor pressures shown by Van Haveren, (1971) it is possible that the higher relative vapor pressures near the surface result from the movement of air in the snow cover. The measurements may thus indicate snowpack ventilation but for reasons quite different from those given by Van Haveren.

A second, most important effect of air movements on vapor pressures inside the snow cover is the previously discussed

spatial variations in vapor pressure and temperature resulting from the rapid changes in temperature caused by ventilation.

(c) The vapor pressure regime

Given the aforementioned constraints, it is possible to make some observations regarding the vapor pressure regime during the period of measurement. Throughout the 9-day period evaporation from the surface prevailed (Figure 15). Only at night, under calm conditions was condensation onto the surface possible. Figure 17 shows that the movement of water vapor by diffusion was mainly upwards, particularly in the uppermost 5 cm. Farther down there was daytime downward migration of vapor, but at the lowest levels, the movement of vapor was, again, mainly upwards. There was a zone of apparent daytime mass loss just below the snow surface. Similarly, there was an apparent nocturnal mass gain in this zone. The explanation for this apparent mass gain must be that ventilation causes a reduction in the steepness of the gradient of the uppermost layer by increasing its effective thermal conductivity. No known energy transfer mechanism could selectively remove the necessary energy for the aforementioned mass gain. The daytime mass loss can be explained by internal absorption of solar radiation and by cooling of the snow surface by ventilation.

The patterns of moisture migration are of importance in snow cover metamorphism. La Chapelle and Armstrong (1977) identified

a vapor pressure gradient of approximately 0.05 mb/cm as a critical limit between "temperature gradient metamorphism" and "equi-temperature metamorphism" (Sommerfeld and La Chapelle, 1970). This limit was periodically exceeded in the lowest 20 cm of the snow cover during the 9-day period. It was exceeded in both positive and negative directions in the uppermost 15 cm of the snow cover. The alternating direction of moisture flow must be quite important to the metamorphic processes in this layer.

CHAPTER VI  
ANALYSIS FOR VENTILATION EFFECTS

Some insight may be gained into the patterns of ventilation by comparing the total heat flux to the conductive heat flux. In this chapter such a comparison is attempted under the constraints imposed by (i) the previously mentioned interpolation error associated with the assumption of semi-linear temperature change at reference level and (ii) the unknown thermal properties of the snow cover and (iii) the unknown distillation effects within the snow cover.

A computer program was written to perform the calculation of both the conductive and the total heat fluxes in a multi-layer model where the snow density can be specified for individual layers and the respective thermal properties of the snow are computed accordingly. The program computes the difference between the two fluxes at four different depths below the snow surface. It also computes the cumulative differences between the fluxes. The output from the program is graphical, obtained directly on the CALCOMP plotter. This makes it convenient to manipulate the properties of the snow cover and to observe the effects of the manipulations.

## 1. Method

The conductive heat flux,  $Q_c$ , through a given depth interval in the snow cover may be estimated by:

$$Q_c = -k(dT/dz) \quad 6.1$$

where  $dT/dz$  is the temperature gradient estimated from the observed temperature difference across a vertical interval in the snow cover.

In the present analysis, the conductive heat flux across a depth interval is compared to the change in heat content of a snow slab below that level. The gradients controlling the conduction into or out of the snow slab are mainly the gradients right at its upper and lower surfaces. Because of the non-linearity of the temperature gradient, the actual conductive heat flux may differ somewhat from the flux inferred from the temperature difference across the intervals. The actual flux will also lag behind the predicted flux somewhat.

The total heat flux at the top of a slab,  $Q_t$ , can be estimated from the known temperature change per unit time,  $\Delta T/\Delta t$  of a given slab of snow and the heat flux at the bottom,  $Q_b$ , of that slab. Thus,

$$Q_t = \rho_s H C_i (\Delta T/\Delta t) + Q_b \quad 6.2$$

where,  $\rho_s$  is snow density ( $g/cm^3$ )

$H$  is the height interval (cm)

$C_i$  is the specific heat of ice (cal/g).

The total heat flux estimate is also slightly affected by the

non-linearity of the temperature gradient. Since the measurement method precludes destructive monitoring of the thermal properties of the snow pack, and since no non-destructive methods were available, the snow density and the thermal properties are unknown and need to be estimated.

Recent reviews of different proposed relations between snow density and thermal conductivity,  $k_s$ , are given by Goodrich (1976), Reimer (1980) and Ohmura (1980). For the present study Abels' (1894) formula was used where

$$k_s = c \rho_s^2 \quad (\text{cal/cm/s/degree C}) \quad 6.3$$

and where  $c$  is a constant that normally ranges from 0.0067 (Abels, 1894) to 0.0085 (Kondratyeva, 1945). Although Kondratyeva's constant was established for snow densities greater than 0.3 g/cm<sup>3</sup>, the latter value rather than the former was used for the initial estimate of the conductive heat flux, for when compared to other, more recent estimates of the thermal conductivity of snow it falls closer to the centre of the range of these estimates than Abels' formula.

The volumetric specific heat was determined using the formula

$$C_s = \rho_s(0.5057 + 0.001863T)\rho_i \quad 6.4$$

where  $T$  is temperature (degrees C) and

$$\rho_i = 0.9168 \text{g/cm}^3 \quad 6.5$$

The accuracy of this estimate depends on the accuracy of the estimated snow density. A density survey at the end of the

measurement period, taken as the snow thermometer was excavated, yielded a density of approximately  $0.2 \text{ g/cm}^3$ . The estimated range in density is from not less than 0.16 to a maximum density equal to that measured at the end of the measurement period.

## 2. Run 1

An initial run was made using a uniform snow density of  $0.2 \text{ g/cm}^3$ . The result is shown in Figure 18.

The two fluxes show apparent differences of several kinds. First, the short term variability is far greater for the total heat flux than for the conductive heat flux. This can be expected since the temperature gradients change only gradually and other factors governing the conductive heat flux also change very slowly.

Secondly, there is an apparent lag of approximately 100 minutes between the two fluxes with the conductive heat flux preceding the total heat flux.

Thirdly, at the lowest level there are large differences between the two fluxes. These differences can be seen throughout the entire depth of the snow cover. The difference is particularly visible at 6100 minutes.

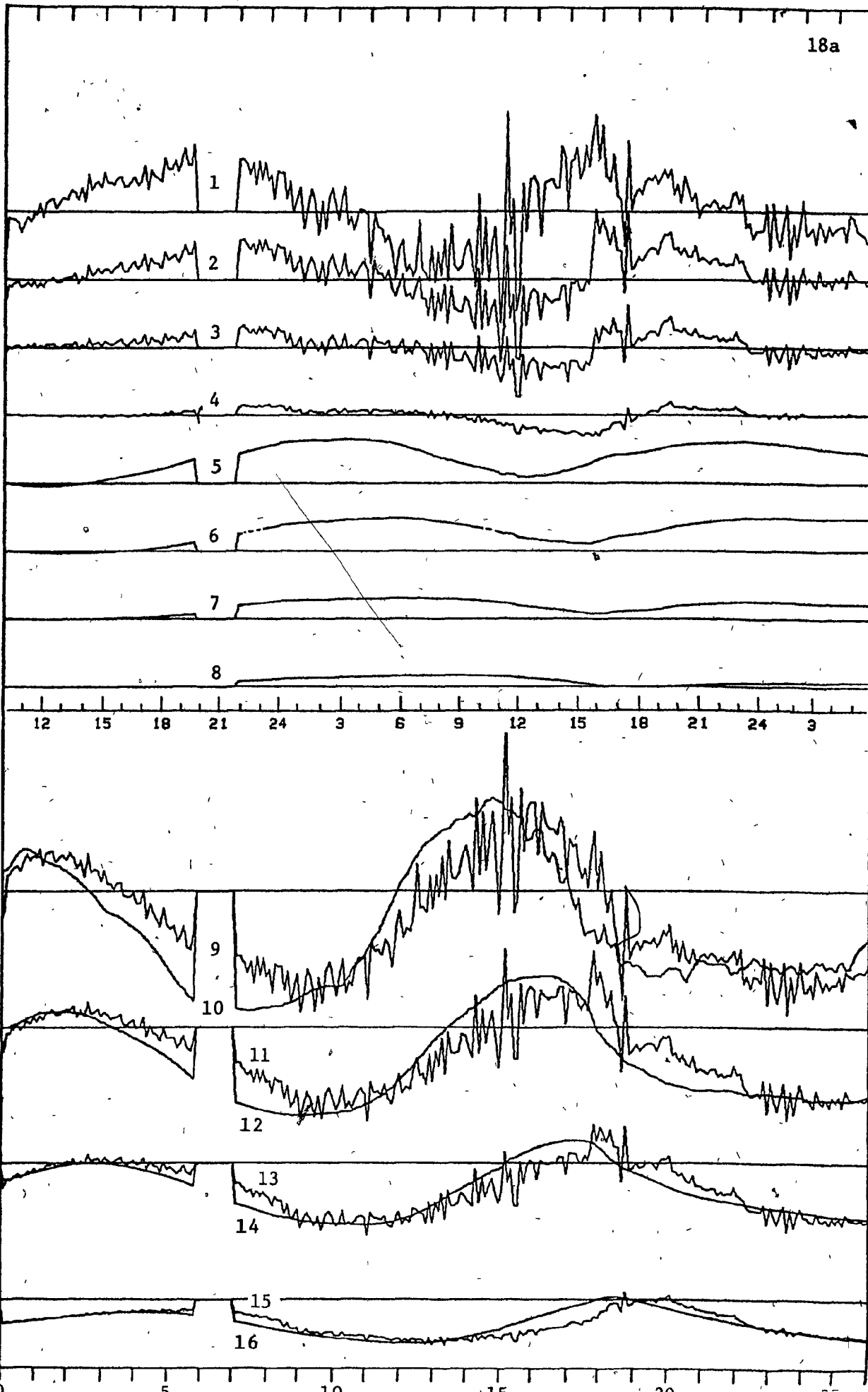
In part, the differences are caused by the method of computation (particularly the time lag). It is also quite apparent that the semi-linear interpolation between thermistor

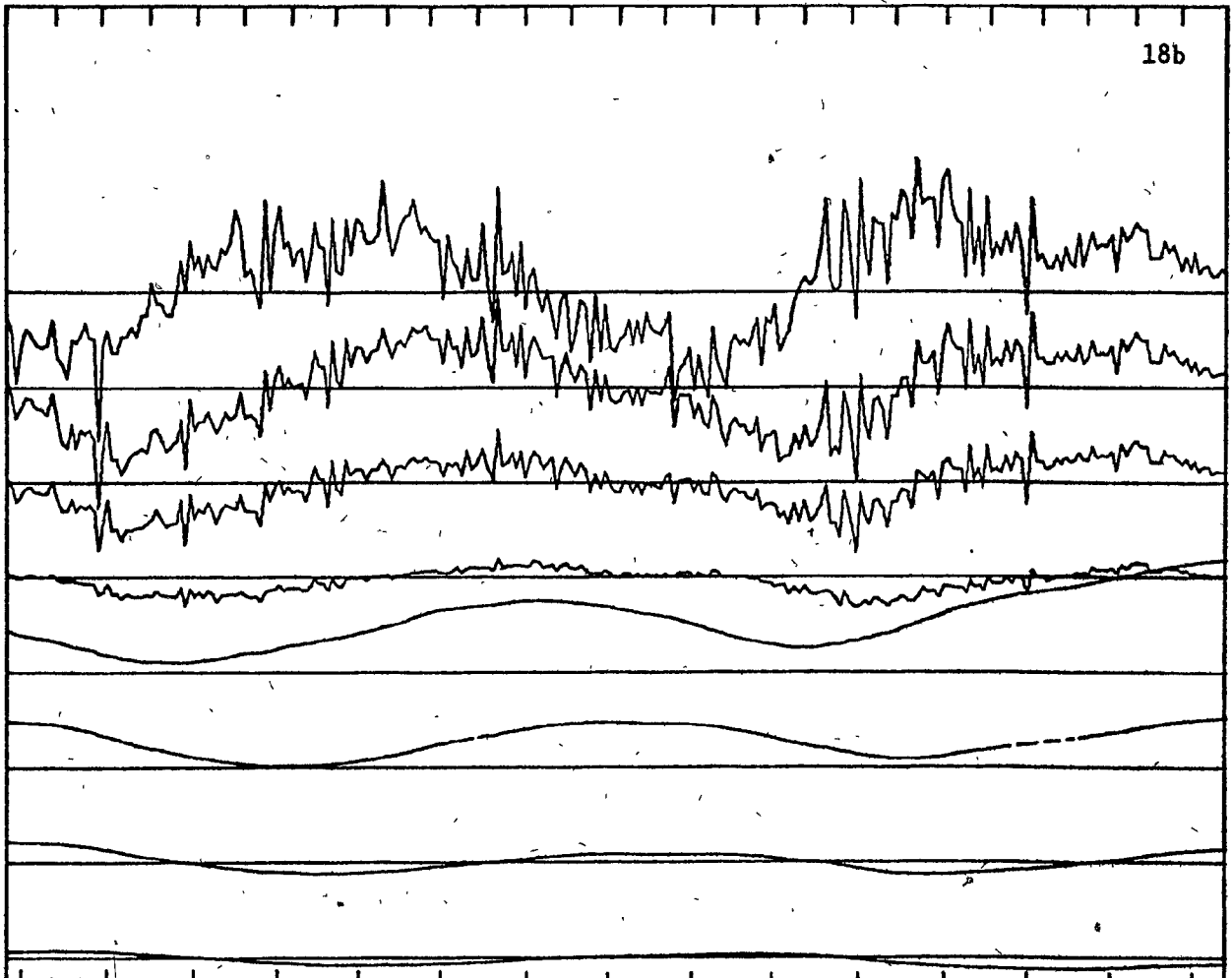
Figure 18. Run 1. Conductive and total heat fluxes

(a.r. - above reference)

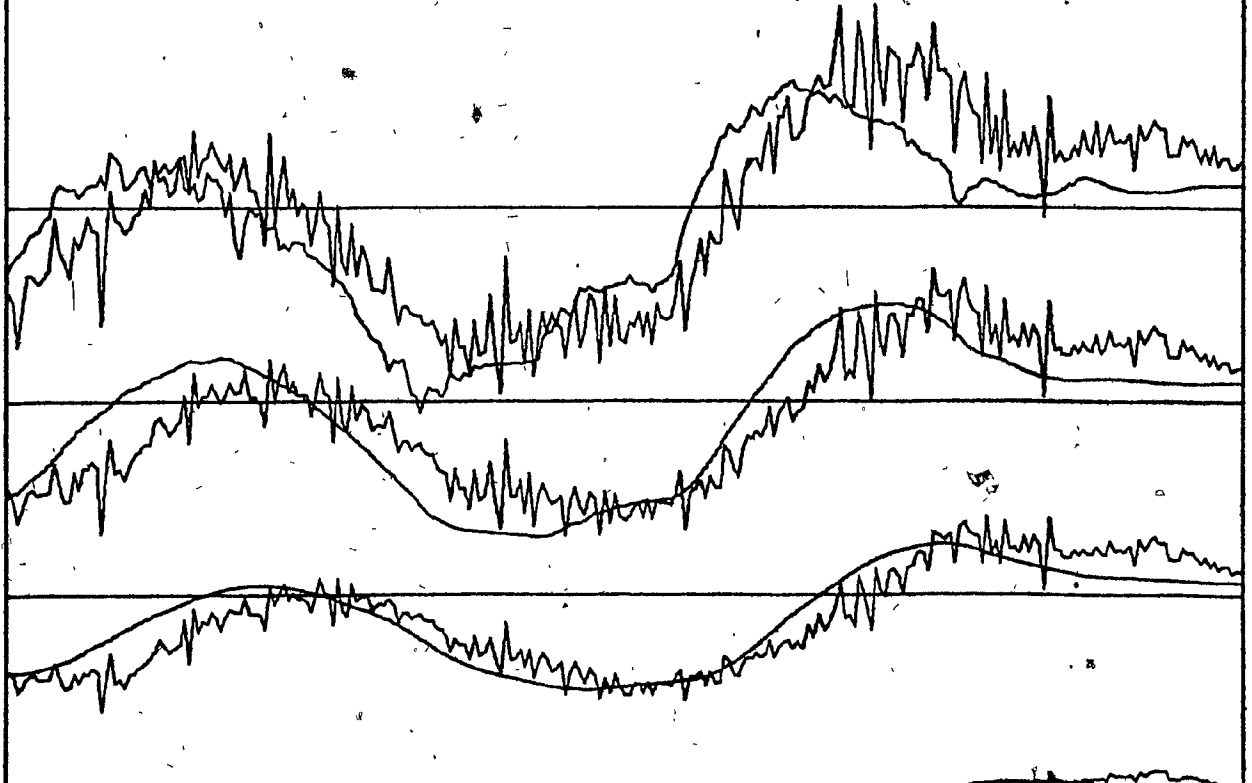
	<u>Scale</u>
1. Total minus conductive heat flux at 30 cm a.r.	1 inch - 0.02 ly min <sup>-1</sup>
2. Total minus conductive heat flux at 25 cm a.r.	1 inch - 0.02 ly min <sup>-1</sup>
3. Total minus conductive heat flux at 20 cm a.r.	1 inch - 0.02 ly min <sup>-1</sup>
4. Total minus conductive heat flux at 10 cm a.r.	1 inch - 0.02 ly min <sup>-1</sup>
5. Cumulative total of 1.	1 inch - 20.0 cal cm <sup>-2</sup>
6. Cumulative total of 2.	1 inch - 20.0 cal cm <sup>-2</sup>
7. Cumulative total of 3.	1 inch - 20.0 cal cm <sup>-2</sup>
8. Cumulative total of 4.	1 inch - 20.0 cal cm <sup>-2</sup>
9. Total heat flux at 30 cm a.r.	1 inch - 0.02 ly min <sup>-1</sup>
10. Conductive heat flux at 30 cm a.r.	1 inch - 0.02 ly min <sup>-1</sup>
11. Total heat flux at 25 cm a.r.	1 inch - 0.02 ly min <sup>-1</sup>
12. Conductive heat flux at 25 cm a.r.	1 inch - 0.02 ly min <sup>-1</sup>
13. Total heat flux at 20 cm a.r.	1 inch - 0.02 ly min <sup>-1</sup>
14. Conductive heat flux at 20 cm a.r.	1 inch - 0.02 ly min <sup>-1</sup>
15. Total heat flux at 10 cm a.r.	1 inch - 0.02 ly min <sup>-1</sup>
16. Conductive heat flux at 10 cm a.r.	1 inch - 0.02 ly min <sup>-1</sup>

The assumed snow density is 0.2 gcm<sup>-3</sup>



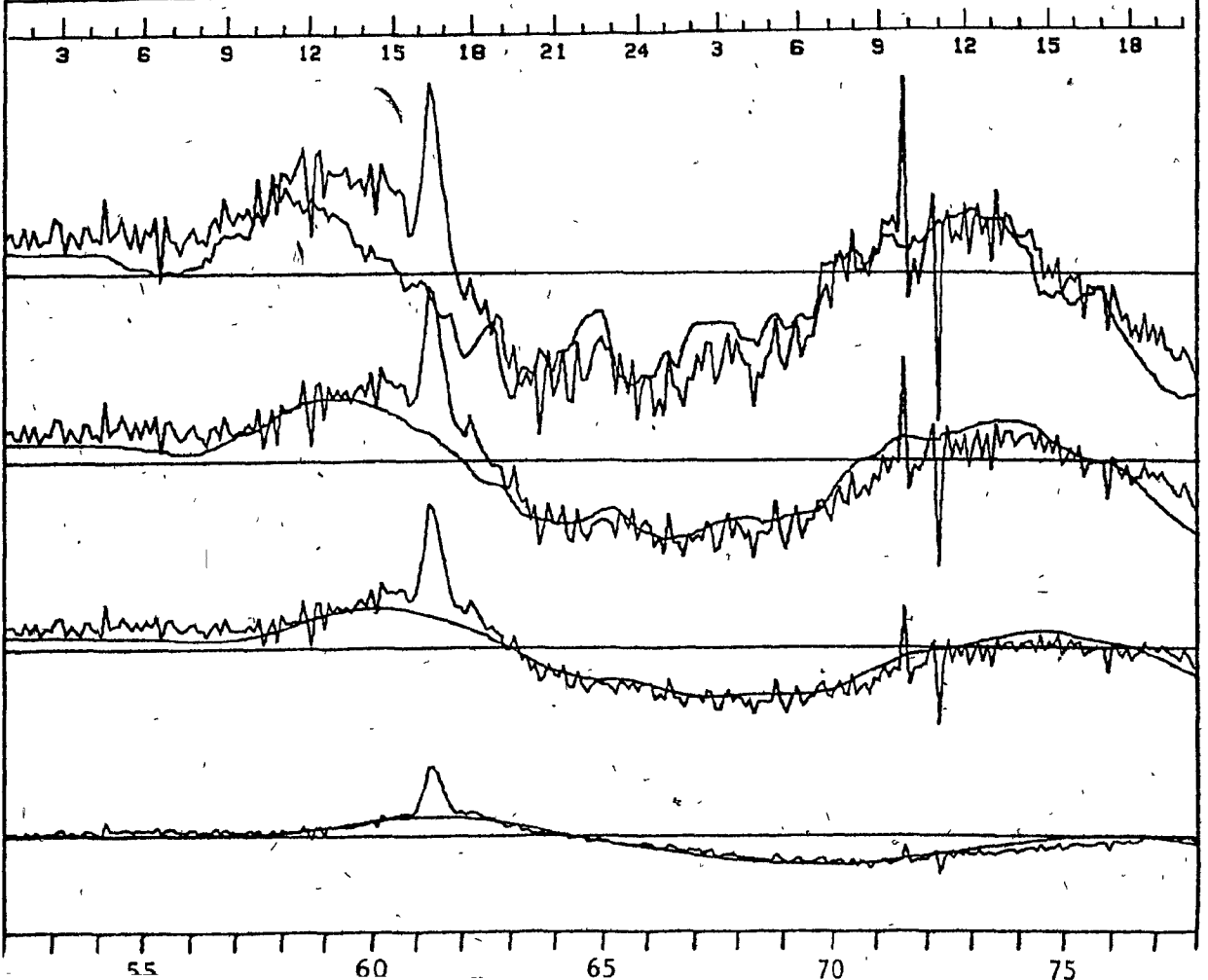
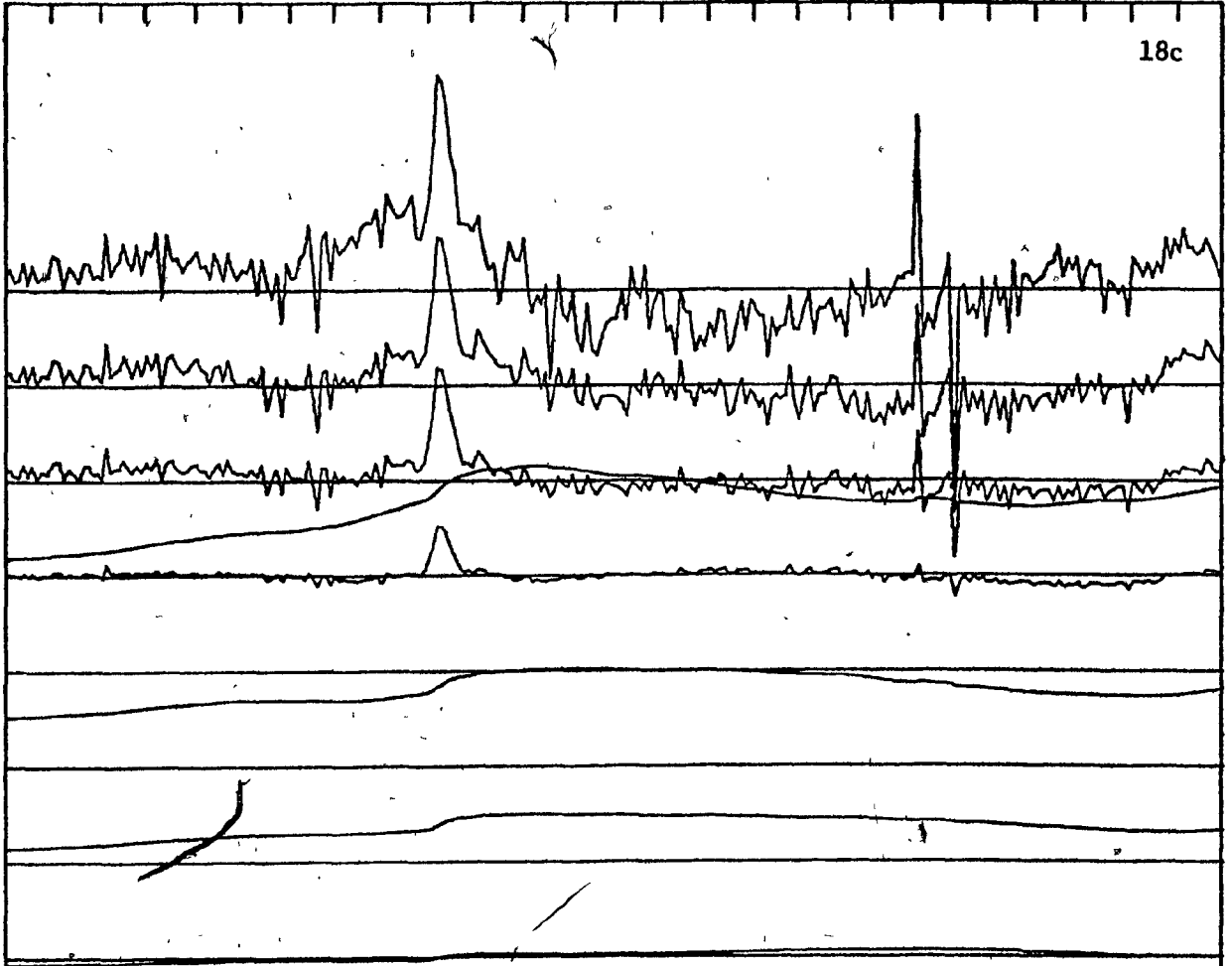


6 9 12 15 18 21 24 3 6 9 12 15 18 21 24

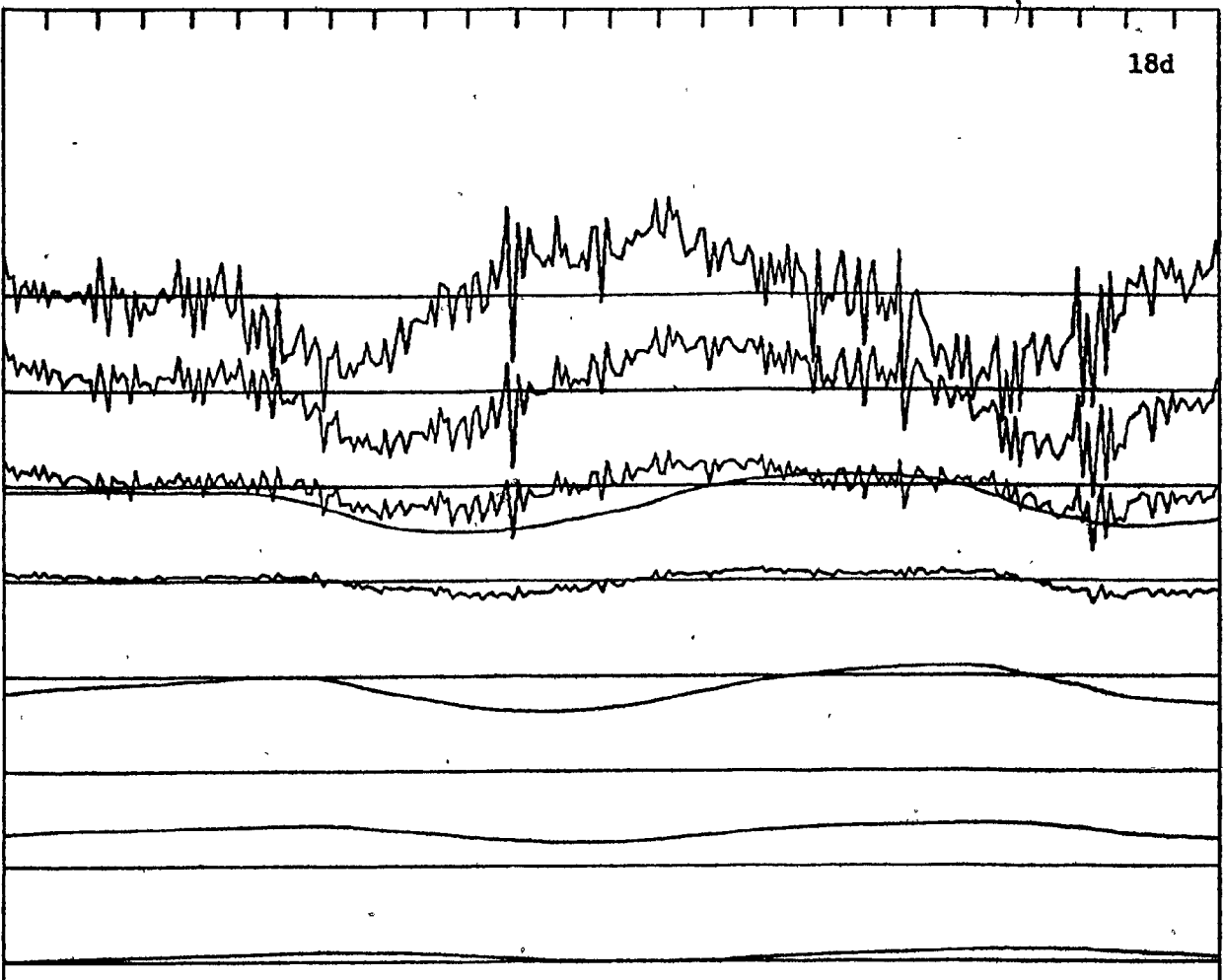


30 35 40 45 50

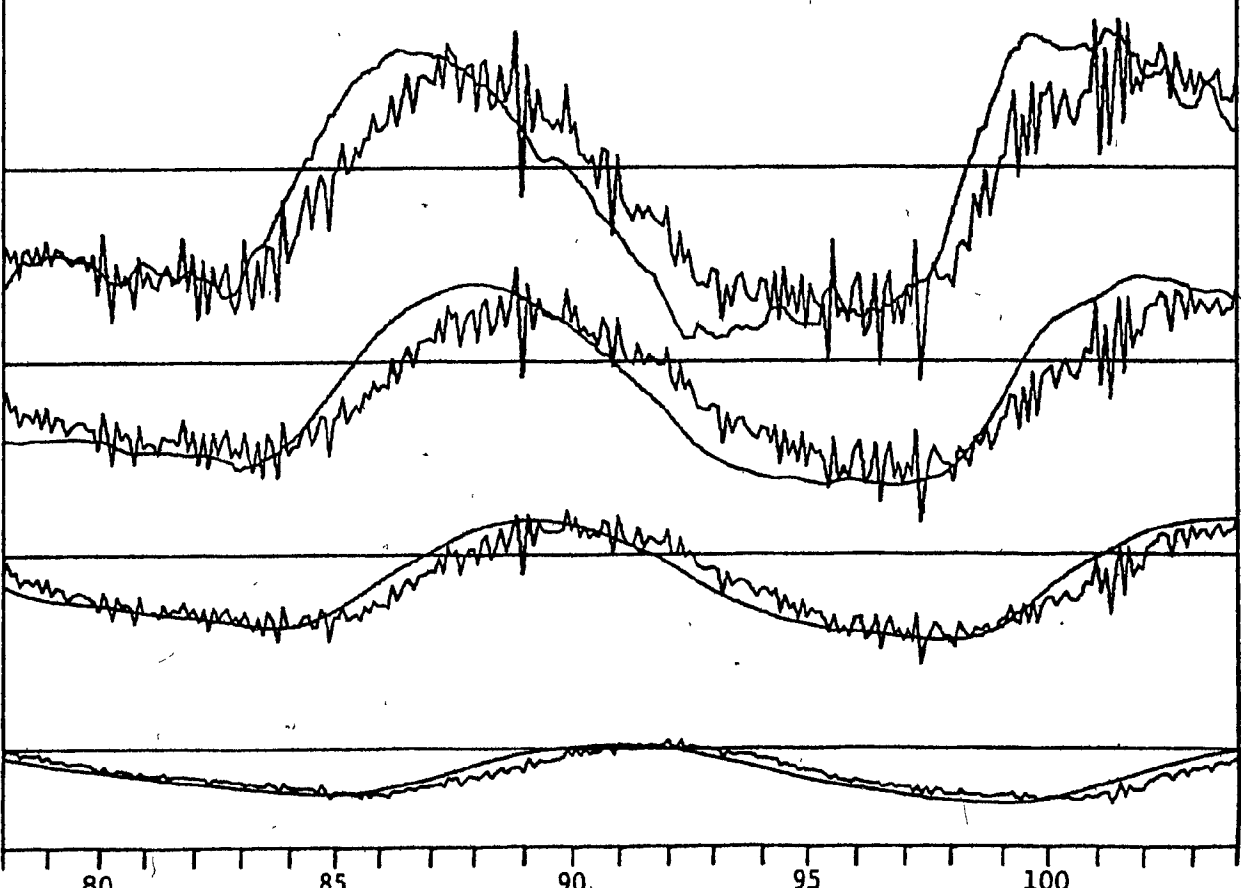
18c



18d

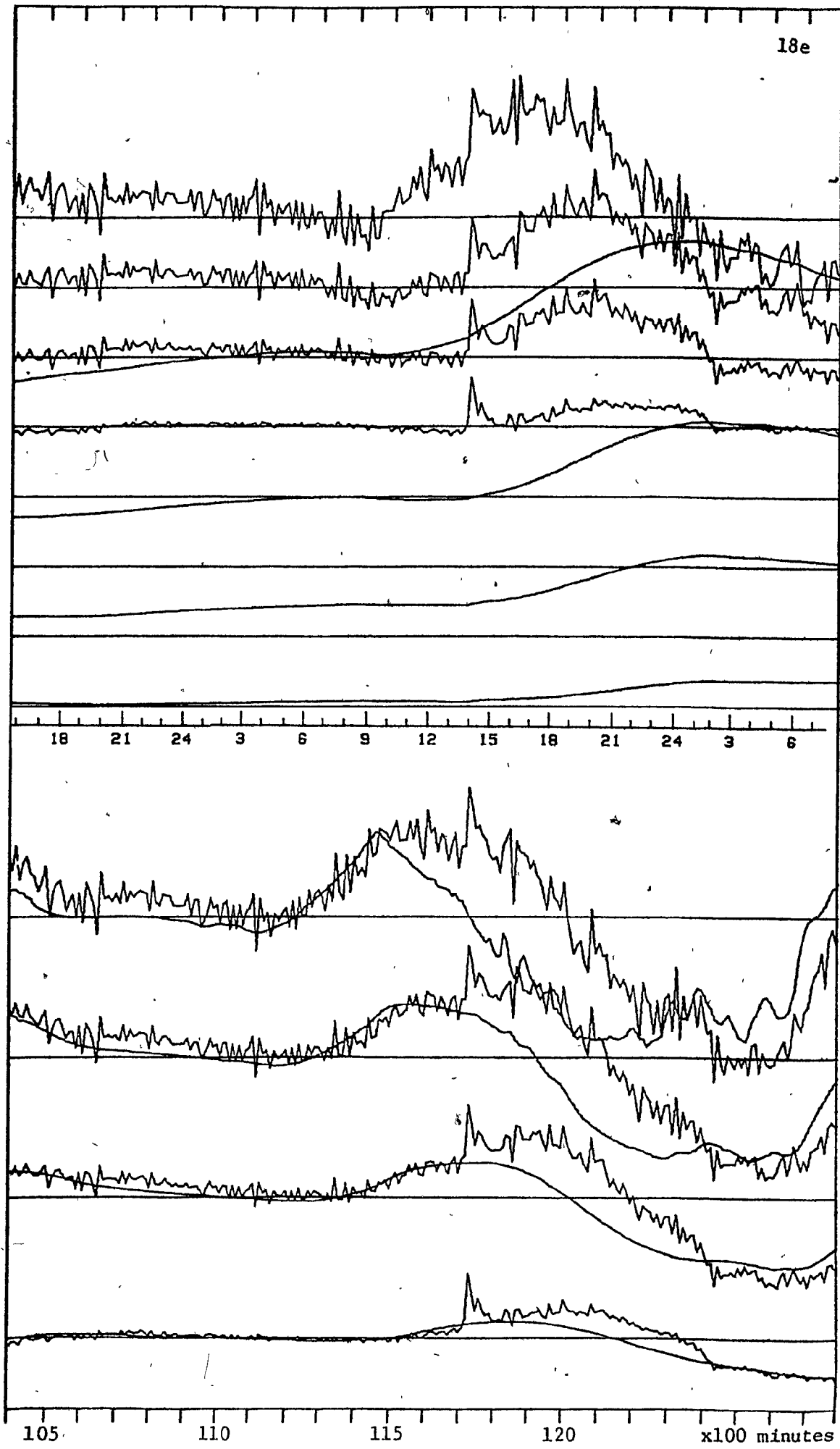


21 24 3 6 9 12 15 18 21 24 3 6 9 12 15



80 85 90 95 100

18e



readings is inadequate. The total heat flux exhibits considerable temporal variations throughout the snow cover, down to the lowest measuring level. This suggests that the sudden changes in temperature extend right to the base of the snow cover. The intermittent reference temperature readings miss the sudden temperature changes. The semi-linear interpolation removes these short-term fluctuations in temperature, not only at the base but throughout the snow column. An error of longer wavelength is also present due to the interpolation over long time intervals when the actual temperature change was strongly non-linear.

If we adjust for the lag by simply delaying the conductive heat flux by an appropriate amount and we assume a perfect fit between the two fluxes at the lowest level (after lag adjustment) and remove the actual difference at that level and the effects of this difference throughout the snow cover, we can filter out the error due to the interpolation over long time intervals. While the conductive heat flux remains unchanged, we are no longer dealing with the total heat flux across the different levels. Instead "total heat flux" now means the effects of change in the heat content of the upper levels of the snow cover added to the conductive heat flux at the lowest level. This, of course, precludes an accurate quantitative evaluation of the ventilation effects. However, the distortion is in most cases small. A qualitative analysis should, therefore, still be meaningful.

The data manipulation described above affects the time lag between the conductive and the total heat fluxes. This is because the previously discussed lag at the lowest level is filtered out. Therefore a change in the assumed thermal conductivity of the snow will change the lag somewhat since it influences the difference between the two fluxes at the lowest level.

### 3. Runs 2, 3, 4 and 5

A second run (Figure 19) shows the output after lag adjustment. In this run the non-conductive heat fluxes are assumed to be equal to the conductive fluxes at the lowest layer. This run shows that on several occasions the conductive heat flux exceeds the total heat flux both in the downward (positive) and upward (negative) directions. When the snow density is modified from 0.20 to a value of 0.16 g/cm<sup>3</sup> (Figure 20), the fit improves somewhat. The nocturnal conductive heat fluxes still at times considerably exceed the total heat fluxes. Similarly, on some days the conductive heat fluxes exceed the total fluxes.

Any further lowering of the snow density would bring it well below the estimated minimum snow density for the experiment. The ratio between the two fluxes can, however, also be changed by altering the value of  $c$  in Abels' formula. A value  $c=0.0060$  gives a reasonable fit for an assumed snow density of 0.20 g/cm<sup>3</sup> (Figure 21). This brings  $c$  outside the normally observed range

Figure 19. Run 2. Conductive and total heat fluxes.

(a.r. - above reference)

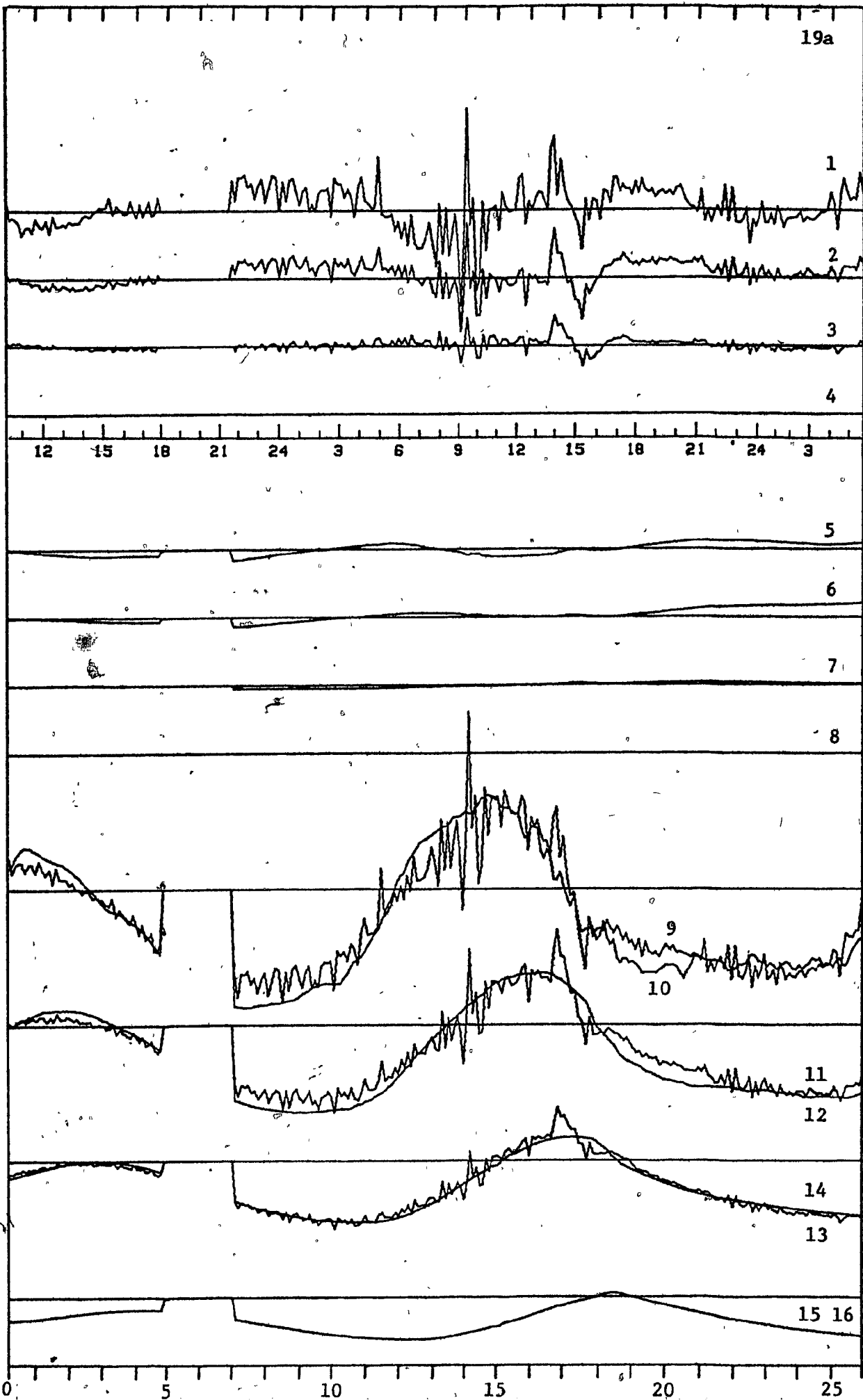
	<u>Scale</u>
1. Total minus conductive heat flux at 30 cm a.r.	1 inch - 0.02 ly min <sup>-1</sup>
2. Total minus conductive heat flux at 25 cm a.r.	1 inch - 0.02 ly min <sup>-1</sup>
3. Total minus conductive heat flux at 20 cm a.r.	1 inch - 0.02 ly min <sup>-1</sup>
4. Total minus conductive heat flux at 10 cm a.r.	1 inch - 0.02 ly min <sup>-1</sup>
5. Cumulative total of 1.	1 inch - 20.0 cal cm <sup>-2</sup>
6. Cumulative total of 2.	1/2 inch - 20.0 cal cm <sup>-2</sup>
7. Cumulative total of 3.	1 inch - 20.0 cal cm <sup>-2</sup>
8. Cumulative total of 4.	1 inch - 20.0 cal cm <sup>-2</sup>
9. Total heat flux at 30 cm a.r.	1 inch - 0.02 ly min <sup>-1</sup>
10. Conductive heat flux at 30 cm a.r.	1 inch - 0.02 ly min <sup>-1</sup>
11. Total heat flux at 25 cm a.r.	1 inch - 0.02 ly min <sup>-1</sup>
12. Conductive heat flux at 25 cm a.r.	1 inch - 0.02 ly min <sup>-1</sup>
13. Total heat flux at 20 cm a.r.	1 inch - 0.02 ly min <sup>-1</sup>
14. Conductive heat flux at 20 cm a.r.	1 inch - 0.02 ly min <sup>-1</sup>
15. Total heat flux at 10 cm a.r.	1 inch - 0.02 ly min <sup>-1</sup>
16. Conductive heat flux at 10 cm a.r.	1 inch - 0.02 ly min <sup>-1</sup>

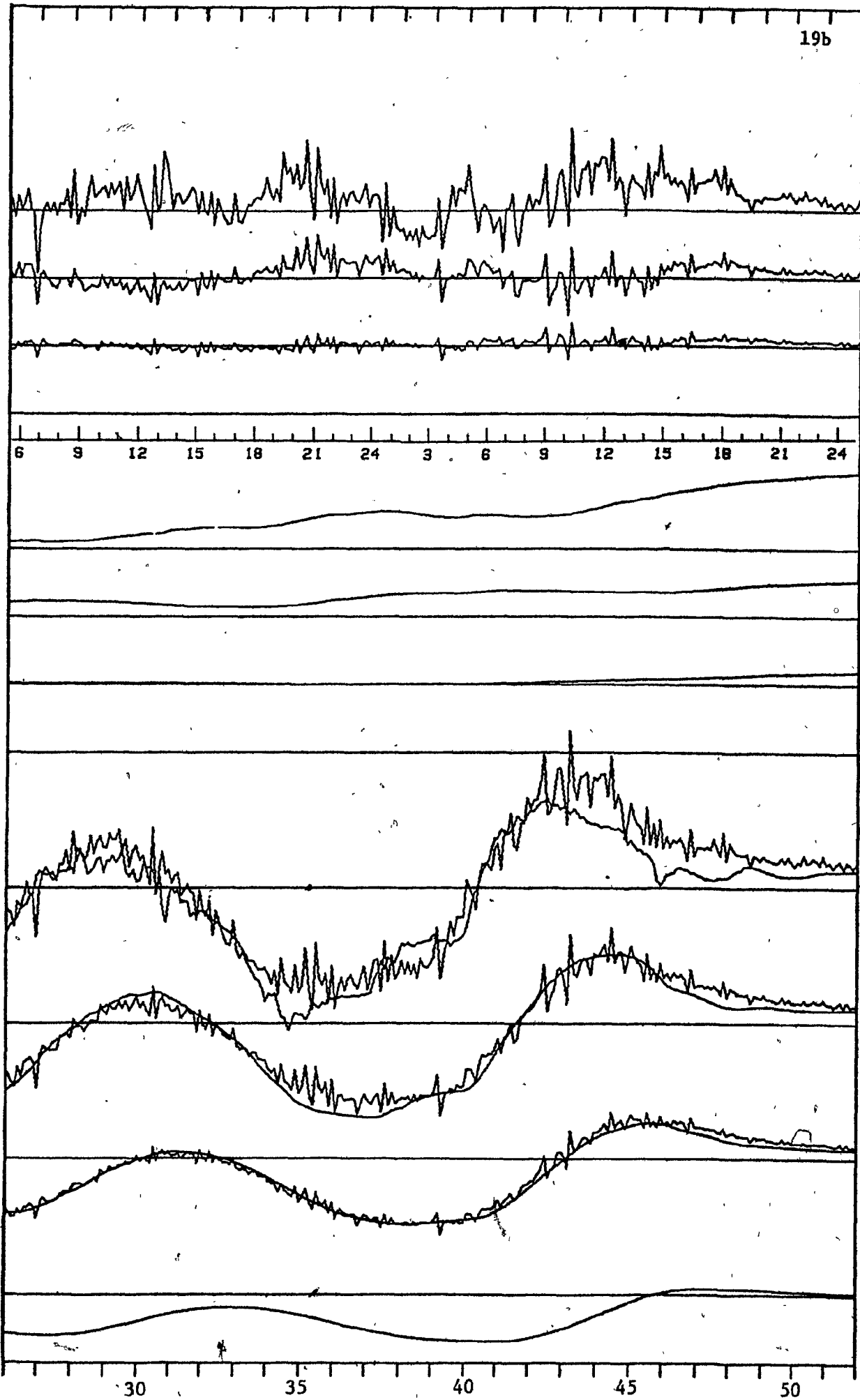
The assumed snow density is 0.2 gcm<sup>-3</sup>.

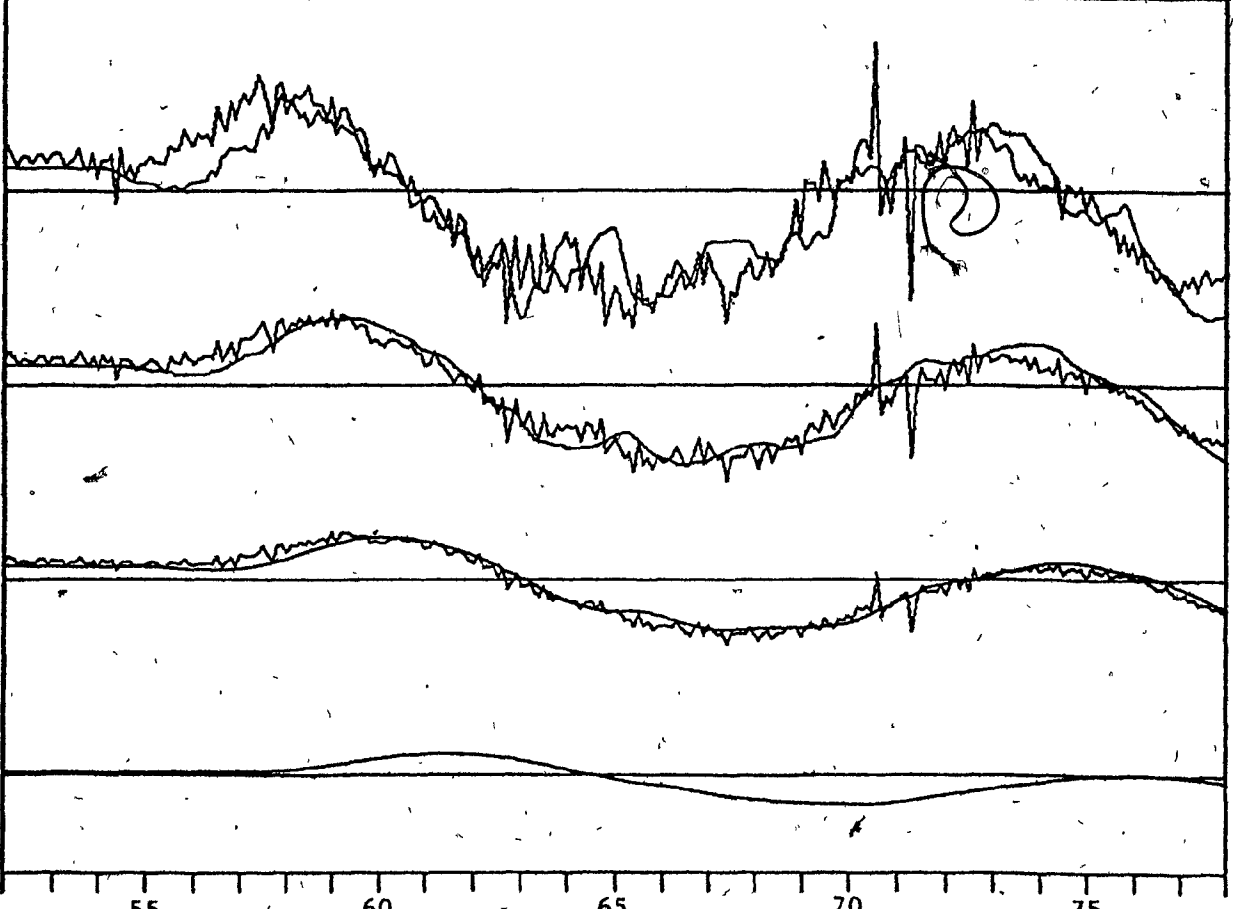
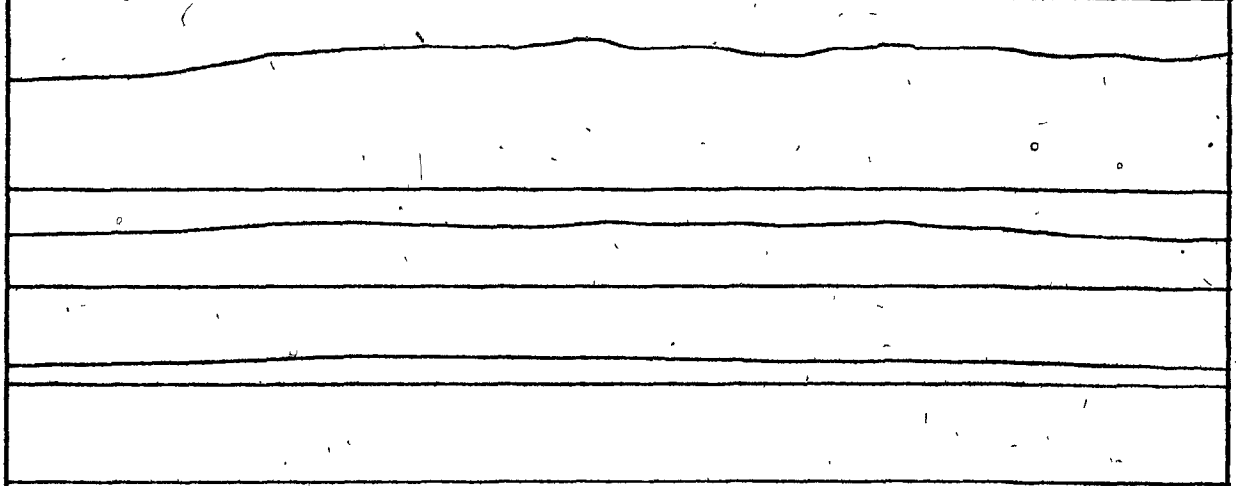
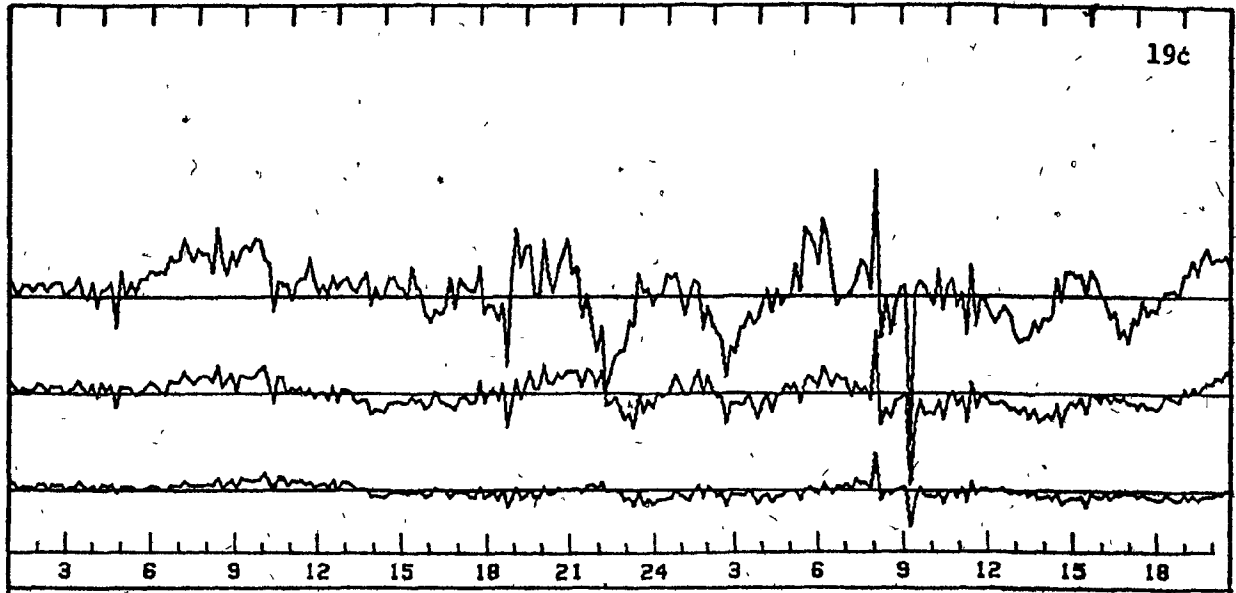
Lag adjustment is 100 minutes.

Total heat flux is set equal to the conductive heat flux at 10 cm a.r.

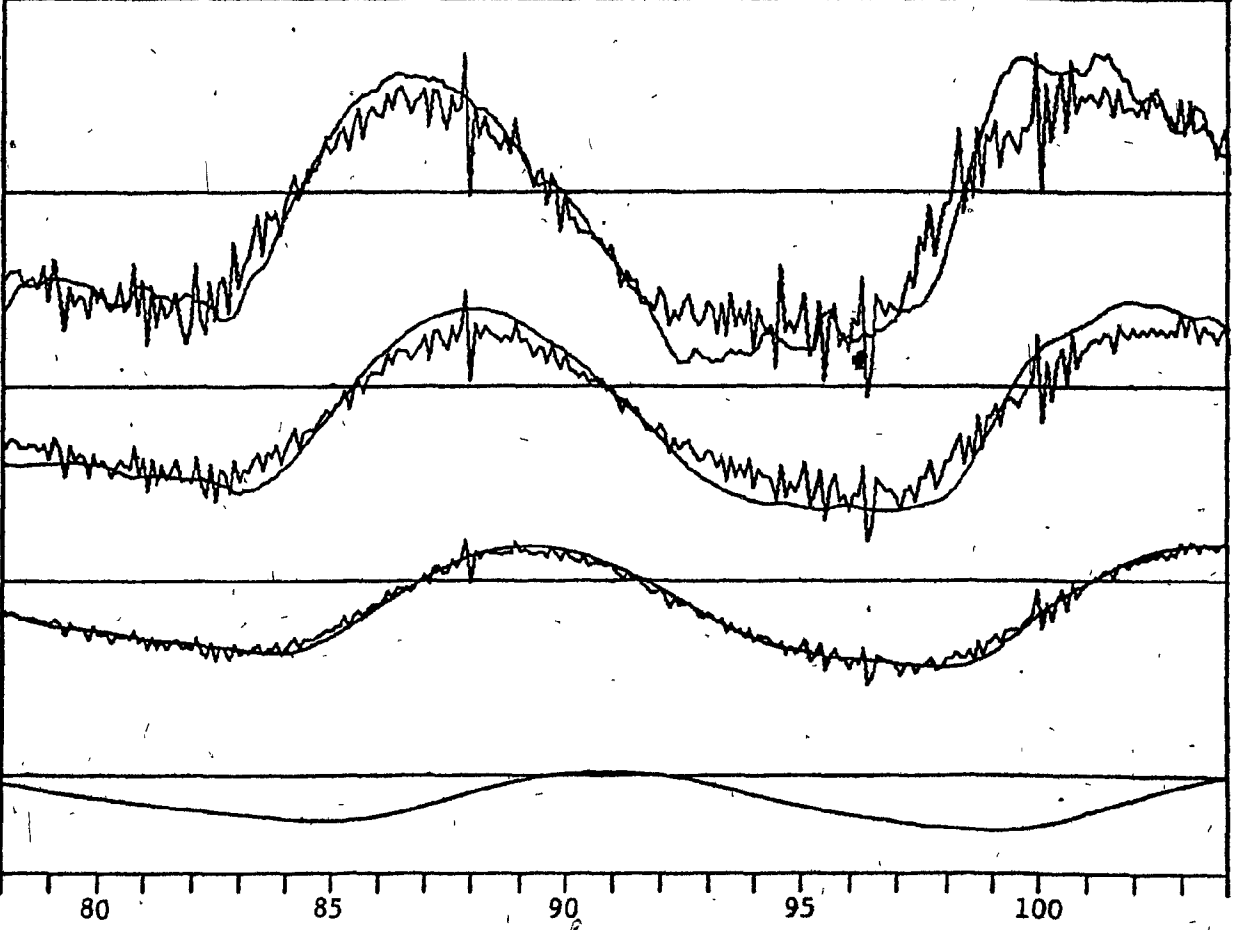
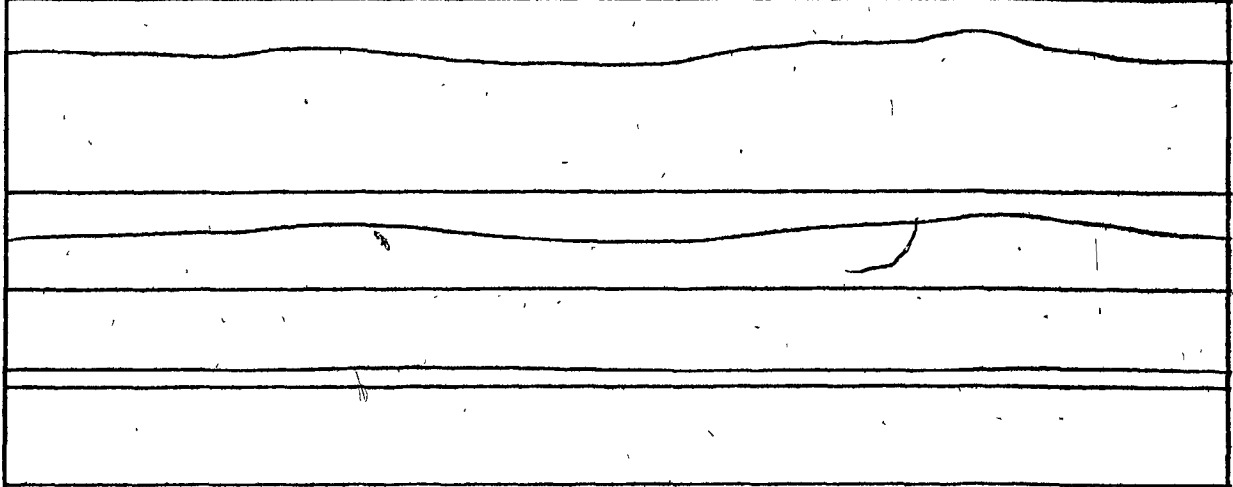
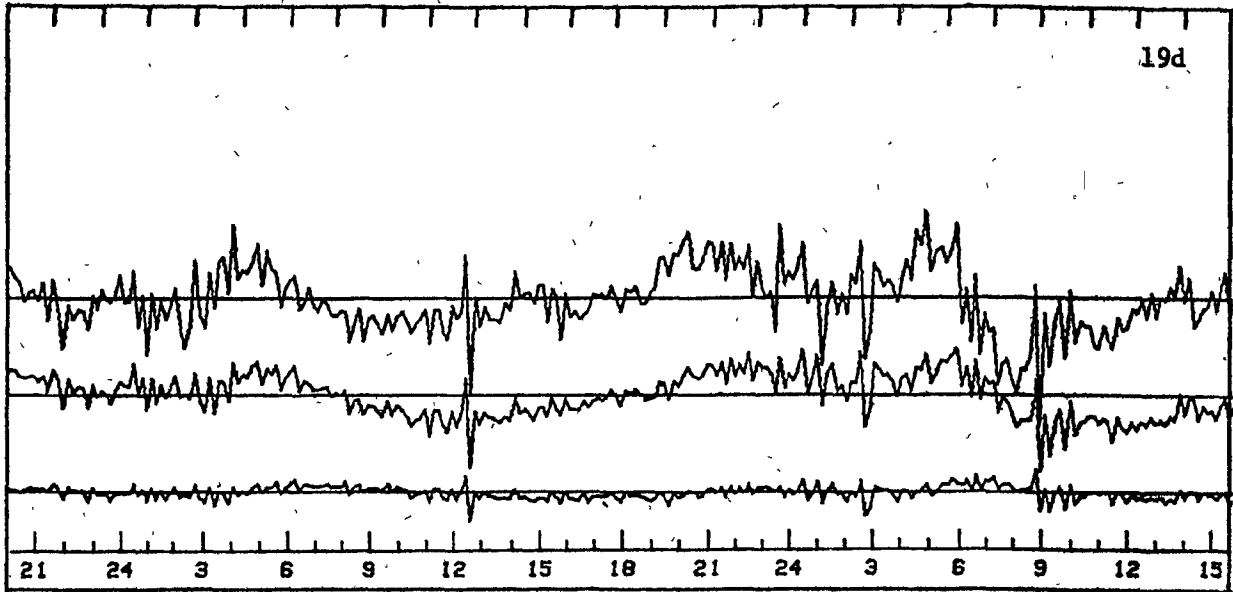
19a







19d



19e

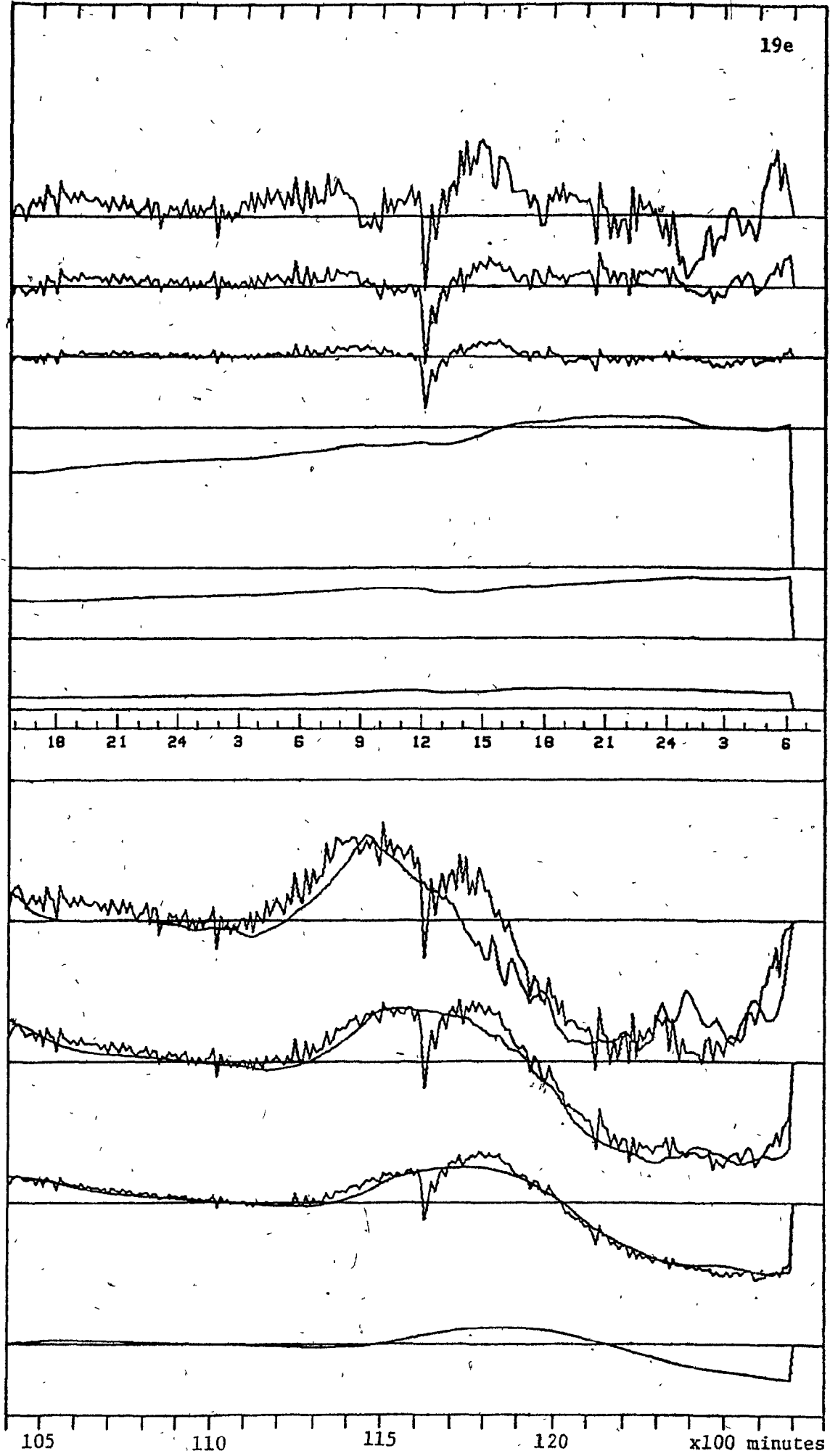


Figure 20. Run 3. Conductive and total heat fluxes.

(a.r. - above reference)

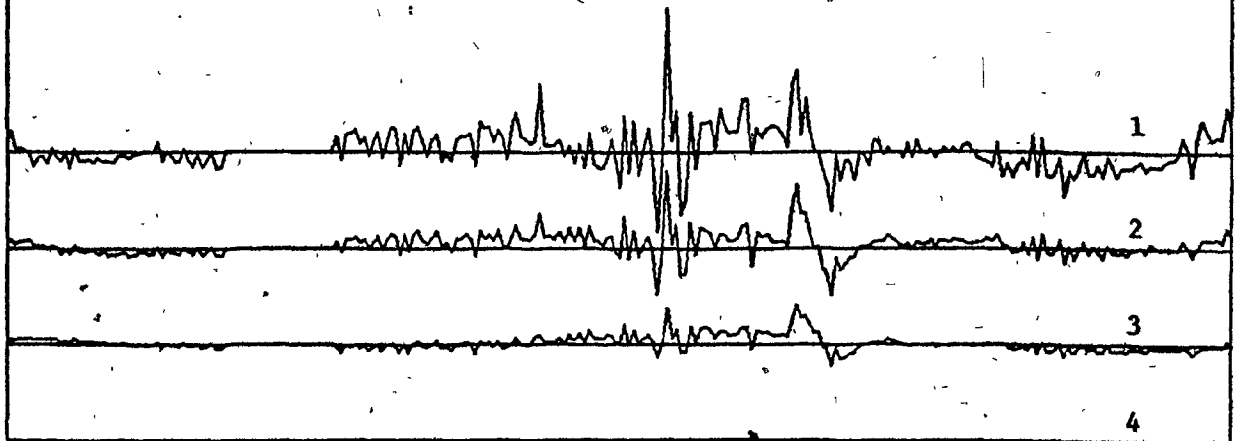
	<u>Scale</u>
1. Total minus conductive heat flux at 30 cm a.r.	1 inch - 0.02 ly min <sup>-1</sup>
2. Total minus conductive heat flux at 25 cm a.r.	1 inch - 0.02 ly min <sup>-1</sup>
3. Total minus conductive heat flux at 20 cm a.r.	1 inch - 0.02 ly min <sup>-1</sup>
4. Total minus conductive heat flux at 10 cm a.r.	1 inch - 0.02 ly min <sup>-1</sup>
5. Cumulative total of 1.	1 inch - 20.0 cal cm <sup>-2</sup>
6. Cumulative total of 2.	1 inch - 20.0 cal cm <sup>-2</sup>
7. Cumulative total of 3.	1 inch - 20.0 cal cm <sup>-2</sup>
8. Cumulative total of 4.	1 inch - 20.0 cal cm <sup>-2</sup>
9. Total heat flux at 30 cm a.r.	1 inch - 0.02 ly min <sup>-1</sup>
10. Conductive heat flux at 30 cm a.r.	1 inch - 0.02 ly min <sup>-1</sup>
11. Total heat flux at 25 cm a.r.	1 inch - 0.02 ly min <sup>-1</sup>
12. Conductive heat flux at 25 cm a.r.	1 inch - 0.02 ly min <sup>-1</sup>
13. Total heat flux at 20 cm a.r.	1 inch - 0.02 ly min <sup>-1</sup>
14. Conductive heat flux at 20 cm a.r.	1 inch - 0.02 ly min <sup>-1</sup>
15. Total heat flux at 10 cm a.r.	1 inch - 0.02 ly min <sup>-1</sup>
16. Conductive heat flux at 10 cm a.r.	1 inch - 0.02 ly min <sup>-1</sup>

The assumed snow density is 0.16 gcm<sup>-3</sup>.

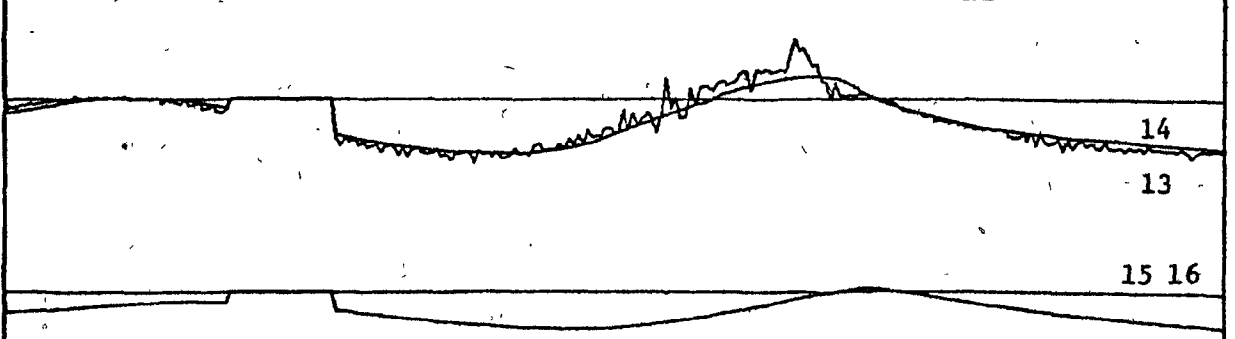
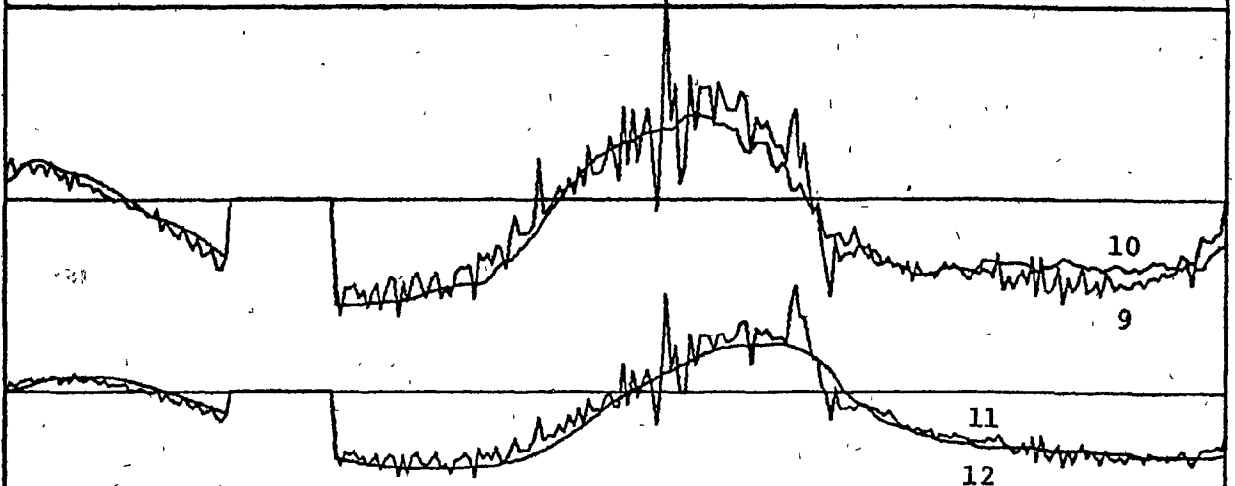
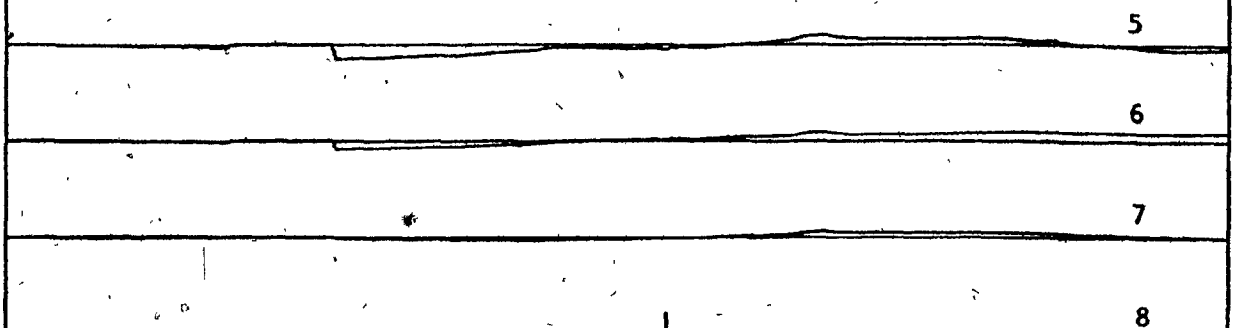
Lag adjustment is 100 minutes.

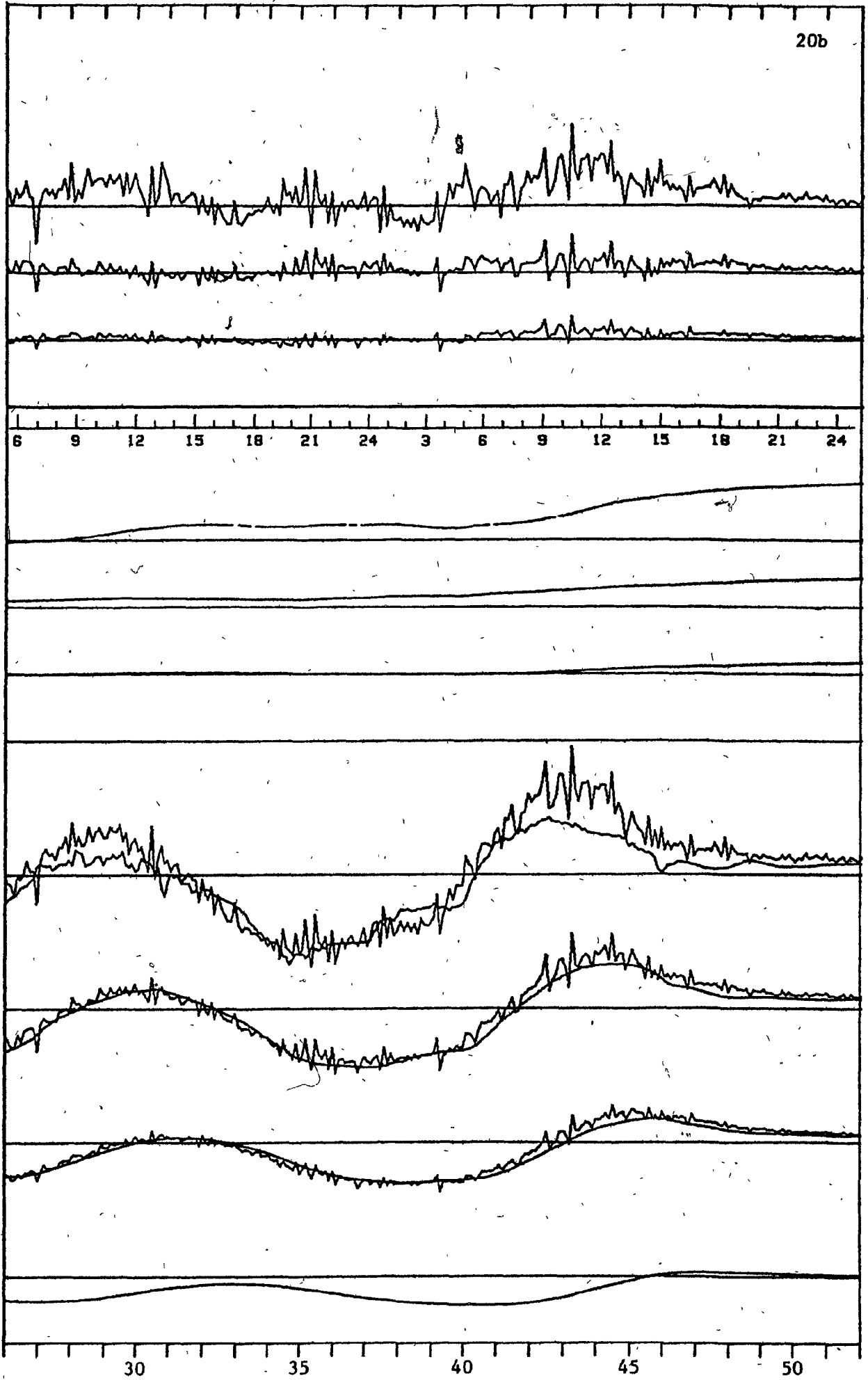
Total heat flux is set equal to the conductive heat flux at 10 cm a.r.

20a

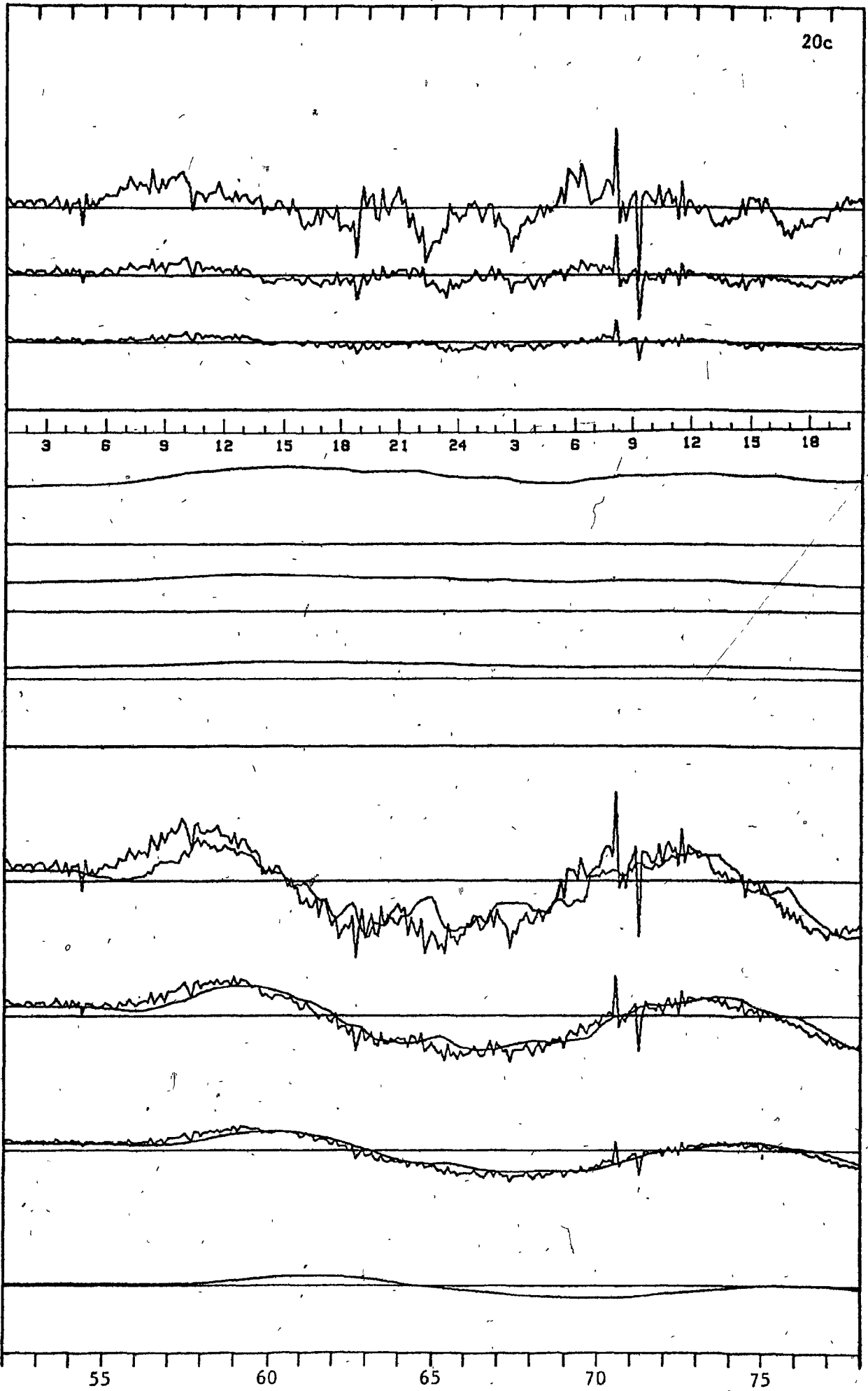


12 15 18 21 24 3 6 9 12 15 18 21 24 3

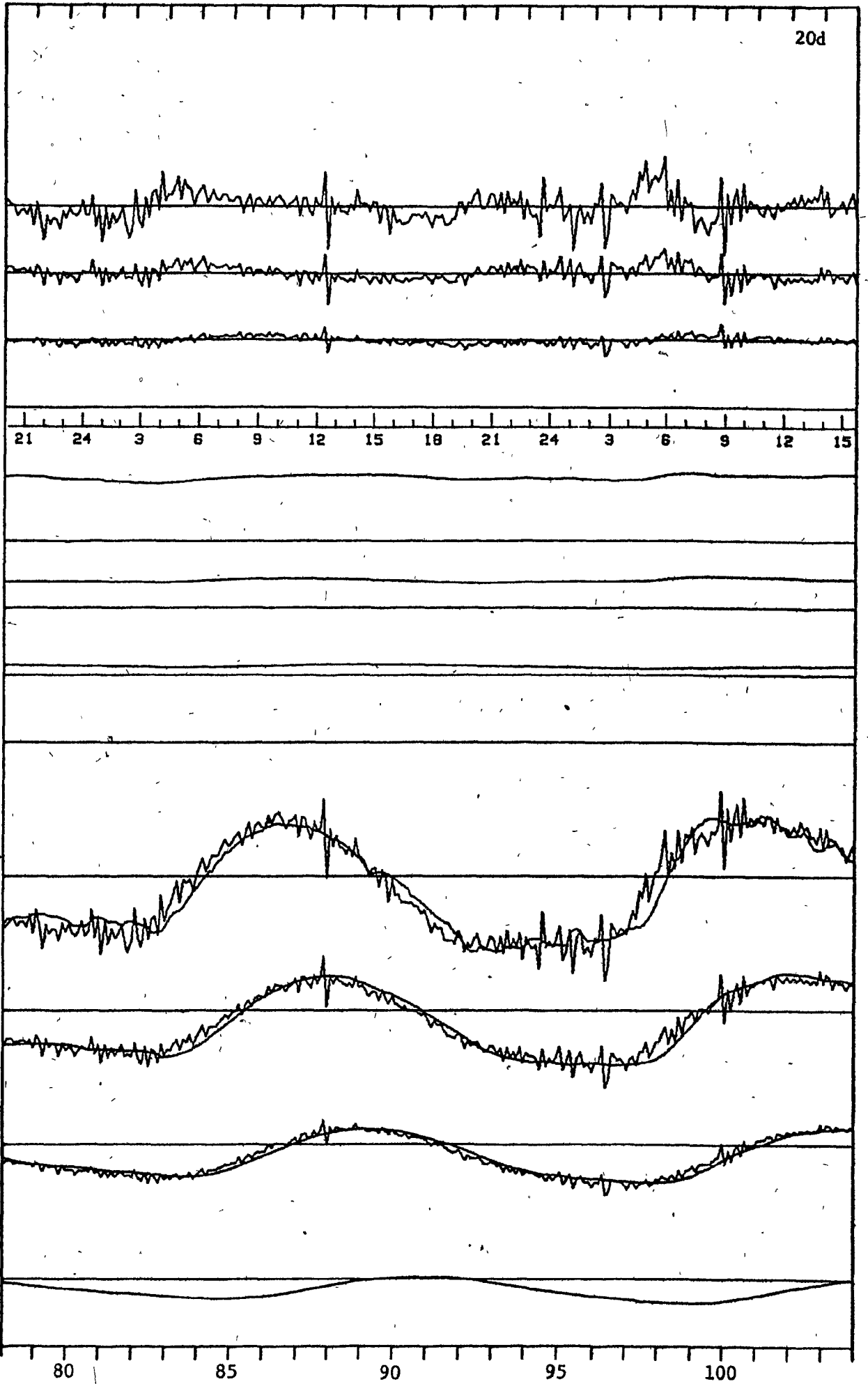




20c



20d



20e

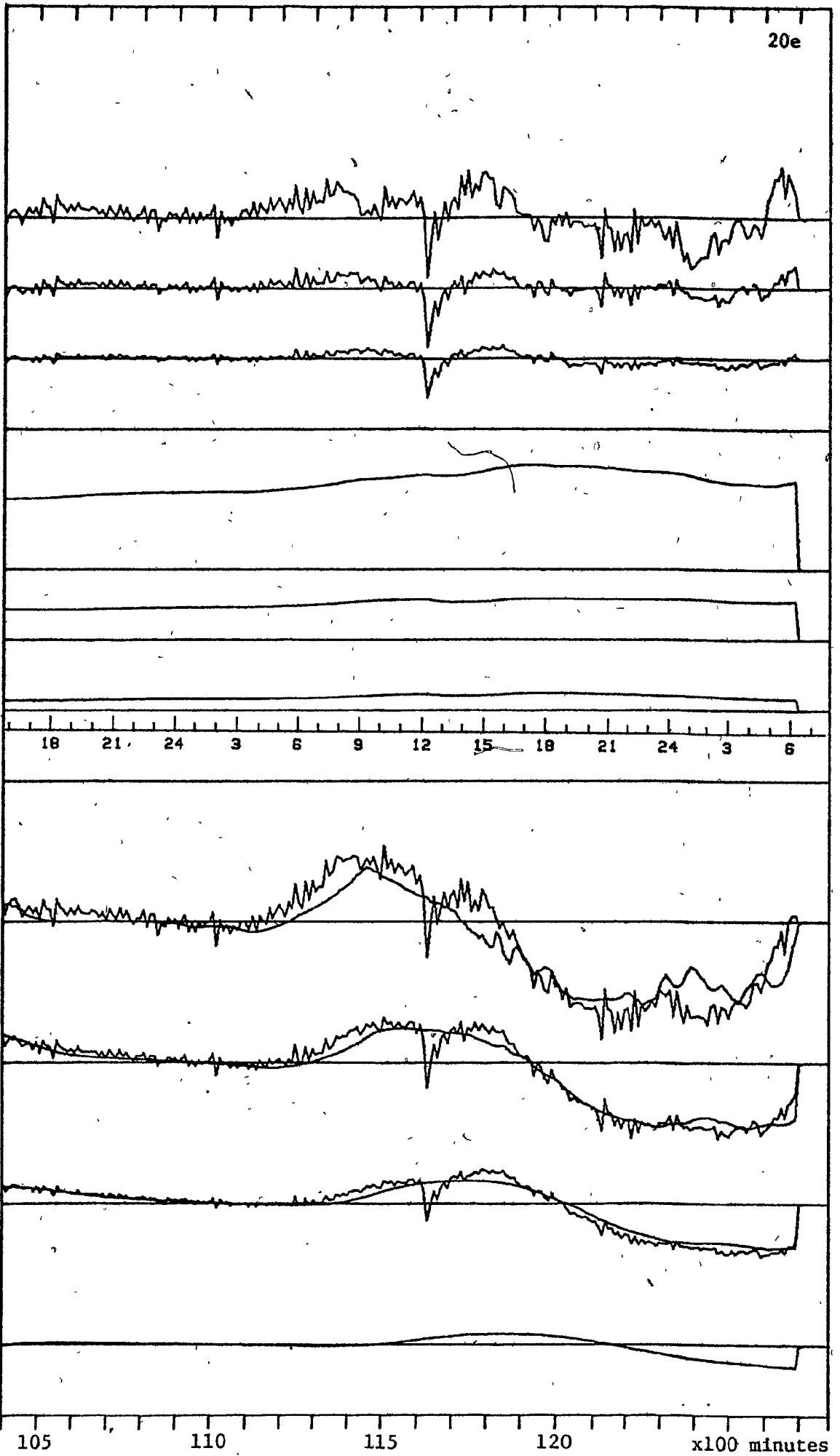


Figure 21. Run 4. Conductive and total heat fluxes.

(a.r. - above reference)

	<u>Scale</u>
1. Total minus conductive heat flux at 30 cm a.r.	1 inch - $0.02 \text{ ly min}^{-1}$
2. Total minus conductive heat flux at 25 cm a.r.	1 inch - $0.02 \text{ ly min}^{-1}$
3. Total minus conductive heat flux at 20 cm a.r.	1 inch - $0.02 \text{ ly min}^{-1}$
4. Total minus conductive heat flux at 10 cm a.r.	1 inch - $0.02 \text{ ly min}^{-1}$
5. Cumulative total of 1.	1 inch - $20.0 \text{ cal cm}^{-2}$
6. Cumulative total of 2.	1 inch - $20.0 \text{ cal cm}^{-2}$
7. Cumulative total of 3.	1 inch - $20.0 \text{ cal cm}^{-2}$
8. Cumulative total of 4.	1 inch - $20.0 \text{ cal cm}^{-2}$
9. Total heat flux at 30 cm a.r.	1 inch - $0.02 \text{ ly min}^{-1}$
10. Conductive heat flux at 30 cm a.r.	1 inch - $0.02 \text{ ly min}^{-1}$
11. Total heat flux at 25 cm a.r.	1 inch - $0.02 \text{ ly min}^{-1}$
12. Conductive heat flux at 25 cm a.r.	1 inch - $0.02 \text{ ly min}^{-1}$
13. Total heat flux at 20 cm a.r.	1 inch - $0.02 \text{ ly min}^{-1}$
14. Conductive heat flux at 20 cm a.r.	1 inch - $0.02 \text{ ly min}^{-1}$
15. Total heat flux at 10 cm a.r.	1 inch - $0.02 \text{ ly min}^{-1}$
16. Conductive heat flux at 10 cm a.r.	1 inch - $0.02 \text{ ly min}^{-1}$

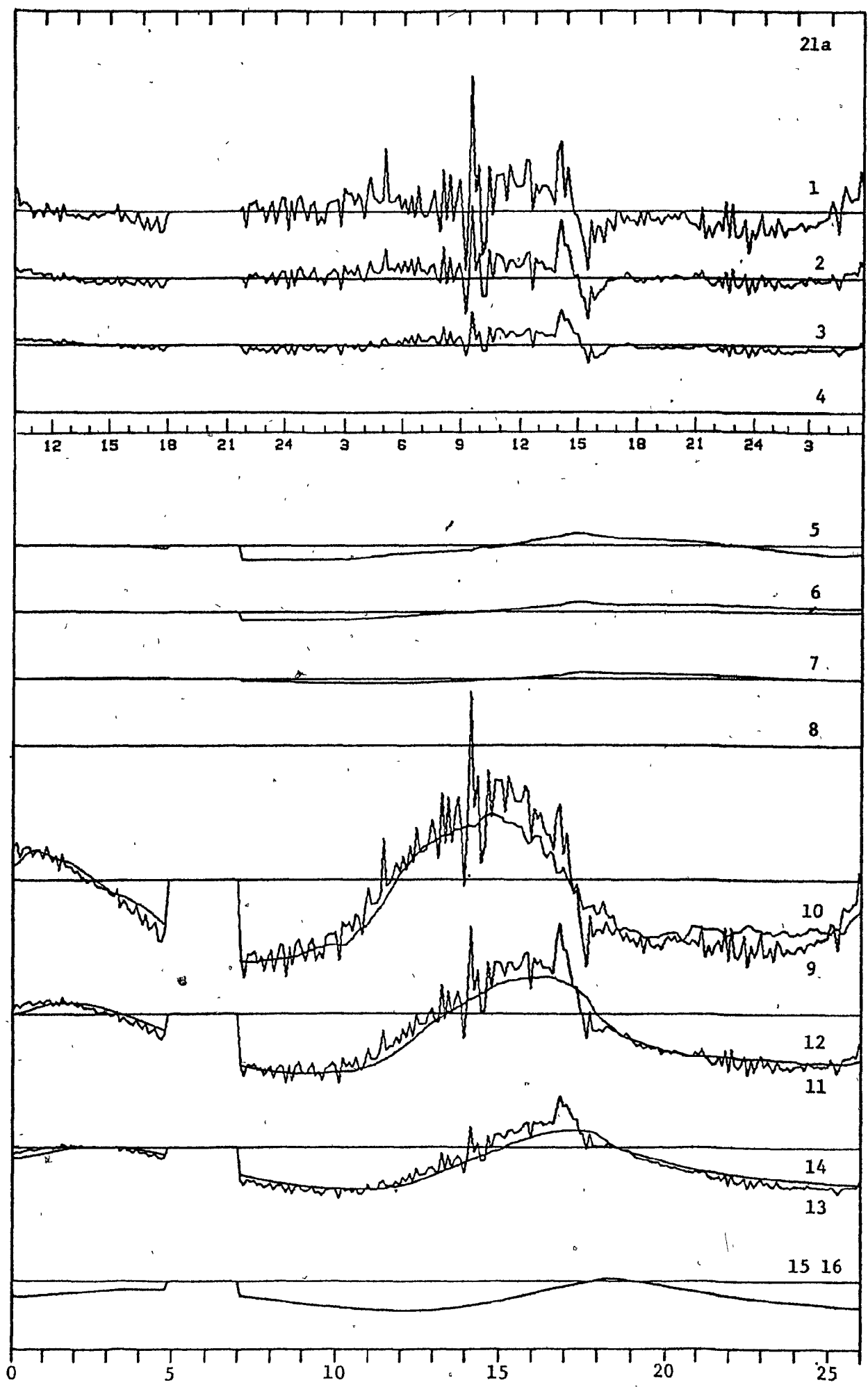
The assumed snow density is  $0.2 \text{ gcm}^{-3}$ .

Lag adjustment is 100 minutes.

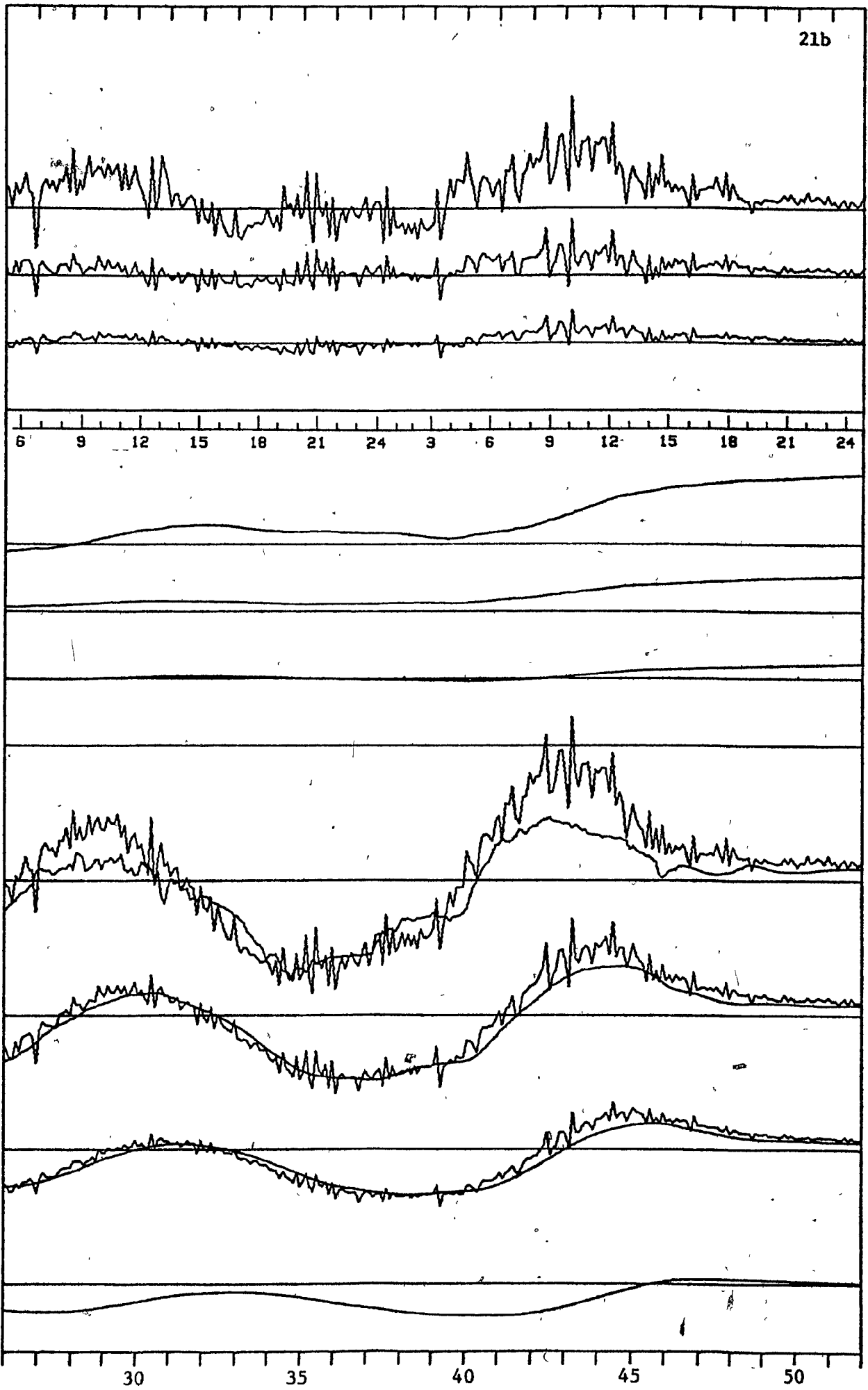
Total heat flux is set equal to the conductive heat flux at 10 cm a.r.

The constant used is 0.0060.

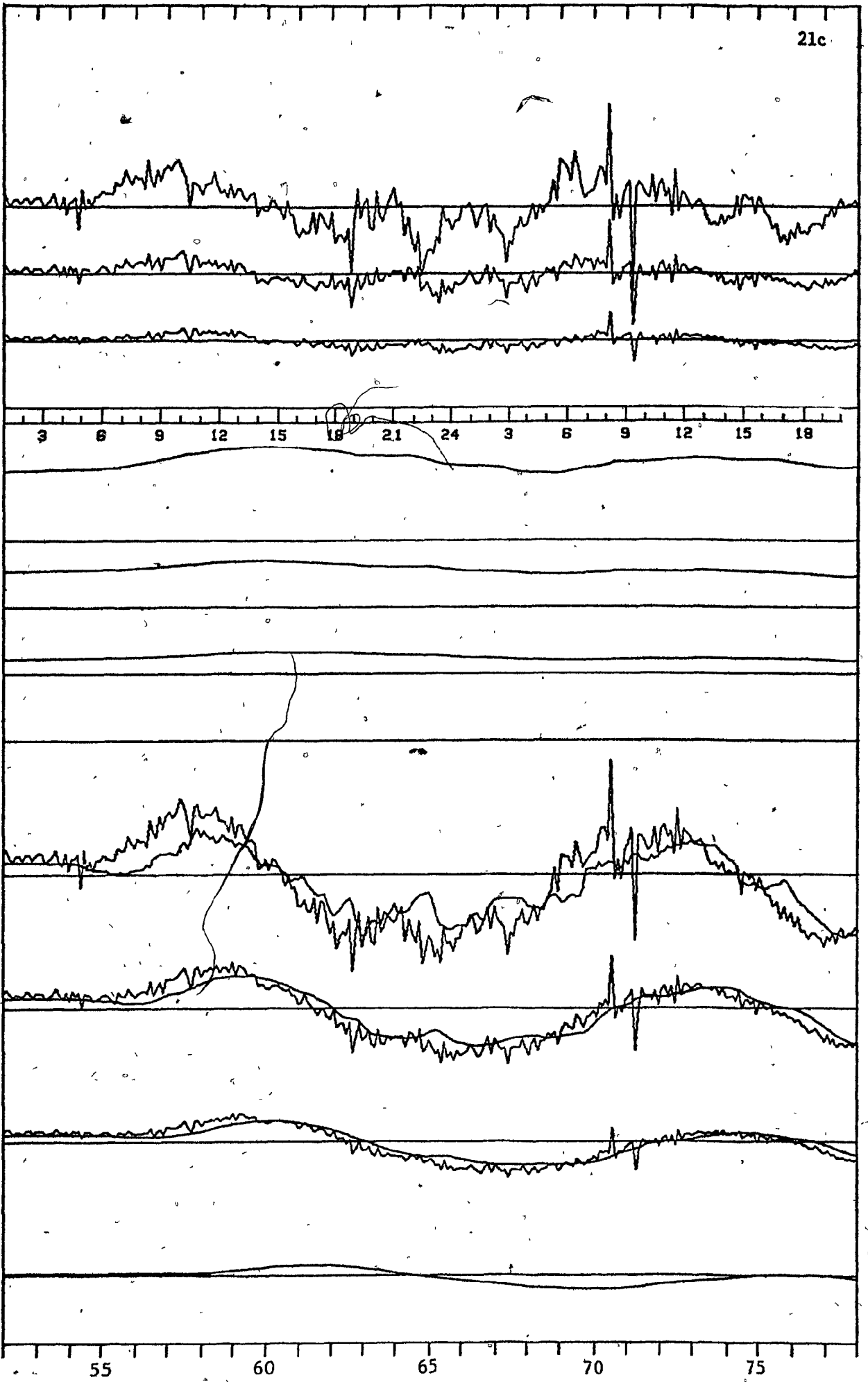
21a



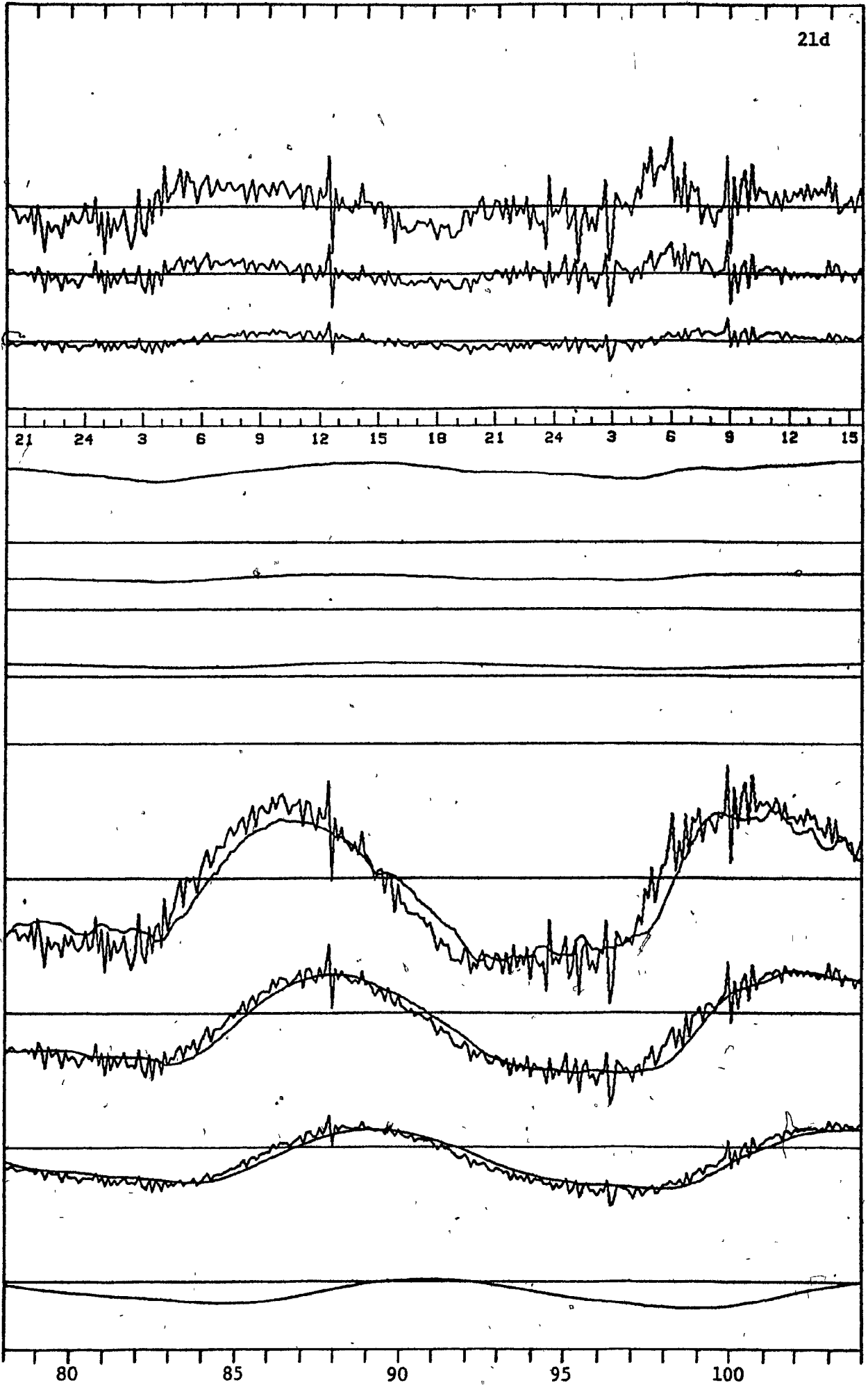
21b



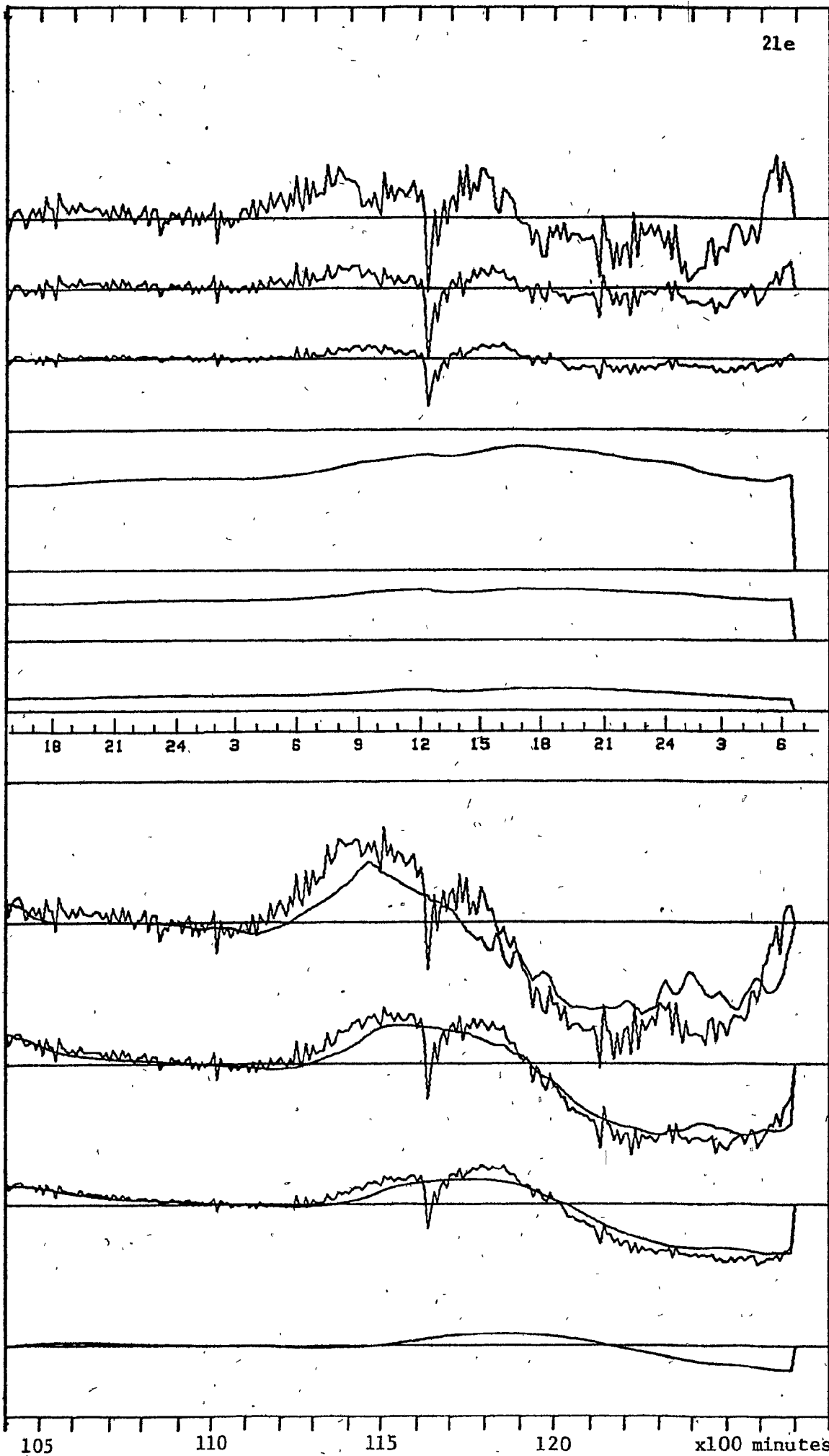
21c



21d



21e



of 0.0068 to 0.0085, possibly as a result of the flux equalization at the base.

Heat gains due to absorption of shortwave radiation are apparent in the form of daytime total heat fluxes exceeding the conductive heat flux. However, if the heating were by radiant absorption only, it would decline much more rapidly with depth than is presently indicated. It is quite possible that the observed heating is related to snowpack ventilation and is caused by downwards redistribution of radiant heat absorbed in the near-surface layers of the snow cover. Although the thermal effects of ventilation appear to be relatively small, Figure 21 shows that ventilation cannot be discounted as unimportant to heat transfers through the snow cover. From about 4000 minutes to about 6000 minutes, a period of warm air advection and fairly high wind speeds, the total heat gain of the snow cover was consistently about 20 to 50 per cent greater than the heat gain by conduction. The net radiation during the night falling within that period was close to zero, and the snow surface temperature was warmer than the temperature inside the snow cover. Another, similar, occasion is in the evening between 10600 minutes and 10800 minutes when, again, the surface temperature was warmer than the internal parts.

There is an apparent strong response to variations in net radiation at night. This response, however, is more apparent than real and is caused by an excessive lag between the two

fluxes. If the lag is reduced to 20 minutes, the effect disappears (Figure 22). This is probably a more appropriate lag for the presently used constants than the 100-minute lag determined for the initial run. The variation in lag time is a result of the assumed lower boundary condition, as previously mentioned.

The reduction in lag time enhances the appearance of absorption of solar radiation. It also adjusts the timing of the radiant absorption to correspond better with astronomic reality. One interesting pattern appears in this figure, namely that the two windiest days are also the two days when the greatest differences between the conductive and non-conductive heat fluxes occur. The effect extends through the entire depth of the snowpack. This may be the previously discussed effect of ventilation redistributing downwards into the snow cover radiant heat absorbed near the surface.

The periods of non-conductive heat gain coincide with the periods of increased variation in the first and second derivatives of temperature (Chapter W). Because of the uncertainty introduced by the various assumptions used, however, this coincidence may be fortuitous.

There are several events when there is a close temporal correspondence between the differences between the total and conductive heat fluxes for different depths within the snow cover. This is valid for fluctuations of both long and short

Figure 22: Run 5. Conductive and total heat fluxes.

(a.r. - above reference)

	<u>Scale</u>
1. Total minus conductive heat flux at 30 cm a.r.	1 inch - 0.02 ly min <sup>-1</sup>
2. Total minus conductive heat flux at 25 cm a.r.	1 inch - 0.02 ly min <sup>-1</sup>
3. Total minus conductive heat flux at 20 cm a.r.	1 inch - 0.02 ly min <sup>-1</sup>
4. Total minus conductive heat flux at 10 cm a.r.	1 inch - 0.02 ly min <sup>-1</sup>
5. Cumulative total of 1.	1 inch - 20.0 cal cm <sup>-2</sup>
6. Cumulative total of 2.	1 inch - 20.0 cal cm <sup>-2</sup>
7. Cumulative total of 3.	1 inch - 20.0 cal cm <sup>-2</sup>
8. Cumulative total of 4.	1 inch - 20.0 cal cm <sup>-2</sup>
9. Total heat flux at 30 cm a.r.	1 inch - 0.02 ly min <sup>-1</sup>
10. Conductive heat flux at 30 cm a.r.	1 inch - 0.02 ly min <sup>-1</sup>
11. Total heat flux at 25 cm a.r.	1 inch - 0.02 ly min <sup>-1</sup>
12. Conductive heat flux at 25 cm a.r.	1 inch - 0.02 ly min <sup>-1</sup>
13. Total heat flux at 20 cm a.r.	1 inch - 0.02 ly min <sup>-1</sup>
14. Conductive heat flux at 20 cm a.r.	1 inch - 0.02 ly min <sup>-1</sup>
15. Total heat flux at 10 cm a.r.	1 inch - 0.02 ly min <sup>-1</sup>
16. Conductive heat flux at 10 cm a.r.	1 inch - 0.02 ly min <sup>-1</sup>

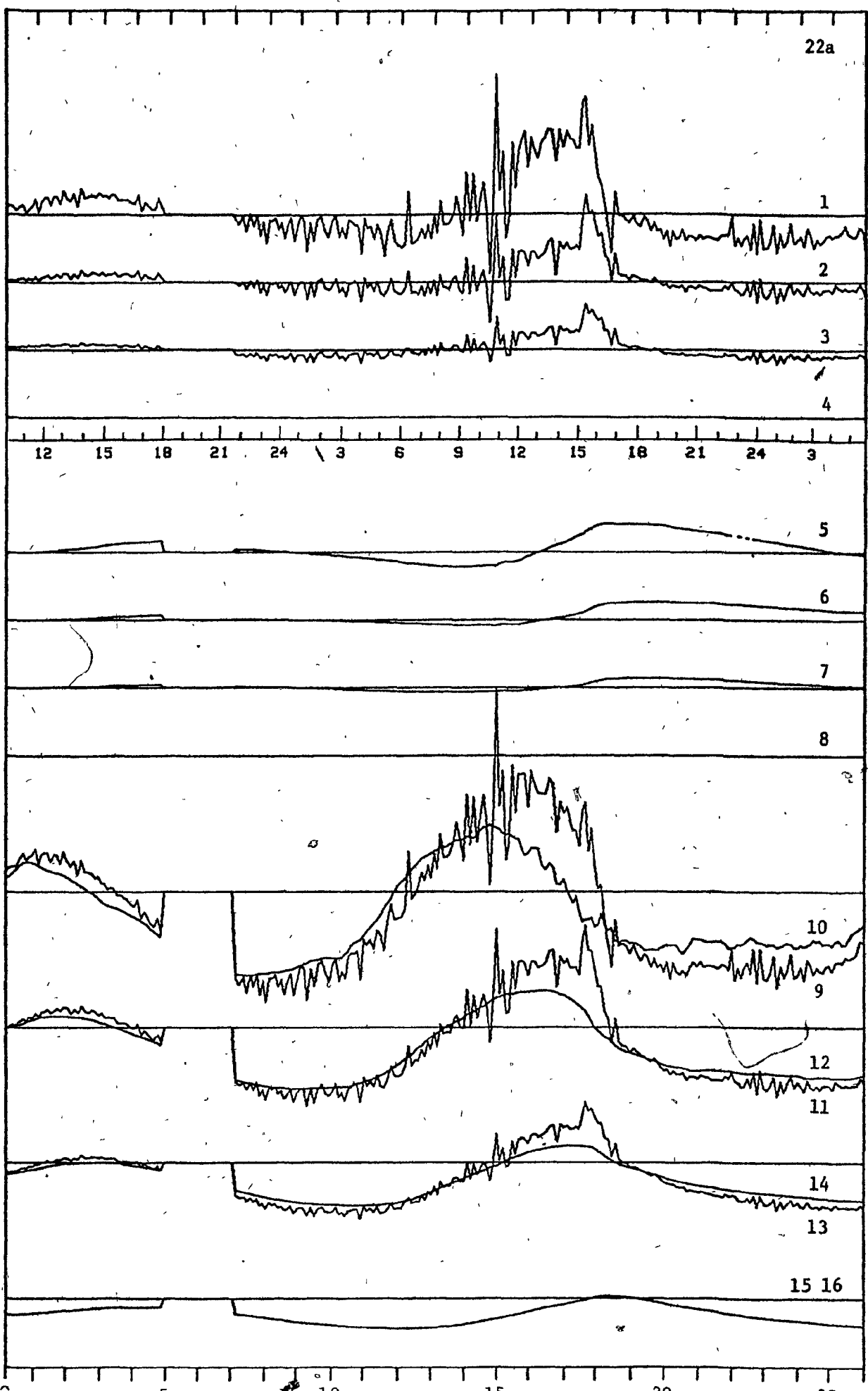
The assumed snow density is 0.2 gcm<sup>-3</sup>.

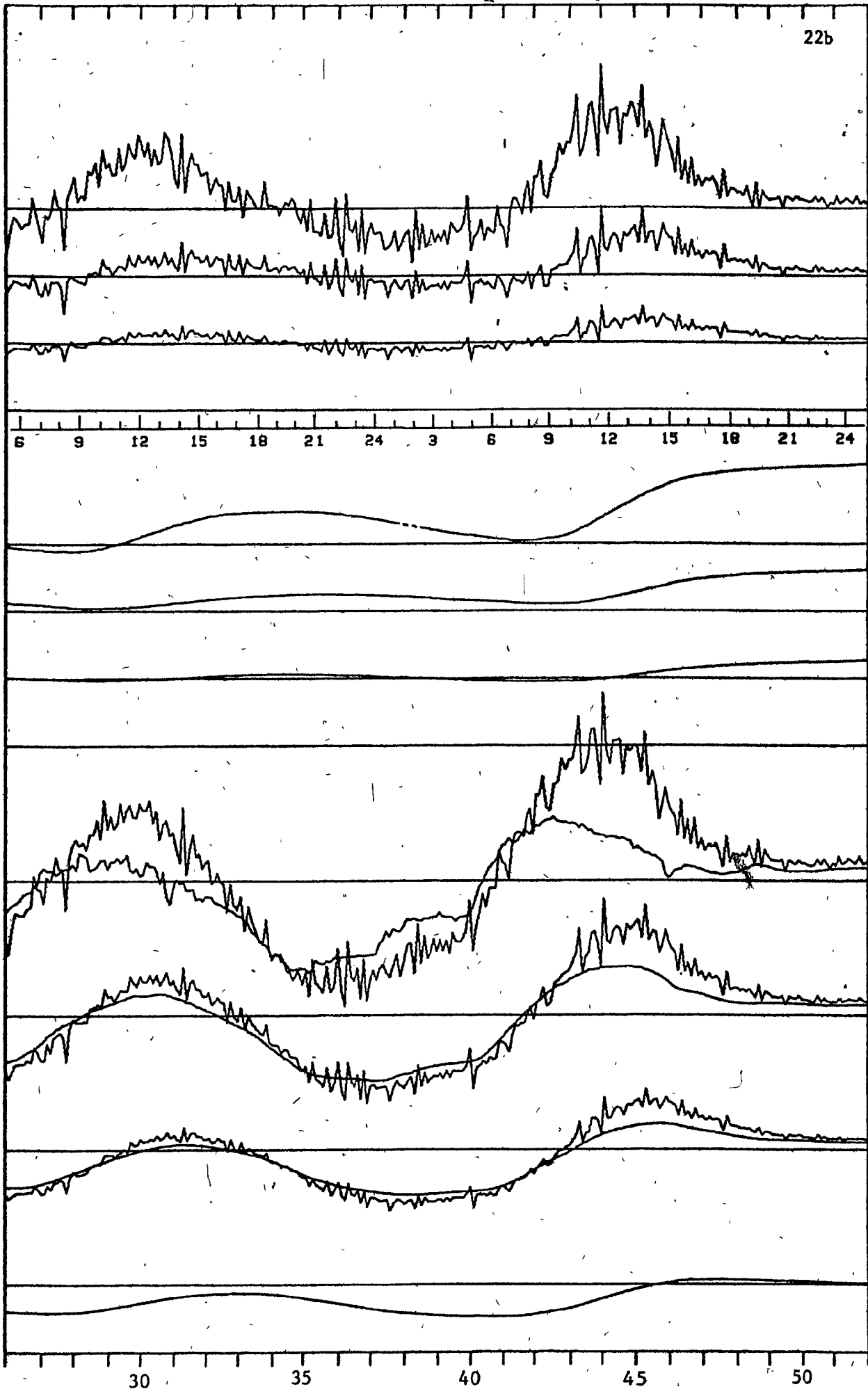
Lag adjustment is 20 minutes.

Total heat flux is set equal to the conductive heat flux at 10 cm a.r.

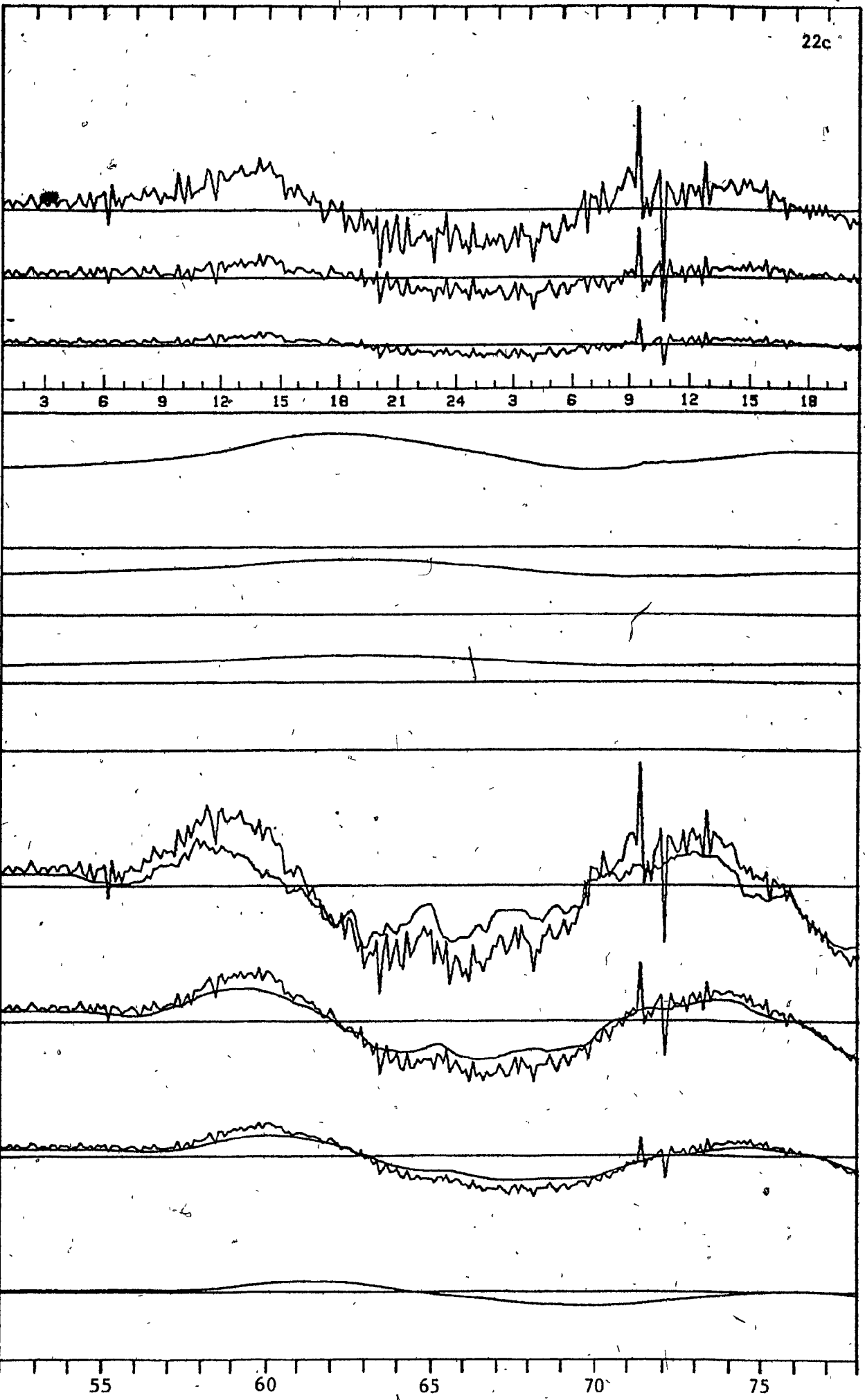
The constant used is 0.0060.

22a

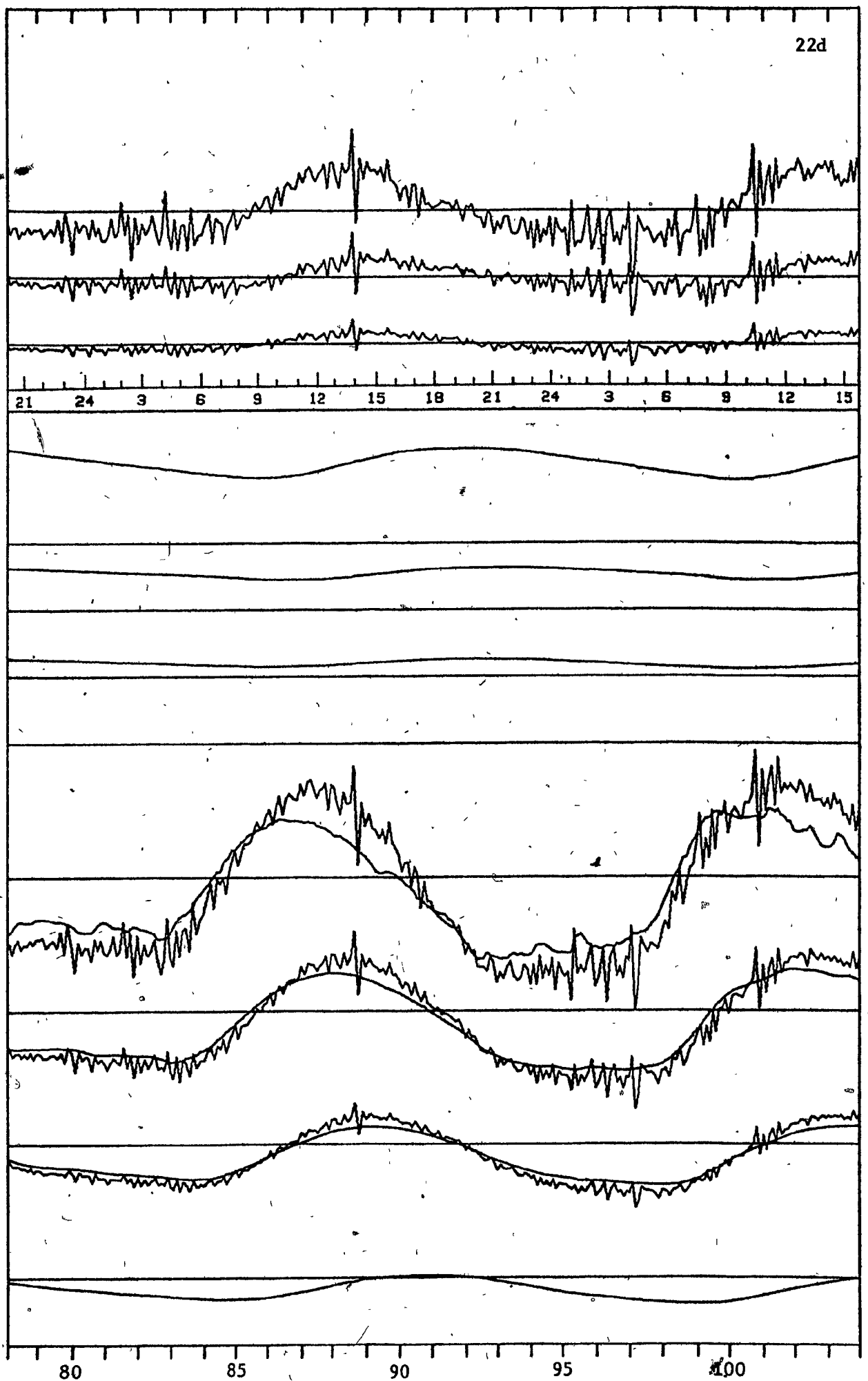




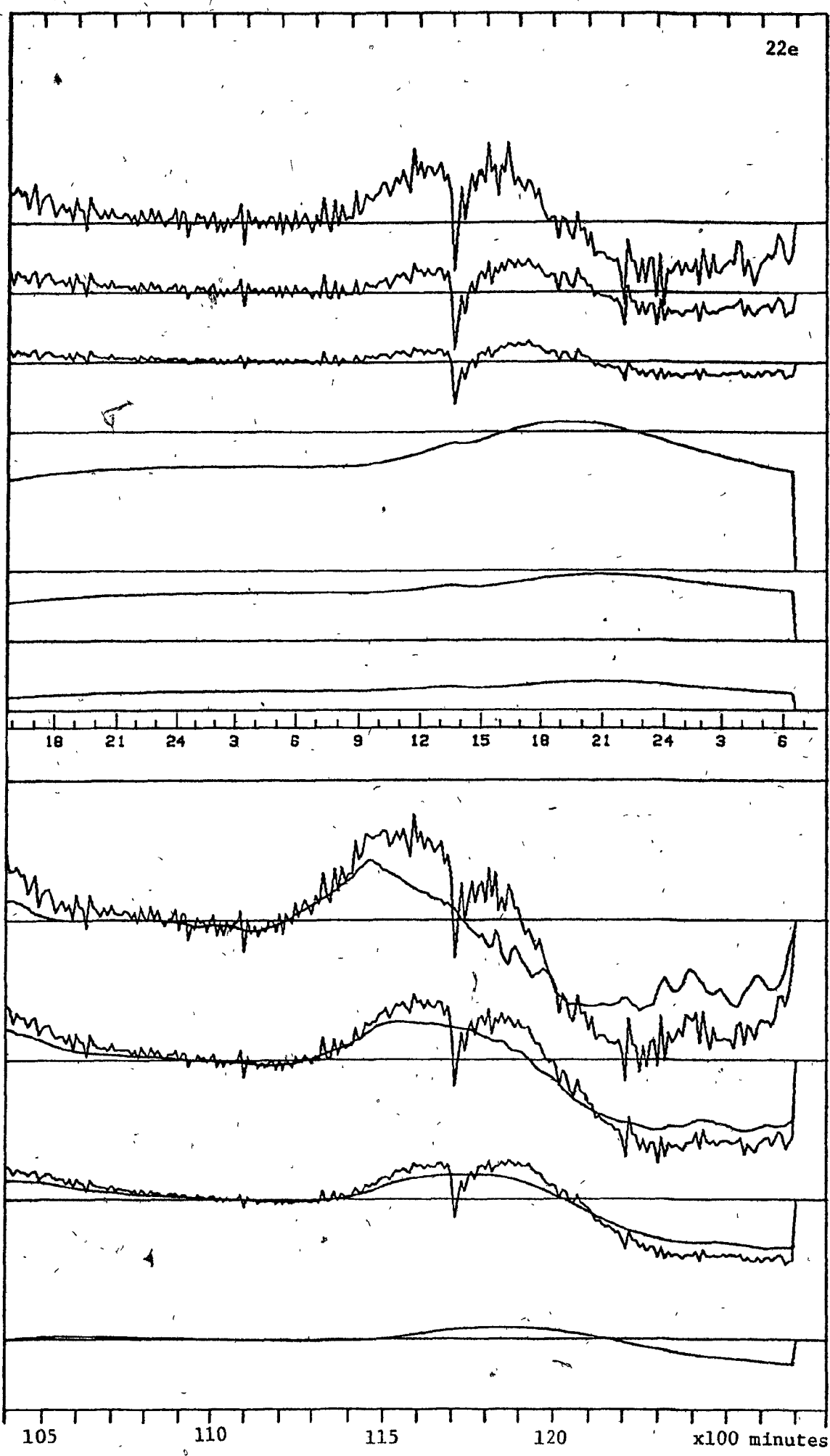
22c



22d



22e



wavelength. This would suggest that the differences are related either to the error introduced by the equalization of the two fluxes at the lowest level or that they are related to ventilation events, simultaneously effective throughout the snowpack. Neither the timing, nor the direction of the differences at the lowest level, however, coincide with the aforementioned pattern, so the pattern is not caused by the artificial equalization of the fluxes at the lowest level. The pattern may thus be related to snowpack ventilation.

One such event occurred at approximately 1800 minutes when a large, positive difference between the conductive and total heat fluxes suddenly changed to a much smaller difference. Not much in the backup information can explain this sudden change. There is a decrease both in windspeed and in wind gustiness at the time and also a decrease in net radiation. However, such events occurred on most afternoons throughout the period of measurement without producing the same spectacular effect. There is, however, also a sharp drop in the temperature difference between the snow surface and the air at 30 cm above the surface that coincides with this particular event. The absolute value of the temperature difference is unknown because of the previously discussed instrument trouble but the relative change in temperature is a real one. The change is from an unstable to a less unstable thermal stratification in the near-surface layer of the air. Coincident with this event there is also a drop in the

relative humidity of the air at screen level. Since the near-surface temperature was higher than the temperature of the lower parts of the snow cover, ventilation would produce a heat gain. The surface temperature also drops sharply at the same time as the change in difference between the two fluxes occurs, possibly as a result of the changing radiation balance, but more likely as a result of cooling by evaporation, caused by the reduced relative humidity of the air. The simultaneity of the change at the different levels suggests that the sudden change in the difference between the total and the conductive fluxes is the result of a sudden reduction in snowpack ventilation.

An event at 1500 minutes is shown as a marked fluctuation in the difference between the two fluxes that extends throughout the snowpack. There were coincident variations in both net radiation, wind speed and relative humidity of the air at this time. A similar event at 7150 minutes is similarly accompanied by fluctuations in windspeed, net radiation and a drop in relative humidity. In addition, there is a reversal in the temperature gradient between the surface and 30 cm above the surface. The change was from unstable to stable stratification and the temperature distribution was such that ventilation would increase the heat gain by the snowpack. These events also suggest effects of snowpack ventilation.

It is evident that many of the observed fluctuations that penetrate through the snow cover are related to events above the

snow surface. However, there is no clear relationship between the difference between the two fluxes and the above-snow events as was anticipated. At times there is an apparent relationship to changes in wind, temperature gradient and relative humidity. On many occasions, however, there are large changes in wind speed with no apparent response in the difference between the two fluxes. On other occasions there is covariance between wind speed variations and variations in the flux differences.

CHAPTER VII  
CONCLUSIONS AND RECOMMENDATIONS

1. Conclusions

A new snow thermometer was designed and manufactured in order to investigate the temporal patterns of snowpack ventilation. The design was successful and enabled an accurate set of snow temperature measurements to be taken through a set of diurnal cycles that include an event of snow surface melting. The high resolution of the temperature measurements allowed some new observations to be made regarding snowpack temperatures.

The study shows that there are temporal variations in temperature inside a snow cover that cannot be explained in terms of conductive or radiative heat fluxes. It is concluded that they are caused by air movements inside the snow.

The thermal effects of the air movements show two distinct patterns. One is particularly apparent in the daytime when the snow surface temperature is near its daily maximum. This coincides with the least stable density stratification of the air immediately above the surface. The pattern thus supports the notion that the surface pressure field drives the air motion inside the snow.

There is a second pattern of irregular changes in temperature that occur at night. This pattern coincides with

steep negative temperature gradients in the snow cover and appears to be caused by the unstable density stratification in the snow cover. This is in agreement with conclusions reached by Bergen (1963).

The relationship between wind above the surface and air movements inside the snow cover is not a simple one. The theory proposed in this thesis suggests that an increase in windspeed may not necessarily result in an increased ventilation rate, but that there may, in fact, be a decrease in ventilation rate beyond a certain, perhaps fairly low, wind speed. The theory also suggests that vapor transfer mechanisms may produce negative feedbacks to ventilation in the presence of steep temperature gradients. It was, however, not possible to verify these aspects of the theory using the present data set.

The snow thermometer design does not encourage downward percolation of meltwater along the sensor array. This allows accurate temperature measurements to be made even when parts of the snow cover are melting. Thus, a temperature maximum of -1.4 degrees C was recorded at 5 centimeters below the surface during a brief period of surface and near surface melt. There was a well developed zero curtain effect during this period.

The data set shows one event of percolation of meltwater from a melting near-surface layer through a snow cover that is well below the freezing point. The mechanism of such percolation has been discussed by Wankiewicz (1976) but it is the first time

that the associated thermal events have been recorded in a natural setting.

It was possible to determine, with reasonable accuracy, the heat balance of the snow cover over 10-minute intervals. The measurements show that although the snow cover may absorb only some 20 per cent of the incident solar radiation, only a small portion of the absorbed radiation is actually used to elevate the temperature of the snow cover itself. A major portion of the absorbed radiation is used to heat the air above the snow. This is accomplished, at least in part, by ventilation of the uppermost few centimeters of the snow cover where most of the radiant absorption occurs. Ventilation of the uppermost few centimeters of the snow cover is suggested as a complement and, perhaps, an alternative to Ohmura's (1980) surface absorption hypothesis. This hypothesis was put forward to explain why the near-surface layers of the snow cover do not melt despite the large amount of solar radiation absorbed by the snow cover.

Snow surface temperatures were monitored with good accuracy. The data set shows rapid temporal variations which are particularly marked at night, in near-calm conditions. A test of three methods of estimating snow surface temperatures indicated that screen air temperature is generally the best estimator. At night, in calm conditions with clear skies, the screen dewpoint temperature is the best estimator. In windy conditions, at night, the best estimate is often given by the screen wet-bulb

temperature.

## 2. Suggested Modification of the Snow Thermometer

The present thermometer suffered from a design error which was due to an assumption, based on available literature, that the temperature variations at the base of the snow cover would be negligible. It was assumed that semi-linear interpolation between intermittent reference thermistor readings would give a sufficiently accurate temperature reference. The temperature measurements show, however, for the first time, that there are sudden changes in temperature that extend throughout the snow cover.

The design error is easily corrected by using a reference thermistor cavity of high thermal inertia. The reference cavity should be linked to the lowest level of the snow thermometer using a fast-response thermopile. The output from the thermopile should be monitored with the other sensors on the scan.

## 3. Suggestions for a Future Experiment

It would have been desirable to repeat the experiment using a correctly designed snow thermometer. However, the experience gained in the experiment showed that a more comprehensive change in the experimental design is necessary.

First, the detailed analysis of minute-by-minute data indicated that a much greater scan rate, of several scans per

second is required in order to study individual ventilation events. This requires a further improvement in the resolution of the data recording system. Such an improvement can be achieved with a better data logger. A digital data logger is required for the necessary speed of response. The output should be directly computer compatible because of the vast amount of data generated.

Secondly, the spatial variations in the surface pressure field should be directly monitored during the experiment. The character of the pressure field is not easily inferred from wind speed measurements - even if the vertical component and the horizontal components were to be simultaneously monitored. The monitoring of surface pressure variations presents its own problems, however, and it is an area of research that still needs considerable attention.

The monitoring of the thermal stratification above the surface, while made less essential by the direct monitoring of the spatial variations in surface pressure, would be greatly facilitated by a high-speed data acquisition system. The large time constant, necessary for a steady signal on the chart recorder, forces a sensor geometry that makes artificial ventilation of the sensor imperative. Using a high-speed data acquisition system, air temperature sensors sufficiently small to eliminate the need for artificial ventilation can be used.

#### 4. Some Suggestions for Future Research

This thesis has provided some, at least tentative, answers to some of the questions regarding snowpack ventilation. However, many more questions were raised than answered. It is clear that much work remains before the factors controlling snowpack ventilation are fully understood. The present work has concentrated on the temporal patterns at a site located in flat terrain. It thus largely ignores the effects of the quasi-stationary surface pressure variations. Yet, these may be the ones mainly responsible for snowpack ventilation in terrain that is not flat.

The spatial and temporal aspects of near-surface turbulence and of the associated surface pressure field is a topic that merits considerable attention. It is important, not only to snowpack and soil ventilation but also to energy exchanges at the surface and to aeolian transport processes.

It is easily imagined that differences in vegetation and topography influence the character of both the quasi-stationary and the mobile pressure fields. The ecological effects, both long-term and short-term, of such variations are unknown.

The vapor transfers within a snow cover merit further attention. Of particular interest in this context is the proposed negative feedback to ventilation in the presence of particularly strong, negative temperature gradients. A relationship between the vapor pressure of the pore air and its velocity is also suggested.

In turbulent transfer theory the assumption is often made that both the horizontal and the vertical components of the flow come to zero near the surface. The present study shows that there is a vertical flow component through the snow surface. The effect of this vertical component on the heat flux estimates obtained by standard gradient measurement methods needs to be investigated.

The vertical component through the surface may be an important factor in aeolian transport processes. The observed snow erosion feature described in the introductory chapter certainly suggests this to be the case. It would be most interesting to know the magnitude of the vertical component at the surface under different conditions. From the point of view of snow drifting and energy exchange it would be particularly interesting to know the influence of the near-surface air permeability on the vertical component through the surface.

The accessory instruments, developed during the course of this study open possibilities for several new investigations. The radiometer probe appears promising for research on radiation penetration into the snow cover. The probe could be modified by adding filters for different spectral bands. The anemometers have already been modified and developed into a low-cost totalizing anemometer that makes spatial wind surveys feasible (Ockwell, 1980). Further understanding of the spatial variations in wind speed is needed and the high cost of anemometers is a

main bottleneck in this field.

Finally, the rapid temperature fluctuations and the ventilation they indicate suggest not only one but two new factors that need to be considered in the theory of snow metamorphism. First, the movement of air influences both mass and heat transfers. Secondly, the rapid fluctuations in temperature can cause spatial variations in the temperature and the vapor pressure of the ice matrix as a result of spatial variations in the thickness of the ice matrix. The latter mechanism may offer an explanation to the rapid "destructive metamorphism" of new snow observed in nature but not predictable from surface curvatures using Kelvin's equation.

## REFERENCES

- Abels, H., 1894: Beobachtungen der taglichen Periode der Temperatur in Schnee und Bestimmung des Wärmeleitungsvermögens des Schnees als Funktion seiner Dichtigkeit.  
Repertorium für Meteorologie, Bd. 16, Nr. 1, p. 1-53.
- Acharya, C. L. and Prihar, S. S., 1969: Vapor losses through soil mulch at different wind velocities.  
Agron. J., No. 61, p. 666 - 668.
- Annersten, L. J., 1964: Investigations of Permafrost in the Vicinity of Knob Lake, 1961-62.  
McGill Sub-Arctic Research Papers, No. 16, p. 51 - 78.
- Atwater, M. and LaChapelle, E. R., 1961: Three Instruments used in Avalanche Hazard Forecasting.  
Miscellaneous Report No. 2, Alta Avalanche Study Center, U. S. Department of Agriculture.
- Bader, H., Haefeli, E., Bucher, E., Neher, S., Eckel, D. and Thams, C., 1939: Der Schnee und seine Metamorphose.  
Beiträge zur Geologie der Schweiz, Geotechnische Serie, Hydrologie, Lieferungs Kummerly und Frey, Bern. U. S. A. S. I. P. R. E. Translation No. 14, 1959, 313 p.
- Bender, J. A., 1957: Air Permeability of Snow.  
U. S. A. S. I. P. R. E. Research Report No. 70, 93 p.
- Benoit, G. R. and Kirkham, D., 1963: The Effect of Soil Surface

Conditions on Evaporation of Soil Water.

Soil Sci. Soc. Am. Proc. 27, p. 495 - 498.

Bergen, J. D., 1963: Vapor Transport as estimated from Heat Flow in a Rocky Mountain Snowpack.

Int. Assoc. Sci. Hydrol. No. 61, p. 62 - 74.

Brown, R. W., 1970: Measurement of Water Potential with Thermocouple Psychrometers: Construction and Applications.

U. S. D. A. Forest Services Res. Paper INT-80. 27 p.

Colbeck, S. C., 1973: Theory of Metamorphism of Wet Snow.

U. S. A. C. R. R. E. L. Res. Rep. 313, 11 p.

Colbeck, S. C., (in press): An Overview of Seasonal Snow Metamorphism.

Review paper presented at the NSF - NRC International Workshop on the Properties of Snow, Snowbird, Utah, April 8 - 10, 1981.

De Quervain, M. R., 1972: Snow Structure. Heat and Mass Flux through Snow.

Proc. International Symposium on the Role of Snow and Ice in Hydrology. UNESCO-WMO, Banff, Canada.

Dien, M., 1937: Bodenatmung. Gerlands Beiträge zur Geophysik, Vol. 51, p. 146 - 166.

Doebelin, E. O., 1976: Measurement Systems, Applications and Design. McGraw-Hill, 772 p.

Evans, R. D., Kraner, H. W. and Schroeder, G. L., 1962:

On site Radon in Surface Soils - Project Vela.

Final Report AFTAC Project Vela T/2031/S/OSR, Edgerton,

- Gerneshausen and Grier Inc., Boston. 93 p.
- Farrell, D. A., Graecen, E. L. and Gurr, C. G., 1966:  
Vapor Transfer in Soil due to Air Turbulence.  
Soil Sci. Vol. 102, p. 305 - 313.
- FitzGibbon, J., 1977: Snowmelt Routing in the Knob Lake  
Drainage Basin. Ph.D. Thesis, Dep. of Geography,  
McGill University.
- Fukuda, H., 1955: Air and Water Movement in Soil due to Wind  
Gustiness. Soil Sci. Vol. 79, p. 249 - 258.
- Gjessing, Y. T., 1975: Filtering Effect of Snow. Int. Assoc.  
Hydrol. Sci. Publ. No. 118, p. 199 - 203.
- Goodrich, L. E., 1976: A Numerical Model for Assessing the  
Influence of Snow Cover on the Ground Thermal Regime.  
Ph. D. Thesis, Interdisciplinary Programme in Glaciology,  
McGill University. 538 p.
- Granberg, H. B., 1978: Measured Thermal Regime within a Snow Cover  
just before the onset of Melt.  
Proc. Modeling of Snow Cover Runoff (S. C. Colbeck and  
M. Ray eds.) p. 279 - 287.
- Hanks, R. J. and Woodruff, N. P., 1958: Influence of Wind on  
Water Vapor Transfer through Soil, Gravel and Straw Mulches.  
Soil Sci. Vol 86, p. 160 - 164.
- Horton, R. E., 1915: The Melting of Snow.  
Monthly Weather Review, 43, p. 599 - 605.
- International Rectifier Corporation, 1966: Solar Cell and Photocell

Handbook HB-30. 136 p.

- Jessop, A. M., 1968: Three Measurements of Heat Flow in Eastern Canada. Canadian Journal of Earth Sci., No. 5, p. 61 - 68.
- Kimball, B. A., 1970: Effects of Air Turbulence upon Gas Exchange from Soil. Ph. D. Thesis, Cornell University. 199 p.
- Kimball, B. A. and Lemon, E. R., 1970: Spectra of Air Pressure Fluctuations at the Soil Surface. J. Geophys. Res., Vol. 75, p. 6771 - 6777.
- Kimball, B. R. and Lemon, E. R., 1971: Air Turbulence Effects upon Soil Gas Exchange. Soil Sci. Soc. Amer. Proc. Vol. 35, p. 16 - 21.
- Kondratyeva, A. S., 1945: Thermal Conductivity of Snow Cover and Physical Processes Caused by the Temperature Gradient. SIPRE, U. S. A. C. R. R. E. L. Technical Translation 22, 1954.
- Kotlyakov, V. M., 1961: Snow Cover in the Antarctic and its Role in modern Glaciation of the Continent. Translated from Russian by Israel Program for Scientific Translations Ltd.
- LaChapelle, E. R. and Armstrong, R. L., 1977: Temperature Patterns in an Alpine Snow Cover and their Influence on Snow Metamorphism. Technical Report, Institute of Arctic and Alpine Research, Univ. of Colorado. 33 p.
- Liljequist, G. H., 1956: Energy exchange of an Antarctic Snowfield. Norwegian-British-Swedish Antarctic Expedition 1949 - 1952.

- Scientific Results, Vol. 2, Part 1, Oslo,  
Norsk Polarinstitutt, 298 p.
- Marlatt, W. E., 1967: Remote and in situ Temperature Measurements  
of Land and Water Surfaces.  
J. Appl. Met., Vol. 6, p. 272 - 279.
- McDonald, J. A. and Herrin, E., 1975: Properties of Pressure  
Fluctuations in an Atmospheric Boundary Layer.  
Boundary-Layer Meteorology, Vol. 8, p. 419 - 436.
- McKay, G. C. and Thurtell, G. W., 1978: Measurements of the  
Energy Fluxes involved in the Energy Budget of a Snow Cover.  
J. Appl. Met., Vol. 17, p. 339 - 349.
- Ockwell, M., 1980: Searching for the best Aerogenerator  
Site. Chinook, Spring 1980, p. 36 - 37.
- Ohmura, A., 1980: Climate and Energy Balance on Arctic Tundra.  
Ph D Diss. ETH Nr. 6587, Zurich, 437 p.
- Oura, H., Ishida, T., Kobayashi, S. and Yamada, T., 1967:  
Studies on Blowing Snow II. In: Physics of Snow and Ice,  
Part 2 (H. Oura ed.), Inst. Low Temp. Sci.,  
Sapporo, p. 1099 - 1117.
- Outcalt, S. I., 1977: The Influence of the Addition of Water  
Vapor Diffusion on the Numerical Simulation of the process  
of Ice Segregation. Frost i Jord, Oslo.
- Palm, E. and Tveitereid, M., 1979: On Heat and Mass Flux through  
Dry Snow. J. Geophys. Res., Vol. 84, No. C2, p. 745 - 749.
- Price, A. G., Dunne, T. and Colbeck, S. C., 1976: Energy Balance

and Runoff from a Subarctic Snowpack.

U. S. A. C. R. R. E. L. Report 76-27, 29 p.

Reimer, A., 1980: The Effect of Wind on Heat Transfer in Snow.

Cold Regions Science and Technology, Vol. 3, p. 129 - 137.

Romell, L. G., 1922: Luftvaxlingen i marken som ekologisk faktor.

Medd. Statens Skogsforskningsinstitut,

Vol. 19, p. 125 - 359.

Scheidegger, A. E., 1960: The Physics of Flow through Porous Media.

Univ. of Toronto Press.

Schlatter, T. W., 1972: The Local Surface Energy Balance and

Subsurface Temperature Regime in Antarctica.

J. Appl. Met., Vol. 11, p. 1048 - 1062.

Schmidt, W. and Lehmann, P., 1929: Versuch zur Bodenatmung.

Sitzber. Akad. Wiss. Wien, Math.-Naturw., Kl IIa, Vol. 9,

No. 10, 138 p.

Scotter, D. R. and Raats, P. A. C., 1969: Dispersion of Water

Vapor in Soil due to Air Turbulence.

Soil Sci., Vol. 108, p. 170 - 176.

Sommerfeld, R. A. and LaChapelle, E. R., 1970: The Classification

of Snow Metamorphism.

Journal of Glaciology, Vol. 9, No. 55, p. 3 - 17.

Tetens, O., 1930: Über einige Meteorologische Begriffe.

Z. Geophys., Vol. 6, p. 297 - 309.

Van Haveren, B. P., 1971: Measurements of Relative Vapor Pressure

in Snow with Thermocouple Psychrometers.

- Proc. Symp. on Thermocouple Psychrometers, Utah State Univ.  
(Ray W. Brown and B. P. Van Haveren eds.), p. 178 - 185.
- Wankiewicz, A., 1976: Water Percolation within a deep Snowpack  
- Field Investigations at a Site on Mount Seymour, British  
Columbia Ph. D. Thesis, Univ. of British Columbia, 177 p.
- Wankiewicz, A., 1978: A Review of Water Movement in Snow.  
Proc. Modeling of Snow Cover Runoff (S. C. Colbeck and  
M. Ray eds.) Hanover, NH, p. 222 - 252.
- Wendler, G., 1971: An Estimate of the Heat Balance of a Valley  
and Hill Station in Central Alaska.  
J. Appl. Met., Vol. 10, p. 684 - 693.
- Yen, Y. C., 1962: Effective Thermal Conductivity of Ventilated  
Snow. J. Geophys. Res., Vol. 67, p. 1091 - 1098.
- Yen, Y. C., 1963: Heat Transfer by Vapor Transfer in Ventilated  
Snow. J. Geophys. Res., Vol. 68, p. 1093 - 1101.
- Yen, Y. C., 1965: Effective Thermal Conductivity and Water Vapor  
Diffusivity of Naturally Compacted Snow. J. Geophys. Res.,  
Vol. 70, p. 1821 - 1825.
- Yosida, Z., 1950: Heat transfer by Water Vapor in a Snow Cover.  
Low Temp. Sci., Vol. 5, p. 93 - 100.
- Yosida, Z., 1955: Physical Studies on Deposited Snow. I. Thermal  
Properties. Low Temp. Sci., Vol. 7, p. 19 - 74.